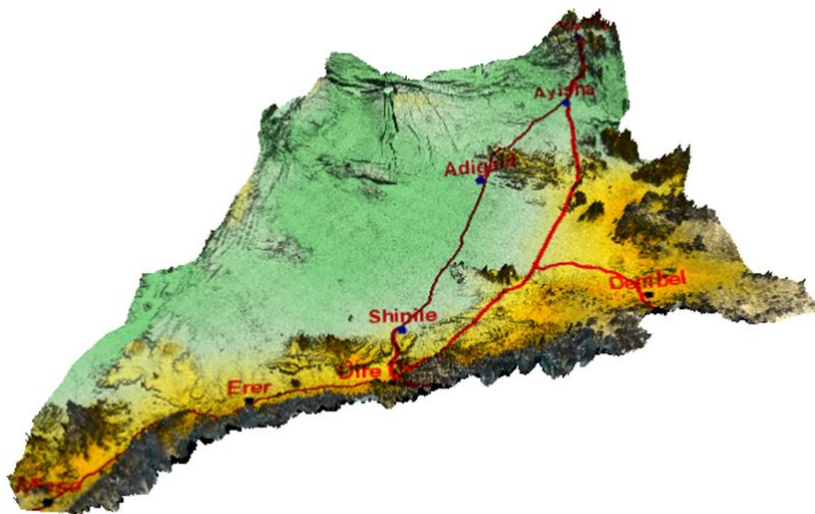


Addis Ababa  
University  
(Since 1950)



**ADDIS ABABA UNIVERSITY  
SCHOOL OF GRADUATE STUDIES  
DEPARTMENT OF EARTH SCIENCES**

**GEOCHEMICAL EVOLUTION OF GROUNDWATER FROM  
PLATEAU TO THE RIFT FLOOR IN SHINILE AREA, EASTERN  
ETHIOPIA**



**A Thesis Submitted to the School of Graduate Studies of Addis Ababa  
University  
In Partial Fulfillment of the Requirements for the Degree of Master of Science  
in  
Hydrogeology  
By  
DIRIBA MENGESHA KEJELA**

**MARCH, 2012  
ADDIS ABABA**

**ADDIS ABABA UNIVERSITY  
SCHOOL OF GRADUATE STUDIES  
DEPARTMENT OF EARTH SCIENCES**

**GEOCHEMICAL EVOLUTION OF GROUNDWATER FROM  
PLATEAU TO THE RIFT FLOOR IN SHINILE AREA, EASTERN  
ETHIOPIA**

**A Thesis Submitted to the School of Graduate Studies of Addis Ababa  
University in Partial Fulfillment of the Requirements for the Degree of Master  
of Science in Hydrogeology**

**By  
DIRIBA MENGESHA KEJELA**

Approved by the Board of Examiners

Name

Signature

---

---

---

---

---

---

---

---

## ACKNOWLEDGEMENT

First of all I would like to thank The Almighty God who is the ultimate means of my success for His endless love and care throughout my life.

I am thankful to Oromiya water works design and supervision enterprise for providing me all the necessary and relevant data and information without which the completion of this work would not have been possible.

I would like to thank my advisor Dr. Seifu Kebede and all Addis Ababa University Earth Science Department instructors for their support in the knowledge of Hydrogeology and Earth Sciences.

I would like to thank my friend Getaneh for his support and for providing me different technical material and advice that was necessary for the completion of this thesis.

I would like to thank all my family for their love, support and encouragement. Thank you mother and father you always want me to have the best in life and I wish you a very long and happy life. My brother Fedhesa thank you for your financial and moral support; you have been there for me. My sisters Shuramo and Ayantu thank you for your love and encouragement. This was possible because of all of you.

## ABSTRACT

The objective of this study was to assess geochemical evolution of groundwater from plateau to the rift floor in Shinile area and to identify geochemical processes responsible for evolution by analyzing hydrochemical data using conventional graphical methods and multivariate statistical methods. For this purpose water chemistry data of eighty seven water samples from the area are analyzed and interpreted. Q-mode Hierarchical cluster analysis (HCA) is used to classify the eighty seven water samples in to five distinct hydrochemical groups. The results of this analysis revealed that in general salinity and concentration of the groundwater increases from highland areas to the rift floor and water type in the study area evolves from Ca-HCO<sub>3</sub> and Ca-Mg-HCO<sub>3</sub> dominated type on the highlands to Na-HCO<sub>3</sub> and Na-HCO<sub>3</sub>-SO<sub>4</sub> dominated type on the escarpment to Mg-Ca-SO<sub>4</sub>-HCO<sub>3</sub>, Ca-Na-SO<sub>4</sub> and Na-Cl-SO<sub>4</sub> types on the rift floor following the direction of the ground water flow.

Principal component analysis, another multivariate statistical method, is employed to analyze the water samples to identify geochemical processes that are responsible for the observed variation in hydrochemistry of the area. The first three principal components accounted for 72.85% of the total variance in the hydrochemistry. The first principal component which explained 46.99% of the observed variance most probably represents dissolution reactions of carbonates and evaporite sediments; the second principal component which explained 15.29% of the observed variance in hydrochemistry most probably represents silicate hydrolysis reaction and the third principal component which accounted for 10.58% of the variance in hydrochemistry most probably represents addition of contaminants to the ground water from anthropogenic sources based on their factor loadings for the different hydrochemical variables.

The relationship among the major ion compositions of the water samples are also analyzed to determine if the geochemical processes suggested based on the PCA results are responsible for the observed variations in hydrochemistry of groundwater in the study area. The results of this analysis clearly indicated the occurrence of dissolution reaction of evaporite deposits and carbonate sediments as well as silicate hydrolysis reactions in the study area confirming the PCA results. Finally water quality of the study area is assessed from domestic use and agricultural point of view and distribution of fluoride and SAR of the area are mapped.

**Key words:** Groundwater evolution, hydrogeochemical processes, hierarchical cluster analysis, hydrochemistry, Principal component analysis, Shinile area.

# Table of Contents

ABSTRACT .....	iv
1. INTRODUCTION .....	1
1.1 Background .....	1
1.2 Literature review and previous works .....	2
1.2.1 Literature Review .....	2
1.2.2 Previous Works .....	4
1.3 Statement of the problem .....	4
1.4 Objective .....	5
1.4.1 General Objective.....	5
1.4.2 Specific Objectives.....	5
1.5 Data Sources and Methodology .....	5
1.5.1 Data Source .....	5
1.5.2 Methodology .....	5
2. GENERAL OVERVIEW OF THE STUDY AREA .....	6
2.1 Location and Accessibility .....	7
2.2 Climate .....	7
2.2.1 Rainfall and Temperature.....	9
2.2.2 Wind Speed, Relative Humidity and Sunshine Hours .....	10
2.2.3 Evapotranspiration .....	11
2.3 Physiography and Drainage of the Study Area .....	12
2.3.1 Physiography .....	12
2.3.1.1 The Southeastern Plateau .....	12
2.3.1.2 The Escarpment.....	12
2.3.1.3 The Afar Depression .....	12
2.3.2 Drainage .....	13
3. GEOLOGY .....	16
3.1 Regional Geology.....	16
3.1.1 Precambrian Basement Rocks.....	16
3.1.2. Late Paleozoic to Early Mesozoic Sedimentary Rocks.....	16
3.1.3 Mesozoic Sedimentary Rocks .....	17
3.1.4 Early Tertiary Sedimentary Rocks .....	18
3.1.5 Tertiary Volcanic Rocks.....	18
3.1.6 Quaternary Sedimentary and Volcanic Rocks .....	19

3.2 Geology of The study Area .....	20
3.2.1 Metamorphic rocks.....	20
3.2.2 Sedimentary Rocks.....	20
3.2.2.1 Adigrat Sandstone .....	20
3.2.2.2 The Hamanlei Limestone .....	21
3.2.2.3 The upper (Amba Aradom) Sandstone.....	21
3.2.2.4 Gypsum and Shale intercalation.....	21
3.2.3 Volcanic Rocks .....	22
3.2.3.1. Pre-Rift Volcanic Rocks.....	22
3.2.3.2 Post Rift Volcanic Rocks .....	22
3.2.4. Unconsolidated Sediments and Lacustrine Deposits .....	24
4. HYDROGEOLOGY .....	26
4.1 General .....	26
4.2 Hydrogeology of the Study Area .....	26
4.2.1 Precambrian Rocks.....	26
4.2.2 Mesozoic Sediments.....	27
4.2.3 Volcanic Rocks .....	27
4.2.4 Recent/Quaternary Sediments .....	29
5. HYDROGEOCHEMISTRY .....	30
5.1 General .....	30
5.2 Data Quality .....	31
5.3 Data Analysis .....	34
5.3.1 Graphical Methods .....	35
5.3.1.1 Piper Diagram .....	35
5.3.1.2 Pie Chart and Stiff Diagrams .....	37
5.3.1.2.1 Results of the pie chart plots .....	37
5.3.1.2.1 Results of the Stiff diagram plots.....	39
5.3.2 Multivariate Statistical Methods .....	41
5.3.2.1 Hierarchical Cluster Analysis .....	41
5.3.2.1.1 Results of the HCA .....	42
5.3.2.2 Principal Components Analysis .....	46
5.3.2.2.1 Results of the Principal Components Analysis .....	47
5.4 Evolution and Spatial Variation of hydrochemistry.....	50
5.5 Hydrogeochemical Processes .....	54

5.6 Hydrochemistry and Water Quality .....	58
5.6.1 Hydrogen ion activity (pH) .....	58
5.6.2 Total Dissolved Solids (TDS) and Electrical conductivity (EC) .....	58
5.6.3 Fluoride .....	61
5.6.4 Other Water Quality Parameters .....	63
5.6.5 Agricultural Water Quality.....	64
6. CONCLUSION AND RECOMMENDATION.....	66
6.1 Conclusion.....	66
6.2 Recommendations .....	69
References.....	70
Appendices.....	74

## List of figures

Figure 2.1 Location map of the study area. ....	8
Figure 2.2 Bimodal distribution of rainfall at some stations in and around the study area. ....	10
Figure 2.3 Average monthly distribution of rainfall at some meteorological stations in the study area. ....	10
Figure 2.4 Graph showing variations in monthly rainfall and actual evapotranspiration in the study area. ....	11
Figure 2.5 3D model map showing the different physiographic regions of the study area. ....	13
Figure 3.1 Simplified Geological map of the study area (modified after OWWDSE, 2011). ....	25
Figure 4.1 Simplified hydrogeological map of the study area (modified after OWWDSE, 2011) .....	28
Figure 5.1 Charge balance graph of the water samples. ....	32
Figure 5.2 Location of the different water samples .....	33
Figure 5.3 piper plots: A= all water samples, B= borehole waters, C= HDW waters, D= river waters and E= spring waters. ....	36
Figure 5.4 Pie diagrams of the group mean samples of the five water groups obtained from HCA. ....	38
Figure 5.5 Stiff pattern diagrams of group mean samples of the five water groups obtained from HCA. ....	40
Figure 5.6 Dendrogram of the Q-mode hierarchical cluster analysis. ....	42
Figure 5.7 Piper diagram of water samples clustered in to the five groups by HCA. ....	44
Figure 5.8 Factor loadings of the variables. ....	49
Figure 5.9 Plots of PC scores for PC1 versus PC2. ....	49
Figure 5.10 Distribution of the HCA water groups in the study area. The red lines indicate inferred direction of groundwater flow. ....	51
Figure 5.11 Stiff and pie diagram plots of the water samples on base map of the area. ....	52
Figure 5.12 Electrical conductivity (EC) map of the study area. ....	53
Figure 5.13 Relationship between the major ions: A= $\text{HCO}_3^-$ vs $\text{Ca}^{2+}$ , B= $\text{SO}_4^{2-}$ vs $\text{Ca}^{2+}$ , C= $\text{Mg}^{2+}$ vs $\text{Ca}^{2+}$ , D=Total cations vs $\text{K}^+ + \text{Na}^+$ , E= Total cations vs $\text{Ca}^{2+} + \text{Mg}^{2+}$ and F = chloro-alkaline indices .....	56

Figure 5.14 Distribution of pH in the study area. ....	59
Figure 5.15 Spatial distributions of TDS in the area. ....	60
Figure 5.16 Relationship between EC and TDS. ....	61
Figure 5.17 Spatial distribution of fluoride in the area. ....	63
Figure 5.18 Spatial distribution of SAR in the area. ....	65

## List of tables

Table 1 Mean concentrations for the groups derived from HCA .....	43
Table 2 Description of water cluster groups .....	45
Table 3 Correlation coefficient among hydrochemical parameters .....	47
Table 4 PCA factor loadings matrix .....	48

## List of acronyms

BH	Borehole
CAI	Chloro-alkaline index
EC	Electrical conductivity
HDW	Hand dug well
HCA	Hierarchical clustering analysis
GW	Groundwater
PCA	Principal Component analysis
OWWDSE	Oromiya Water Works Design and Supervision Enterprise
TDS	Total dissolved solids
WHO	World Health Organization

# 1. INTRODUCTION

## 1.1 Background

Groundwater is the sub-surface water that occurs beneath the water table in soils and geologic formations that are fully saturated (Freeze and Cherry, 1979). It is one of the most valuable natural resources, which supports human health, economic development, and ecological diversity. Because of its several inherent qualities (e.g., consistent temperature, widespread and continuous availability, excellent natural quality, limited vulnerability, low development cost, drought reliability), it has become an important and dependable source of water supplies in all climatic regions including both urban and rural areas of developed and developing countries (Todd, 2005). Of the 37 Mkm<sup>3</sup> of freshwater estimated to be present on the earth, about 22% exist as groundwater, which constitutes about 97% of all liquid freshwater potentially available for human use (Foster, 1998).

The Ethiopian rift consists of three major regions with distinct volcanic and tectonic characteristics representing different stages of rifting. These are the broadly rifted zone of southwestern Ethiopia, the Main Ethiopian Rift (MER) of central Ethiopia, and the Afar Depression. The study area which is located in Shinille zone of Somali regional state is found in the Affar Depression part of the Ethiopian rift.

The presence of many lakes and geothermal fields within a complex rift attracted major geoscientific and limnological investigations since the second half of the 20th century. Many of the geoscientific investigations related to hydrogeology and hydrochemistry revealed the importance of water–rock interactions in influencing the water quality in different parts of the Ethiopian rift and adjacent escarpments (Craig et al., 1977; Teklehaimanot et al., 1987; Darling et al., 1996; Gizaw, 1996; Chernet et al., 2001). Very few studies provided information on how groundwater quality is influenced along flow paths at regional scale all the way from the Ethiopian highlands to the rift (Ayenew, 2005; Kebede et al., 2005). This study attempts to provide this information, that is, how groundwater quality and chemistry is affected along flow paths from the highland along the escarpment to the rift floor in the study area by using conventional graphical and multivariate statistical analysis methods to analyze the different water samples collected from the study area.

## 1.2 Literature review and previous works

### 1.2.1 Literature Review

Literature shows the always-increasing potentiality of chemometric methods in obtaining useful information from environmental data, which hardly could be otherwise correlated and interpreted (Belkihiri *et al.* 2011). In particular many examples can be found of the application of multivariate analysis to sets of variables collected for surface and ground waters. Multivariate statistical techniques, cluster analysis (CA) and factor analysis (FA), are effective means of manipulating, interpreting and representing data concerning groundwater pollutants and geochemistry.

Statistical classification of geochemical data by Q-mode hierarchical cluster analysis (HCA) has been proven to provide a suitable basis for objective classification of water composition into hydrochemical facies (Meng and Maynard, 2001; Güler *et al.*, 2002, Güler and Thyne 2003; Kebede *et al.*, 2005). HCA is a multivariate statistical technique intended to classify hydrochemical observations so that the members of the resulting groups or subgroups are similar to each other and distinct from the other groups. The characteristics of the groups or sub-groups are not predetermined but can be obtained after the classification. The results obtained in HCA are justified according to their values in interpreting the data and in indicating realistic hydrochemical patterns representing field conditions. It is therefore not the number of members of a group that determines the robustness of HCA. It is possible that many single member groups that do not belong to any of the multi-member groups are placed in separate groups. This classification is useful especially to understand geological controls on water chemistry under conditions where useful geochemical data are available but clear hydrogeologic models have not yet been developed. The advantage of HCA is that many variables can be used to classify waters. In order that the variables have equal weight the raw chemical data will be logtransformed and standardized. This restricts the influence of or the biases caused by the variables that have the greatest or the smallest variances or magnitudes on the clustering result. A detailed description of the advantages and uses of the HCA in hydrochemistry and the mathematical formulation behind HCA is thoroughly discussed in Güler *et al.* (2002).

Ayene *et al.* (2009) have used multivariate statistical method of Q-mode hierarchical analysis with conventional geochemical methods to classify and understand the spatial variation of

hydrochemical facies and the underlying causes in relation to the groundwater movement and accounting the different volcanic rock sequences and geomorphological zones. In this study samples collected from over 120 wells and limited surface water were analyzed from Ziway Shala basin of the Main Ethiopian Rift. These samples were classified in to seven subgroups which represent different geochemical facies of groundwater from Ca-MgHCO<sub>3</sub> type water of the highland with low TDS to NaHCO<sub>3</sub> dominated and more saline water type of the rift floor.

(Belkhiri *et al.*2011) have used hierarchical cluster analysis with principal component analyses to analyze hydrochemical data of 54 water samples taken from the Ain Azel aquifer of eastern Algeria to extract principal factors corresponding to the different sources of variation in the hydrochemistry with the objective of defining the main controls on the hydrochemistry at the aquifer scale. The study finds, from Q-mode HCA that there are three main classes of hydrochemical facies namely the less saline water (group 1: Ca-Mg-HCO<sub>3</sub>), mixed water (group 2: Mg-Ca-HCO<sub>3</sub>-Cl) and blended water (group 3: Mg-Ca-Cl-HCO<sub>3</sub>). Results of this study clearly demonstrated the usefulness of multivariate statistical analysis in hydrochemistry.

Aynew *et al.*(2007) have used environmental isotopes( $\delta^2\text{H}$ ,  $\delta^{18}\text{O}$  and limited  $^3\text{H}$ ) and hydrochemical analysis supported by conventional field hydrogeological investigations to conceptualize the groundwater and surface water interaction at regional and sub-regional scale in the Awash river basin. This study revealed that recent meteoric water is the major source of recharge in the area. Three distinct groundwater zones were identified associated with the highlands, transitional escarpment and the rift. Towards the rift, the ionic concentration and isotopic enrichment ( $\delta^2\text{H}$  and  $\delta^{18}\text{O}$ ) increases following the groundwater flow paths, which is strongly controlled by axial rift faults. From the hydrochemical and isotope data this study identified five categories of ground water in the basin. These are (1) the depleted, high TDS, Na-HCO<sub>3</sub> type thermal waters of the upper Awash basin; (2) the depleted, low TDS, low  $^3\text{H}$  waters which occur in deeper basaltic or ignimbritic aquifers between the head waters of Awash and Metahara; (3) the shallow, isotopically enriched, high  $^3\text{H}$  (often  $>2$  TU), low TDS( $<1000$  mg litre<sup>-1</sup>), Ca-Mg-HCO<sub>3</sub> type waters in the highland aquifers; (4) the isotopically enriched, high TDS ( $>1500$  mg litre<sup>-1</sup>), thermal or groundwater from deep wells east of lake Beseka and in Asaiyata areas; and (5) the isotopically enriched, intermediate TDS (500–1500 mg litre<sup>-1</sup>) thermal waters in the axial part of the rift between Addis Ababa and Metahara.

### **1.2.2 Previous Works**

A comprehensive hydrogeology of Shinile area is studied by Oromiya Water Works Design and Supervision Enterprise for Shinile zone ground water potential assessment project.

Hydro-geology of Dire Dawa area which includes part of the study area is studied by Tesfamichael Keleta (1961) and several ground water augmentation reports by Mezmure Hailemicheal (1980), ketema Tadesse (1981), Greitzer (1961), and others have also described geology and hydrogeology of the area.

An environmental isotope and hydrochemical study to conceptualize the surface water and groundwater interaction and the groundwater flow pattern in relation to the geological setting has been studied by (Ayenew et al., 2008) Environmental Isotopes And Hydrochemical Study Applied to Surface Water and Groundwater Interaction tn the Awash River Basin. The ground water flow, depth of circulation and geochemical evolution of the upper and lower Awash Basin have been studied by (Seifu kebede et al., 2007) Ground Water Origin and Flow along Selected Transects in Ethiopian Rift Volcanic Aquifers.

Numerical ground water flow modeling in the southern part of the study area around Dire Dawa town has been conducted by Minala Bushura (unpublished Msc Thesis, 2007).

### **1.3 Statement of the problem**

Quality of groundwater is crucial for utilization of groundwater for domestic and agricultural purposes. High salinity and fluoride concentrations in groundwater are major problems in arid, semi-arid and rift valley regions in our country. As the study area is located in the rift valley and has arid to semi-arid climate this study tries to determine the geochemical changes that the groundwater undergoes from the highland plateau to rift floor and the impact of this change on groundwater quality and use of the groundwater for domestic and agricultural purposes.

## 1.4 Objective

### 1.4.1 General Objective

The general objective of this research is to assess and understand the geochemical evolutions that the groundwater in the study area undergoes from the plateau to the rift floor by using conventional graphical and multivariate statistical analysis methods.

### 1.4.2 Specific Objectives

- To determine the chemical processes of water - rock interactions that led to the present observed hydrochemistry of ground water in the area
- To assess water quality from domestic and agricultural point of view
- To map the distribution of important hydrochemical parameters in the study area.
- To map distribution of hydrochemical facies in the area

## 1.5 Data Sources and Methodology

### 1.5.1 Data Source

Secondary hydrochemical data obtained from Oromiya Water Works Design and Supervision Enterprise collected for ground water potential assessment of Shinile zone has been used for this study. This data contains major element geochemistry (Calcium- $\text{Ca}^{2+}$ , Magnesium- $\text{Mg}^{2+}$ , Sodium- $\text{Na}^+$ , Potassium  $\text{K}^+$ , Chloride  $\text{Cl}^-$ , Bicarbonate- $\text{HCO}_3^-$ , Fluoride- $\text{F}^-$ , Sulphate- $\text{SO}_4^{2-}$ , TDS) and physical (EC, Temperature, and pH). These data consists of 87 water samples collected from different part of the study area. Out of this water samples 7 samples are from rivers, 4 samples are from springs 30 samples are from hand dug well and 46 samples are from bore holes.

In addition metrological data from National Metrology Agency, geological and hydrogeological data from Ethiopian Geological Survey has been used to describe climatic, geological and hydrogeological setting of the study area.

### 1.5.2 Methodology

Cluster analysis is used to determine if the samples can be grouped into statistically distinct hydrochemical groups that may be significant in the geologic context. A number of studies used

this technique to successfully classify water samples (Alther, 1979; Williams, 1982; Farnham *et al.*, 2000; Alberto *et al.*, 2001; Meng and Maynard, 2001). Comparisons based on multiple parameters from different samples were made and the samples were grouped according to their ‘similarity’ to each other. Classifications of samples according to their parameters are known as Q-mode classifications. In the present study Q-mode hierarchical cluster analysis (HCA) will be used to classify the samples into distinct hydrochemical groups. The Ward’s linkage method (Ward, 1963) was used in this analysis. A classification scheme using Euclidean distance (straight line distance between two points in c-dimensional space defined by c variables) for similarity measurement, together with Ward’s method for linkage, produces the most distinctive groups where each member within the group is more similar to its fellow members than to any member outside the group (Güler *et al.*, 2002). Eleven hydrochemical variables measured (consisting of EC, pH, Na, K, Ca, Mg, F, Cl, NO<sub>3</sub>, HCO<sub>3</sub>, SO<sub>4</sub>, ) will be utilized in this analysis. Conventional graphical method is also used to describe and analyze the water samples based on their major cations and anion constituents.

PCA was used to extract the principal factors corresponding to the different geochemical processes that are the sources of variation in hydrochemistry and evolution of groundwater of the study area and to analyze correlations among the different major ion composition of the water samples.

Relationships between major ion compositions of the water samples are analyzed and interpreted to confirm the PCA results and to identify additional geochemical processes occurring in the study area..

In addition geographical information system software (ArcView) is used with other software like Surfer and Global Mapper to produce different maps of the study area like geological map, hydrogeological and water quality maps showing distribution of the different chemical constituents in the water samples of the area.

## 2. GENERAL OVERVIEW OF THE STUDY AREA

### 2.1 Location and Accessibility

The study area which covers most part of Shinille zone is found in the northern part of Somali Regional State in the eastern part of Ethiopia. The study area is bounded by the Ethio-Somali international border to the east, by the Ethio- Djibouti international border to the north and by Dire Dawa Administrative Council (DDAC) and by Oromia National Regional States to the south. Geographically the study area is located between 678160-972501E and 1012495-1233635N metric coordinates. The area extends for 174 Km from north to south and for 242 Km from east to west covering a total area of 34793 square kilometers.

The study area can be reached from Addis Ababa through the 500 kilometers long asphalted road to Dire Dawa. Shinille town, the capital of Shinille Zone is situated at 12 kilometers north of Dire Dawa. The Dire Dawa-Dure-Aysha-Deweale all-weather gravel road makes up the main access road to the eastern part of Shinille Zone. Several seasonal roads branch off to the east and to the west making a network of roads and seasonal trails in the study area (Figure 2. 1).

### 2.2 Climate

H. Zerai and J. Sima (1986) have summarized the climate of Shinille Zone and its adjoining areas in to the following five major climatic zones.

1. **Semi-arid zone:** (*Kefil Bereha*): This climatic zone lies between altitudes of 600 to 1200 m above mean sea level. It occurs in the lowland areas of Shinille Zone. It is characterized by high annual mean temperatures (20 to 25 degree celsius). It is indicated that this climatic zone is characterized by high evapotranspiration which exceeds the annual precipitation. Mean annual rainfall in this zone is in the range of 300 to 600 mm.
2. **Hot Subtropical Zone** (*Kolla*): This climatic zone occurs along the escarpment area. It lies at altitudes of 1200 to 1900 meters above mean sea level, and it is characterized by medium to high annual mean temperatures (18 to 20 degree celsius). The hot subtropical climatic zone gets mean annual rainfall of 600 to 1000 mm.

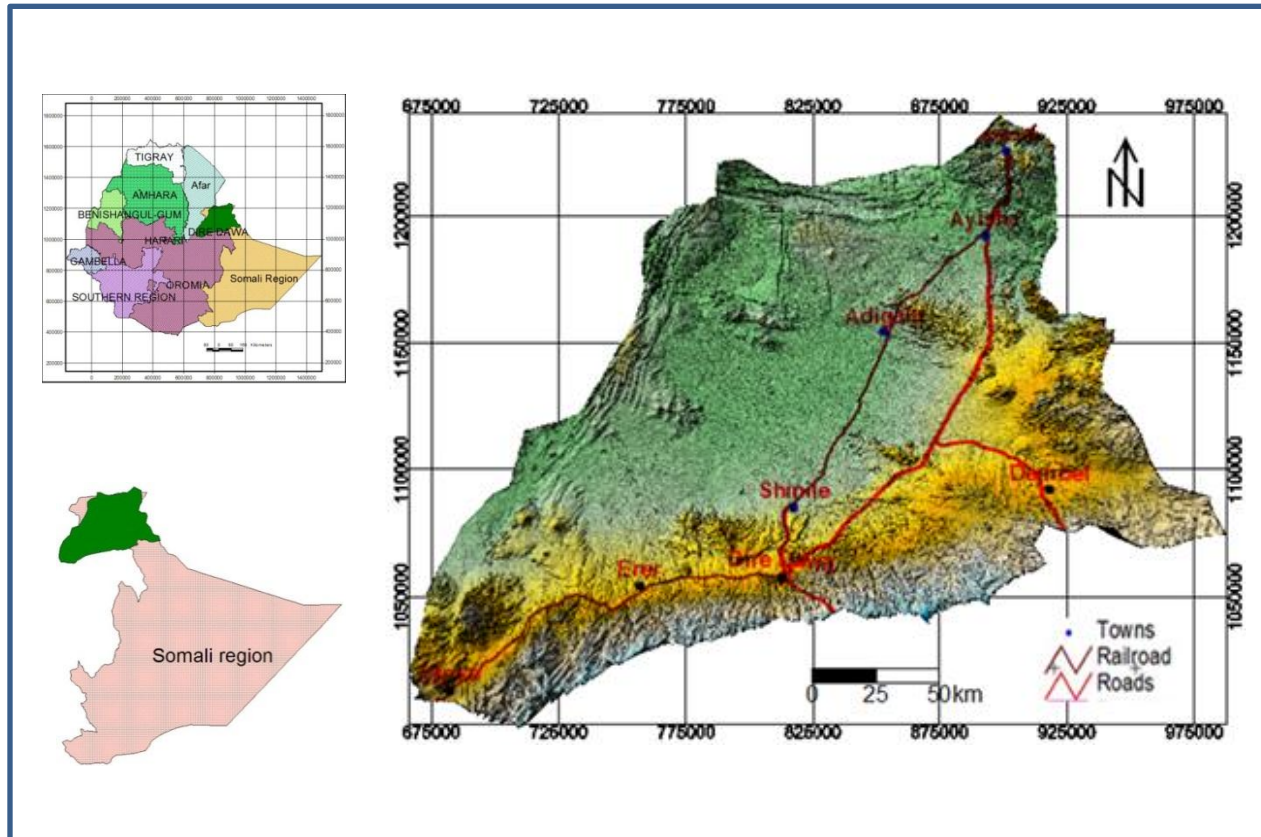


Figure 2.1 Location map of the study area.

3. **Hot Subtropical Zone (*Kolla*):** This climatic zone occurs along the escarpment area. It lies at altitudes of 1200 to 1900 meters above mean sea level, and it is characterized by medium to high annual mean temperatures (18 to 20 degree celsius). The hot subtropical climatic zone gets mean annual rainfall of 600 to 1000 mm.
4. **Humid Subtropical Zone (*Woinadega*):** This zone occurs on the Eastern Plateau, at altitudes of 1900 to 2500 meters above mean sea level. It is characterized by low (14 to 18 degree Celsius) temperatures. The mean annual precipitation of this zone exceeds 1000 m.
5. **Cold-Humid Subtropical Zone (*Dega*):** This zone occurs along the tops of mountain chains of the Eastern Plateau, which lie at altitudes of more than 2500 m above mean sea

level. The cold-humid subtropical zone is characterized by very low mean annual temperatures (less than 14 degree Celsius). The mean annual precipitation of this zone exceeds 1500 mm.

According to this classification most part of the study area falls in the semi-arid climatic zone. The study area is characterized by arid and semi-arid climate. The moisture for precipitation in the area originates from south-east equatorial air stream, which moves northwards within tropical convergence zone (ITCZ), (NMSA, 1996). The climate is typical of equatorial region modified by altitude.

The project area is part of South and Southeastern Ethiopian moisture region that have two distinct dry periods (December to February and July to August) and two rainy seasons (March to May and September to November).

### **2.2.1 Rainfall and Temperature**

The area gets bi-modal rainfall. It gets small rains from March to May. The small rains are generally erratic. In some cases, the small rains start earlier (February) and continue up to May. In other cases, the small rains may not occur at all. The main rainy season is normally from June to September (figure 2.2). The mean annual rainfall of the study area is 531, 368.2 and 312.7 for eastern Awash basin and 217, 134 and 215 for Ayisha basin calculated by arithmetic mean, Thiessen polygon and isoheytal methods (OWWDSE 2011).

According to monthly maximum and minimum temperature data records of Dire Dawa, Alemaya and Jijiga stations collected from National Meteorological Agency (NMA) the mean annual maximum temperature of the study area varies from 23°C to 34°C; while the mean minimum temperature varies from 11°C to 19°C. The mean annual temperature of the area estimated according to the data of the three stations varies from 17°C to 25°C.

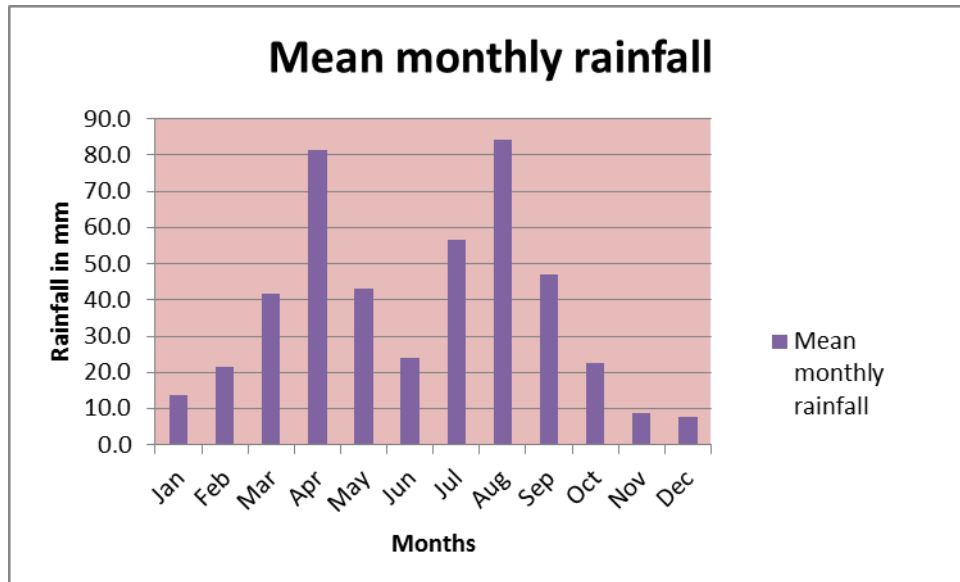


Figure 2.2 Bimodal distribution of rainfall at some stations in and around the study area (after OWWDSE 2011).

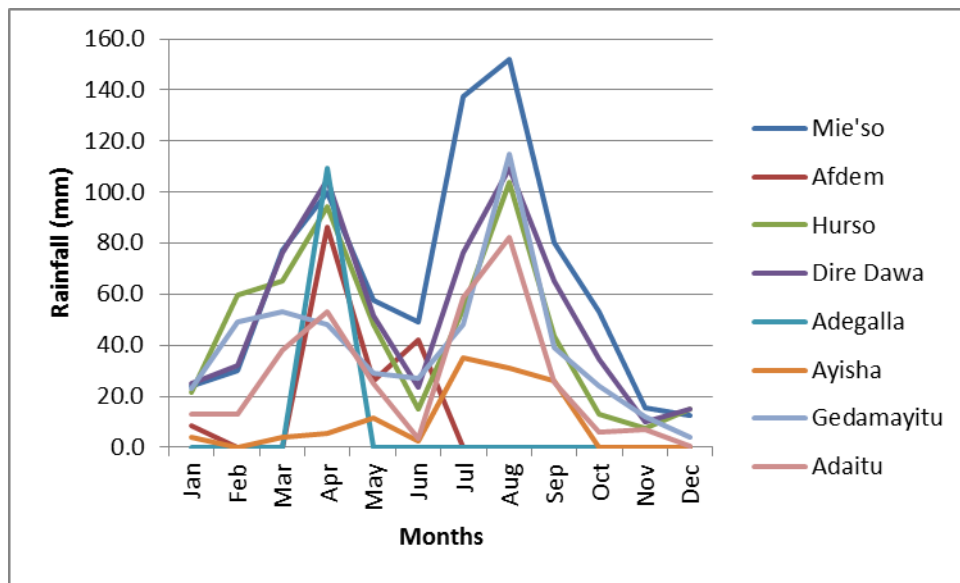


Figure 2.3 Average monthly distribution of rainfall at some meteorological stations in the study area (after OWWDSE 2011).

### 2.2.2 Wind Speed, Relative Humidity and Sunshine Hours

The mean annual relative humidity, wind speed and sunshine duration estimated according to Jijiga station were about 55%, 5m/sec and 6.8hours respectively (OWWDSE 2011).

### 2.2.3 Evapotranspiration

The actual evapotranspiration for the two sub-basins in the study area, namely, Eastern Awash and Ayisha basins are 719.3mm and 529.6mm respectively as obtained by Thornthweite and Mather soil water balance model and potential evapotranspiration of the two basins calculated by FAO's New LocClim estimator v1.10 software which uses Penmann- Monttheith equation is 1660mm and 1857mm (Oromiya Water Works Design and Supervision Enterprise Shinile zone ground water potential assessment project 2011).

The maximum evapotranspiration occurs during the month of October which is equal to 144mm and the minimum evapotranspiration is equal to 19.9mm and occurs during the month of December (OWWDSE 2011). Actual evapotranspiration in the study area is greater than precipitation for most of the months of the year and this is expected as the study area gets more recharge from the southern Oromiya highland precipitation than the precipitation in the study area (figure 2.4).

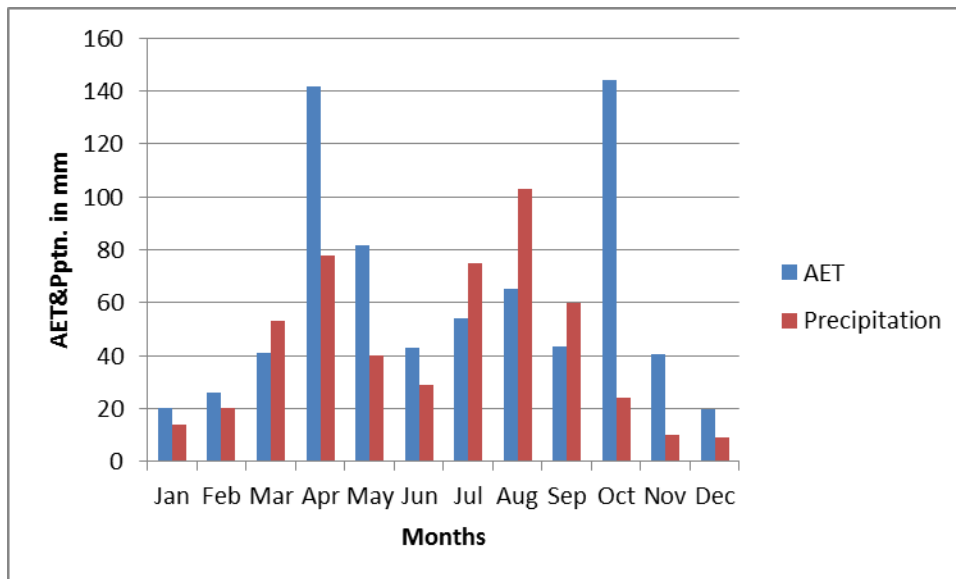


Figure 2.4 Graph showing variations in monthly rainfall and actual evapotranspiration in the study area (OWWDSE 2011).

## **2.3 Physiography and Drainage of the Study Area**

### **2.3.1 Physiography**

The geomorphology of the study area and adjacent areas has been categorized into three distinct physiographic units (M. Hailemeskel 1964). The Marda Range, which occurs west of Jijiga, southwest of Shinille Zone is considered as a fourth geomorphologic feature (Shachnai 1972). The three major physiographic features of the study area are: The Southeastern (eastern) Plateau, the Escarpment and the Afar Depression. The study area encompasses the southern part of the Afar Depression, the Escarpment and the northern part of the Southeastern Plateau.

#### **2.3.1.1 The Southeastern Plateau**

A regional watershed occurs in the southern part of the study area south of Shinille Zone. This watershed which extends from the Chiro area in the west to the Jijiga area in the east is the main source of water for the lowland areas of Shinille Zone in the north and for the Wabi Shebelle Basin in the south. Elevations of 3,405 m and 3138 m above mean sea level are recorded for Gara Muleta and Gondela mountains which occur along the watershed (H. Zerai 1986).

#### **2.3.1.2 The Escarpment**

The most prominent physiographic element of the study area is the escarpment which occurs in the southern margin of Shinille Zone. The escarpment occurs south of the latitude which passes through Dire Dawa and it consists of a set of parallel to sub parallel east-west oriented normal faults which down throw blocks of Mesozoic sedimentary rocks and Tertiary volcanic rocks to the north. Conspicuous fault scarps occur in the Dembel and Sanajif areas of eastern Shinille Zone. In the Dembel area, blocks of metamorphic and sedimentary rocks are downthrown to the north along EW-oriented regional faults. The total throw down of the blocks (800 m) from the eastern plateau up to the foot of the escarpment of the Dembel area in southeastern Shinille Zone is lower than the total throw down of blocks (1200 m) in Dire Dawa area (Shachnai, 1972).

#### **2.3.1.3 The Afar Depression**

Shinille Zone lies at the southern part of the Afar Depression and most part of the study area lies in this physiographic region. The plains of Shinille Zone gently slope to the north in this area. The lowest recorded elevation is 445 meters above mean sea level and it occurs in the Mogoda

area in northwestern Shinille Zone east of Adaytu town. The recorded altitude of the alluvial plains of central and eastern Shinille Zone varies from 581 m above mean sea level at Harriso, which is located in northern Shinille Zone to 1317 m above mean sea level at Dembel, located in southeastern Shinille Zone. The foot of the escarpment in the Dembel area has an elevation of 1335 m above mean sea level.

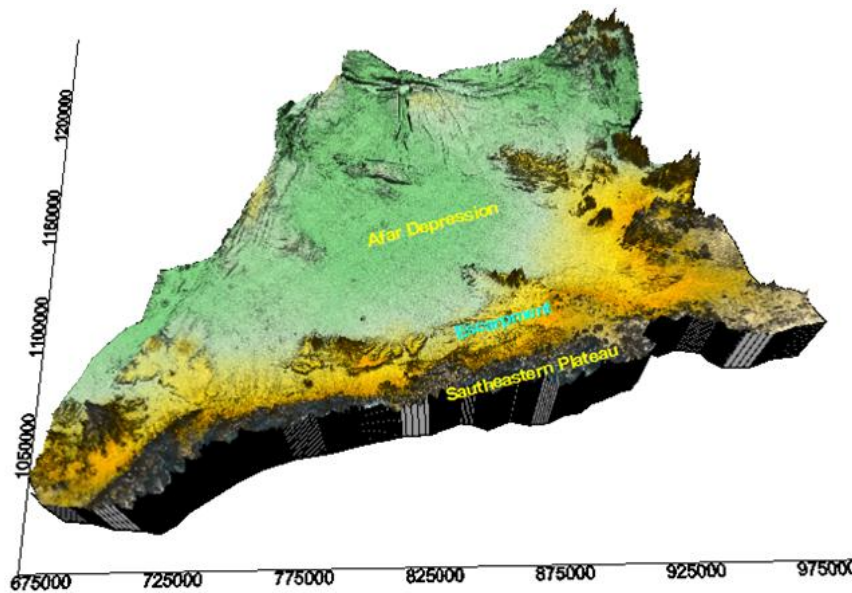


Figure 2.5 3D model map showing the different physiographic regions of the study area.

### 2.3.2 Drainage

The drainage systems of the study area which is mostly comprised of intermittent streams and wadis and some perennial rivers generally originate from the highlands of the escarpment area and recharge the alluvial sediments of the plains. The plains of Shinille Zone gently slope to the north and to the northwest, and as a result, the seasonal streams and flood plains flow to the north and to the north-northwest. In eastern Shinille Zone, seasonal streams from the Somalia and Oromia highlands drain to the southwest and northeast and tribute to the Kulen Valley which ultimately recharges the alluvial sediments of the Warouf and Horre areas which are situated in the central part of Shinille Zone.

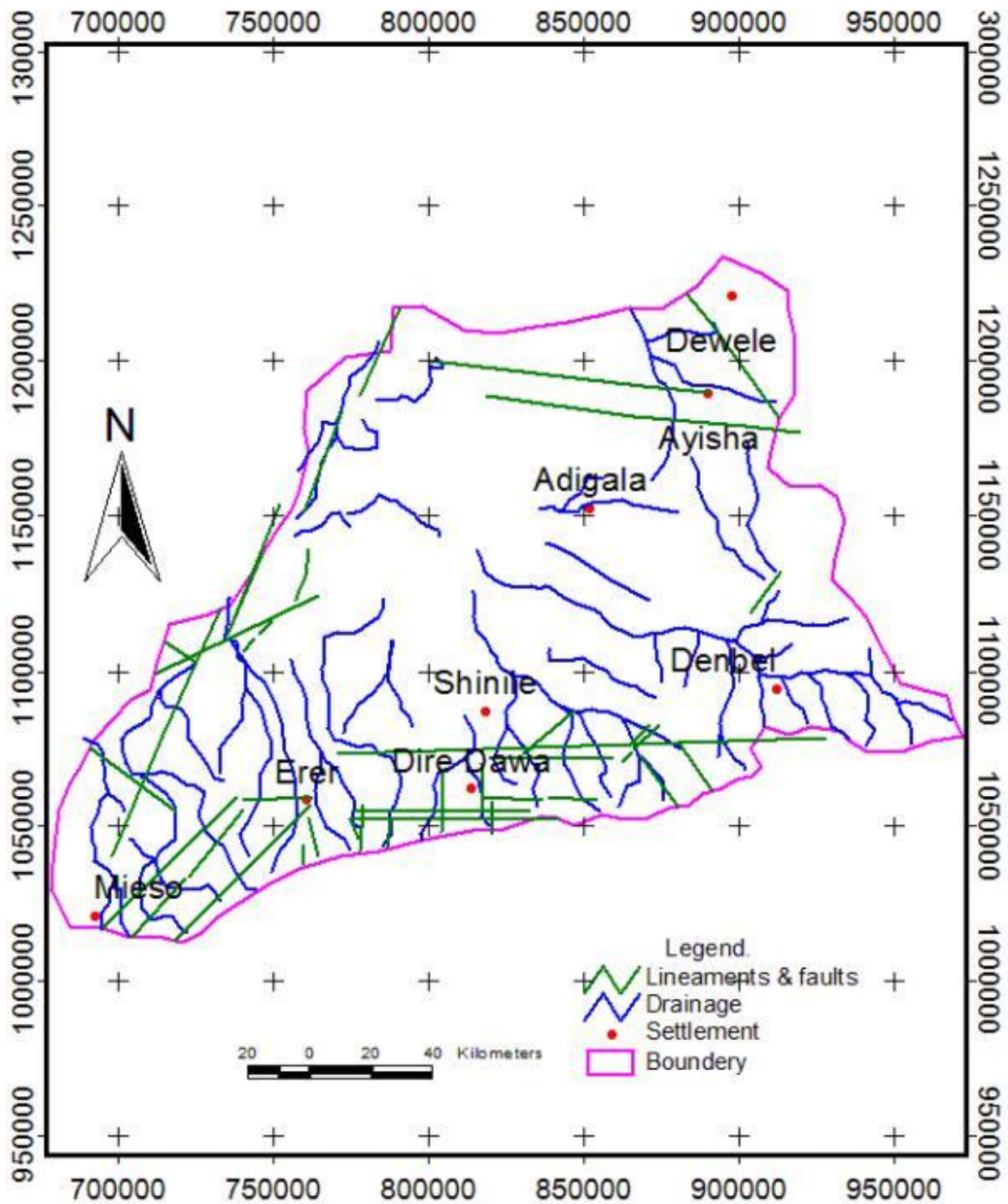


Figure 2.6 Drainage and structural map of the study area.

The waters of Southeastern Plateau and Eastern Escarpment also flow in to the central parts of Shinille Zone. Numerous seasonal streams and prominent flood plains of the Harmukale and Harawe valleys recharge the alluvial sediments of the Harawe-Warouf area. The drainage of southern Shinille Zone which covers the Dire-Dawa-Erer and Bike-Afdem areas generally flow to the north-northwest, north-south, and to the northwest. The seasonal stream of Dire Dawa area converges in to the Dechatu flood plain which passes through the central part of Dire Dawa city. The Dechatu flood plain recharges the groundwater resources of the alluvial sediments of Meto, Bisley and Harawe areas which are situated in central Shinille Zone (Figure 2.6 shows drainage of the study area).

## 3. GEOLOGY

### 3.1 Regional Geology

The geologic units in Ethiopia fall in to one of the following three categories; the Precambrian basement, late Paleozoic to early tertiary sediments and the Cenozoic volcanic and associated sedimentary rocks. The Paleozoic era of Ethiopia is an era of erosion and denudation. Minor occurrences of continental sedimentary rocks which are deposited during Late Paleozoic to Early Mesozoic times occur in the northern, southern and eastern parts of Ethiopia underlying thick Mesozoic sedimentary succession. The following is summary of regional geology is based on the Geological Map of Ethiopia and the accompanying explanatory notes (Mengesha *et al*, 1996).

#### 3.1.1 Precambrian Basement Rocks

High-grade migmatitic rocks of amphibolite to granulite facies occur in western, eastern, and southern Ethiopia. Low-grade metamorphic rocks of green schist facies cover extensive areas in the northern and western parts of Ethiopia, and occur as narrow belts within the high-grade rocks in southern Ethiopia. In the east, high-grade metamorphic rocks are exposed as discontinuous lenses along the eastern escarpment mainly as a result of regional uplift and subsequent step faulting. The high-grade rocks of eastern Ethiopia contain intercalations of low-grade metamorphic rocks of volcanic and sedimentary origin. The low-grade metamorphic belts of Ethiopia are usually intruded by felsic and mafic intrusions. Intrusions of gabbroic to granitic composition occur in several places in the western, northern, eastern and southern parts of the country. The mafic and felsic intrusions are commonly intruded by pegmatite dikes and veins of quartz.

#### 3.1.2. Late Paleozoic to Early Mesozoic Sedimentary Rocks

Sedimentary rocks of continental origin which are composed of sandstone, tillites, and conglomerates occur in northern and eastern Ethiopia. In the north, Edaga Arbi glacial and Enticho Sandstone represent the Late Paleozoic to Early Mesozoic rocks. In the east, the continental sedimentary rocks of Late Paleozoic to Early Mesozoic time are represented by the Calub Sandstone, Gumburo Sandstone and Bokh Shale. The Gura Sandstone from southeastern and the Permian Sandstone from the southwestern parts of Ethiopia are also categorized as Late Paleozoic to Early Mesozoic sedimentary rocks (Mengesha Tefera, et al., 1996). In Eastern

Ethiopia, the Waju Sandstone, which is mapped below the Adigrat Sandstone along the Ramis and Soka Valleys in the south-central part of the Dire Dawa map sheet (S.M. Berhe, 1985, Mengesha Tefera et al., 1996) belongs to this category.

### 3.1.3 Mesozoic Sedimentary Rocks

At the onset of the Mesozoic shallow seas spread initially over the Ogaden region and then extended further north and west as the land continued to subside. Sandstone was deposited on the old land surface, followed by the deposition of shale and limestone as the depth of water increase. In the west of the country sedimentation ended up with the deposition of clay, silt, sand and conglomerate as the sea reduced during the Jurassic. The sea invaded again in the lower cretaceous, and the sedimentation sequence was repeated.

This process resulted in very thick succession of sedimentary rocks which cover most parts of the Southeastern Plateau and parts of the Afar Depression. In addition, both clastic and chemical sedimentary rocks occurred in the Blue Nile Basin of central Ethiopia and in the Mekelle Outlier of northern Ethiopia. The sedimentary rocks are comprised of different types of sandstones, limestones, dolomites, marls, shales and anhydrites. Mesozoic sedimentary rocks, which are comprised of the Adigrat, Hamanlei and Amba Aradom formations mainly crop out along the southern escarpment of the Rift Valley in eastern Ethiopia (Mengesha Tefera 1986, S.M. Berhe 1985, T. Yihune and Haro, 2008). The Adigrat Formation mostly occurs at the base of the Mesozoic sequence except in some localities where the Late Paleozoic to Early Mesozoic rocks underlie it. The Adigrat Formation is commonly composed of continental clastic rocks which are dominantly comprised of fine- to medium-grained and cross-bedded sandstone with minor interbeds of siltstone and conglomerates. In most outcrops, the Adigrat Sandstone is ferruginous and lateritic, especially towards the top of the formation. In northern Ethiopia, the Adigrat Formation is overlain by the Antalo Formation. The Antalo Formation is mainly comprised of limestone with intercalations of shale and minor gypsum. In the Dire Dawa-Harar and Ogaden areas, the Adigrat Formation is overlain by the Hamanlei Formation, which constitutes Jurassic fossiliferous limestone of southeastern and eastern Ethiopia.

### 3.1.4 Early Tertiary Sedimentary Rocks

Deposition of both clastic and chemical sediments continued in eastern and southeastern Ethiopia during the Early Tertiary period. The Tertiary sedimentary rocks include the Jesoma, Auradu Taleh, and Karkar Formations. The Jesoma Formation mainly consists of variegated sandstone with minor intercalations of shale and lateritic beds. It unconformably lies over Mesozoic sedimentary rocks. The Jesoma Formation represents one of the transgressive units which formed as the sea retreated to the SW. The Jesoma formation is overlain by limestone of the Auradu Formation, which is characterized by the presence of iron-coated concretions of chert at its lower section and by the occurrence of chalk and gypsum intercalations towards its upper part. The upper part of the Tertiary sedimentary rocks are categorized in to two formations\_ the Taleh formation and the Karkar Formation. Both formations occur in eastern Ogaden. The Taleh Formation is mainly comprised of interbeds of anhydrite and fossiliferous limestone. The Karkar Formation which makes up the youngest Tertiary sedimentary formation is comprised of intercalations of cavernous limestone, shale and gypsum.

### 3.1.5 Tertiary Volcanic Rocks

The Tertiary Period of Ethiopia is characterized by widespread volcanism. Thick piles of volcanic rocks are deposited in the northern, central, southwestern and eastern parts of Ethiopia during the Tertiary Period. The Tertiary basalts of northern, western and eastern Ethiopia underlie most parts of the Northwestern and Southeastern plateaus, and these rocks age generally referred to as the Trap Series. Rocks of the Trap Series basically occur in the Northwestern and Southeastern plateaus mostly unconformably resting over Mesozoic Formations. In some instances the Trap Series rests on Late Paleozoic to Early Mesozoic sedimentary rocks and on Precambrian metamorphic rocks. These groups of rocks commonly called trap basalts include Ashangi formation, Aiba formation, Tarmaber formation and Alaji formation. The basaltic rocks of the Marda Range of eastern Ethiopia, which occurs west of Jijiga, are also mapped as the Ashangi formation by Mengesha et al., (1996), and described as mega dikes and sills (Shachnai 1972).

### 3.1.6 Quaternary Sedimentary and Volcanic Rocks

The Quaternary Period of Ethiopia has been principally an era of basic and felsic volcanism and deposition of lacustrine, marine and alluvial sediments. Extensive outcrops of Quaternary and Recent volcanic rocks occur within the rift floor of the Main Ethiopian Rift. In addition, in situ weathering of all of the rock types have given rise to the development of eluvial soils. Erosion along the escarpment and the plateaus produced thick unconsolidated sediments of mainly fluvio-alluvial origin. Carbonate precipitates occur in the form of travertine materials or beds within or at the margins of the rift valley.

Detrital sedimentary rocks of the Danakil Group (Red Series) make up the oldest quaternary sedimentary rocks of the Afar Depression (Garland, 1972). The Red Series consists of conglomerates, sandstones, clays and interbeds of basaltic and acidic lavas. The Red Series unconformably lies on the Mesozoic Formations and on metamorphic rocks of Precambrian age. Unconsolidated sediments of Quaternary age occur in several places throughout the country. The Hadar Formation and The Omo group are among these Quaternary sediments which have received detail investigation. The Hadar Formation occurs along the Awash Valley close to the Western Escarpment of the Main Ethiopian Rift. The thickness of the formation reaches up to 200 meters. The Hadar Formation hosts hominid and mammalian fossils. It is comprised of intercalations of silts, clays, and sandstones with intercalations of several tuffaceous beds and layers of basaltic flows.

Volcanic processes continued during the Quaternary period within the rift floor and at the margins of the Ethiopian Rift. Volcanic centers which started in the Northwestern Plateau during the Tertiary Period migrated from north to south during Quaternary (Kazmin, 1979). The migration of the volcanic centers is mainly controlled by tectonic features. Quaternary volcanism produced a thick pile of stratified basaltic rocks with minor associations of felsic extrusions within the rift valley. These rocks are referred to as the Afar Series. The Afar Series is comprised of thick (500 to 1500 m) succession of basaltic flows with minor interbeds of alkaline to per alkaline felsic rocks. Ignimbritic and trachytic to rhyolitic rocks of the Nazret Series which mainly occur along the Main Ethiopian Rift (MER), and along the rift margins also belong to this period

## **3.2 Geology of The study Area**

According geological map of Shinile zone prepared by (OWWDSE 2001) all of the three types of rock formations occur in the study area and they are described in detail as follows. Geological map of the study area is presented in figure 3.2.

### **3.2.1 Metamorphic rocks**

Metamorphic rocks occurring in the study area are the High-grade gneisses and migmatitic rocks which extensively out crop in the southeastern and eastern parts of Shinille Zone. The high-grade gneisses include, granitic gneisses, quartzo-feldspathic gneisses, and, biotite-amphibole gneisses. The granitic and biotite-amphibole gneisses occur in the southeastern part of Shinille Zone in association with thin intercalations of gabbros and amphibolites. In the southern margin of Shinille Zone, the high-grade gneissic rocks and migmatites occur in association with pelitic (fine clastic) and psamitic (coarse-clastic) metamorphic rocks and beds of marble.

Outcrops of migmatitic rocks and granitic gneisses are also mapped out in the northeastern part of Harar map sheet (T. Yihune and Workineh Haro, 2008) which constitutes parts of southeastern Shinille Zone which occur to the south and southeast of Arabi town and in Dure area. Extensive outcrops of metamorphic rocks are also exposed on the surface along the eastern escarpment of the rift valley in the Dengego-Harar area.

### **3.2.2 Sedimentary Rocks**

Extensive outcrops of Mesozoic sedimentary rocks occur in the south along the southern escarpment and within the Harrarghe Plateau of the Oromia Highlands. The Mesozoic sedimentary rocks are constituted by sandstones, limestones and shale. At least two major sandstone units, the lower (Adigrat) and the upper (Amba Aradom) formations are identified in the region.

#### **3.2.2.1 Adigrat Sandstone**

The Adigrat Sandstone makes up the lowest Mesozoic formation in the area of study. It unconformably rests over Precambrian metamorphic rocks in the Chelenko-Dengego area. The Adigrat Sandstone also occurs in southeastern part of the study area unconformably resting over strongly deformed biotite-amphibole gneisses and pegmatites. The Adigrat Sandstone varies

from pink to brown color in fresh outcrops. It is mainly constituted by feldspar indicating its low degree of maturity. In most outcrops, the Adigrat sandstone occurs as massive and intact rock mass which occasionally displays cross beds. Along the escarpment, the Adigrat Sandstone strongly weathers to yellow color and it becomes friable.

### **3.2.2.2 The Hamanlei Limestone**

Thick beds of limestone formation rest over the Adigrat Sandstone in the southern and southeastern parts of the study area. The limestone formation of the area is referred to as Hamanlei Formation (S.M. Berhe, 1985). T. Yihune et al., (2008) have subdivided the limestone successions of the Harar area in to Lower and Upper Limestone.

The Limestone Formation of the study area occurs sandwiched in between two sandstone formations, the Adigrat Sandstone and the Amba Aradom (Upper) Sandstone formations. In eastern Ethiopia, the limestone succession gets much thicker as compared to the north. In the study area yellow to grey, crystalline limestone occur in the southeast near Dembel and Hagar Wayne areas and in the surroundings of Dire Dawa. Thick succession of limestone is found in the northeastern part of the study area near Dewelle, where the limestone is encountered in association with outcrops of the Amba Aradom (Upper) Sandstone.

### **3.2.2.3 The upper (Amba Aradom) Sandstone**

The Upper Sandstone unconformably lies over the limestone formation and it is unconformably overlain by Tertiary volcanic rocks. Thicknesses of over 100 meters of the Upper Sandstone are recorded near Karamille on top of the Eastern Plateau. The Upper Sandstone of the Karamille area is strongly ferruginous, weathered and kaolinized. The Upper Sandstone also occurs extensively along the foot of the escarpment in southern Shinille Zone and in the Adelle-Dewelle area in the northeastern part of the study area.

### **3.2.2.4 Gypsum and Shale intercalation**

Thin interbeds of shale and gypsum occur at the contact of the Hamanlei limestone and the overlying Upper Sandstone south of Dewelle. The gypsum beds of the Dewelle area are being exploited as raw material for the production of cement. A thin bed of blue to brown shale is also

encountered at the contact of the Upper Sandstone with the underlying limestone formation northeast of Dire Dawa along the road to Harmukale.

### 3.2.3 Volcanic Rocks

#### 3.2.3.1. Pre-Rift Volcanic Rocks

This Volcanic rocks extruded prior to the onset of rifting during the tertiary period. And they are generally referred to as the Trap Series. The volcanic rocks of the Trap Series are comprised of horizontally layered olivine basalts, trachy-basalts, and silicic rocks. In Eastern Ethiopia, the Trap Series crops out on the northern part of the Southeastern Plateau and along the margins of the rift valley. The Tertiary volcanic rocks generally rest on the Mesozoic sedimentary succession and on the Precambrian metamorphic rocks. The lower part of the Trap Series is basically made up of stratoid basaltic rocks and pyroclastic falls, whereas the upper part is comprised of felsic flows and pyroclastic falls. The Tertiary volcanic rocks found in the study area constitute the following units.

- **Tertiary Stratoid Basalts-** These rocks are indicated to constitute Alaje Formation (S.M. Berhe, 1985). They are found along the escarpment in the study area and they occur in association with blocks of limestone and Upper Sandstone as a result of block faulting. They are generally fine-grained, strongly fractured, amygdaloidal and strongly weathered. In most outcrops, the basaltic units are intruded by thin silica and carbonate veinlets
- **Tertiary Silicics-** This unit is mainly comprised of alkaline rhyolites and ignimbrites (S.M. Berhe 1985). The Tertiary silicic rocks occur along the margin of the rift, overlying the Tertiary stratoid basaltic rocks and underlying the Afar Series volcanic rocks. These rocks extensively crop out in the Bike area. West of Bike, they are massive and east of Bike the rocks are strongly deformed as a result of the regional EW faulting. Strongly deformed and foliated silicic rocks are also encountered in the southwestern margin of Shinille Zone at Kurfa Sawa on the road to Mulu.

#### 3.2.3.2 Quaternary Volcanic Rocks

These rocks are extruded after the opening of the Main Ethiopian Rift and the Afar Depression, and mainly occur along the floor and margins of the rift. The Quaternary volcanic rocks occur as

intercalations within ancient and modern alluvial sediments indicating the existence of concomitant processes of sedimentation and volcanism in the Rift Valley during the Quaternary period. The volcanic rocks of the Afar Series, like the Trap Series, are stratoid volcanic rocks which are dominated by fissural-type basaltic flows. Rocks of the post rift volcanism which occur in the study area are described below

- **Lower Afar Basalt**- This unit crops out in the western, southeastern and northeastern parts of Shinille Zone, and forms the oldest volcanic rock of the Afar Series rocks in the area. It makes up the lower part of the Quaternary stratoid basaltic rocks of the Afar Depression. The Lower Afar basalt is separated from the upper Quaternary stratoid basalts by the existence of felsic domes and flows and deposition of unconsolidated alluvial sediments.
- **Trachytic Domes and Flows**- This unit occurs in the western, southern and northeastern parts of the study area. The emplacement of the trachytic rocks is controlled by the regional faults which have given rise to the formation of the Rift Valley.
- **Scoria Cones and Flows**- Scoriaceous volcanic cones occur in southeastern, northern and southwestern parts of study area. In southeastern part at Gorgorhi village near Dembel, the scoriaceous rocks are characterized by the presence of holes which can be considered as mega vesicles. The red-brown scoriaceous basalt of the Gorgorhi area is cemented with off-white carbonate material. In the west, vast exposures of scoria occur along the western margin of Shinille Zone east of the Gedamaytu-Gewane asphalted road.
- **Upper Afar Basalt**-The upper basaltic flows of the Afar Depression are widespread in the study area and they are found overlying either on felsic volcanic rocks or on unconsolidated sediments. Rocks of this category are fine-grained and vesicular basaltic layers.
- **Recent Volcanic Rocks** -These rocks occur in the southwestern, northwestern and southeastern parts of Shinille Zone. In all cases, the recent (Holocene) volcanic rocks occur in association with trachytic to rhyolitic rocks and scoriaceous cones and flows. In the southwestern part, the recent volcanic rocks extruded at the intersections of the NNE, NW and EW faults. These rocks are basaltic in composition and appear as fresh lava flows which are devoid of any soil or vegetation.

### 3.2 .4. Unconsolidated Sediments and Lacustrine Deposits

Unconsolidated sediments of Quaternary age occur in several places of the study area. The Quaternary sediments in the area include the thick alluvium of the plains, eluvial soils which commonly occur at the foot of the escarpment, lacustrine sediments, river channel sediments and slope deposits. Travertine beds are commonly encountered in association with the eluvial cover sediments resting on weathered rocks.

- **Eluvium and travertine-** Thin layers of eluvial soil have developed on top of the Tertiary volcanic rocks and Mesozoic sedimentary rocks in the Magala Adi area along the foot of the escarpment. Beds of travertine are reported in the Melka Jebdu and Hurso areas (Tofic Sabat, 2008). In addition, beds of travertine were encountered west of Dire Dawa on the road to Lege Odda along the foot of escarpment. Several beds of travertine are also found in southwestern Shinille Zone on the Miesso-Mulu road, and along seasonal stream channel southwest of Afdem along the road to Alijir.
- **Alluvium-** Thick succession of alluvial deposits cover most parts of the plains of the study area. The thickness of the alluvial deposit is estimated from 100 meters (K. Taddesse, 1982) to 400 m (T. Keleta, 1964). Recent water-well drilling operations (OWWDSE, 2011) indicate the thicknesses of the alluvial deposits to vary from 174 meters in the Biyo Bahi area to the east to more than 250 meters in the central part in Aydora area.

In addition notable amounts of channel deposits, lacustrine deposits, calcrete, and slope deposits (talus) deposits occur in different parts of the area and these are indicated on the geological map of the study area.

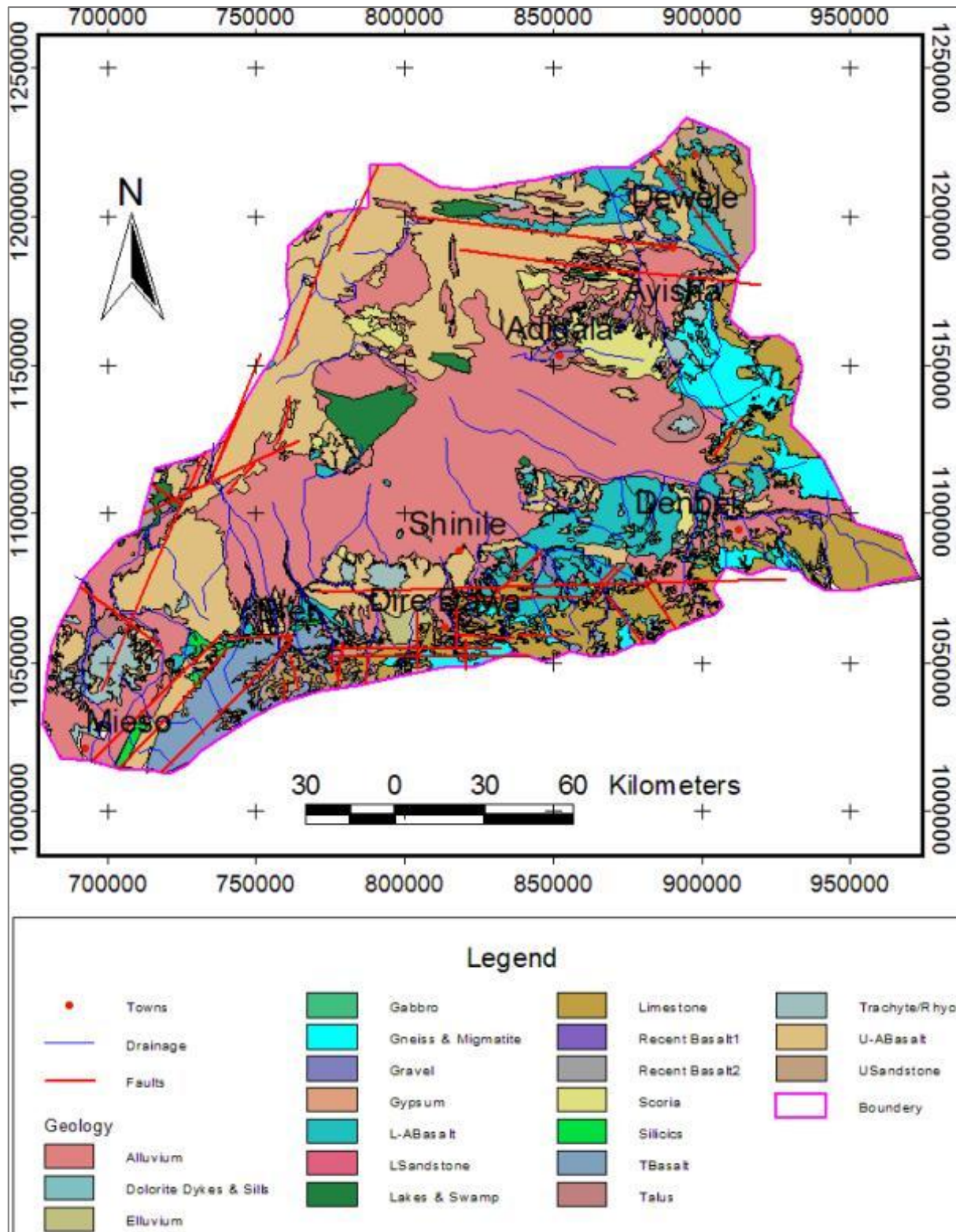


Figure 3.1 Simplified Geological map of the study area (after OWWDSE, 2011).

## 4. HYDROGEOLOGY

### 4.1 General

Ethiopia has huge groundwater potential, mostly localized in the volcanic terrain covered with Quaternary deposits (Tenalem Ayenew, 2006). Morphological configuration of the Ethiopian Rift controls groundwater recharge and discharge situation in and around the rift areas of the country. The higher altitude plateaus marking the East and the West escarpments stand as regional recharge inducing zones whilst the elongated and extensive rift floor behaves as a regional discharge zone. Transverse faults that connect the low lying valley and the surrounding mountains where considerable amount of rainfall is generated are the main conduits of recharge to the arid and semi-arid rift floor. The intersection between NNE and E-W fault systems is considered as a hydrogeological window through which groundwater is channeled to the rift from the mountains (Seifu Kebede and et.al, 2006).

### 4.2 Hydrogeology of the Study Area

Hydrogeology is the study of the relationship between groundwater and geologic formations. The water bearing capacity of geological formations is determined by their porosity and permeability which can be of primary or secondary nature. In general metamorphic and volcanic rocks have little or no primary permeability and they are very poor aquifers unless they are affected by geologic processes such as weathering and tectonism which induce secondary porosity and permeability in which case they can become good aquifers. Unconsolidated sediments have high primary permeability and they can be very good aquifers depending on their grain size. Consolidated sedimentary rocks can also be good aquifers but their water bearing capacity is governed by their degree of cementation and their grain size. Based on these criteria the different types of rock formations occurring in the study area are classified and described below.

#### 4.2.1 Precambrian Rocks

Geological and water works related activity conducted by various individuals and organizations indicate that metamorphic terrain in most parts of Ethiopia is characterized by poor groundwater resources except in areas affected by deep seated secondary fractures (Tamiru Alemayew, 2006, Hambisa Gobena, 1997, MoWR, 2005). In the study area groundwater availability in this terrain

is limited to the areas affected by fractures and fault zones. Generally they are massive and exhibit very low yield and permeability

### **4.2.2 Mesozoic Sediments**

These formations consist of limestone and sandstones. The limestone shows solution cavities, karstification, big fractures and inter-connected sinkholes and the sandstones are mostly fractured with mixed grain sizes. Mesozoic formations in the study area are known to have appreciable quantity of groundwater which is evidenced by many production wells tapping them. Resources Development study for Dire Dawa Administrative Council by WWDSE in 2004 characterized Mesozoic formations as potential aquifers, Haseliso well field and Hurso Military camp water supply wells tap the Mesozoic sandstone where the wells discharge range from 5l/s to 50l/s. Similarly, 156m deep well drilled in 2009 at Biyo Baye village in the study area has two major aquifers; 58m thick basalt and the rest 86m is highly weathered, fractured and altered sandstone which is only partially penetrated. Transmissivity of 440.92m<sup>2</sup>/day and 359.74m<sup>2</sup>/day is obtained from recovery and continuous pumping test respectively (OWWDSE 2010).

### **4.2.3 Volcanic Rocks**

Volcanic rocks occupy considerable part of study area. They are commonly found covering the southern escarpment and highlands, the northern, northwestern and western plain areas. Water bearing capacity of volcanic rocks is mainly governed by the presence of structures such as fractures and joints which induce secondary permeability. As these structures are mainly caused by tectonic processes and the study area is tectonically active because it is located in the Afar depression part of the MER volcanic rocks of the study area are mostly good aquifers. This is mainly true for the basic volcanic rocks since numerous sharp fault escarpments, regional networks of normal faults such as conspicuous horst graben structures mainly having NNE/SSW and EW orientations characterize the volcanic terrain of the area. Basaltic formations in the study area are generally good aquifers and they include Lower Afar stratoid Basalts, Trap Basalts and the Upper Afar Basalts as inferred from various bore hole log data obtained from Alidege plain and some water supply wells drilled in the area. Pump test result for some of these wells shows range of discharge of 4-50l/s depending on the well diameter (OWWDSE, 2011) appendix 2.

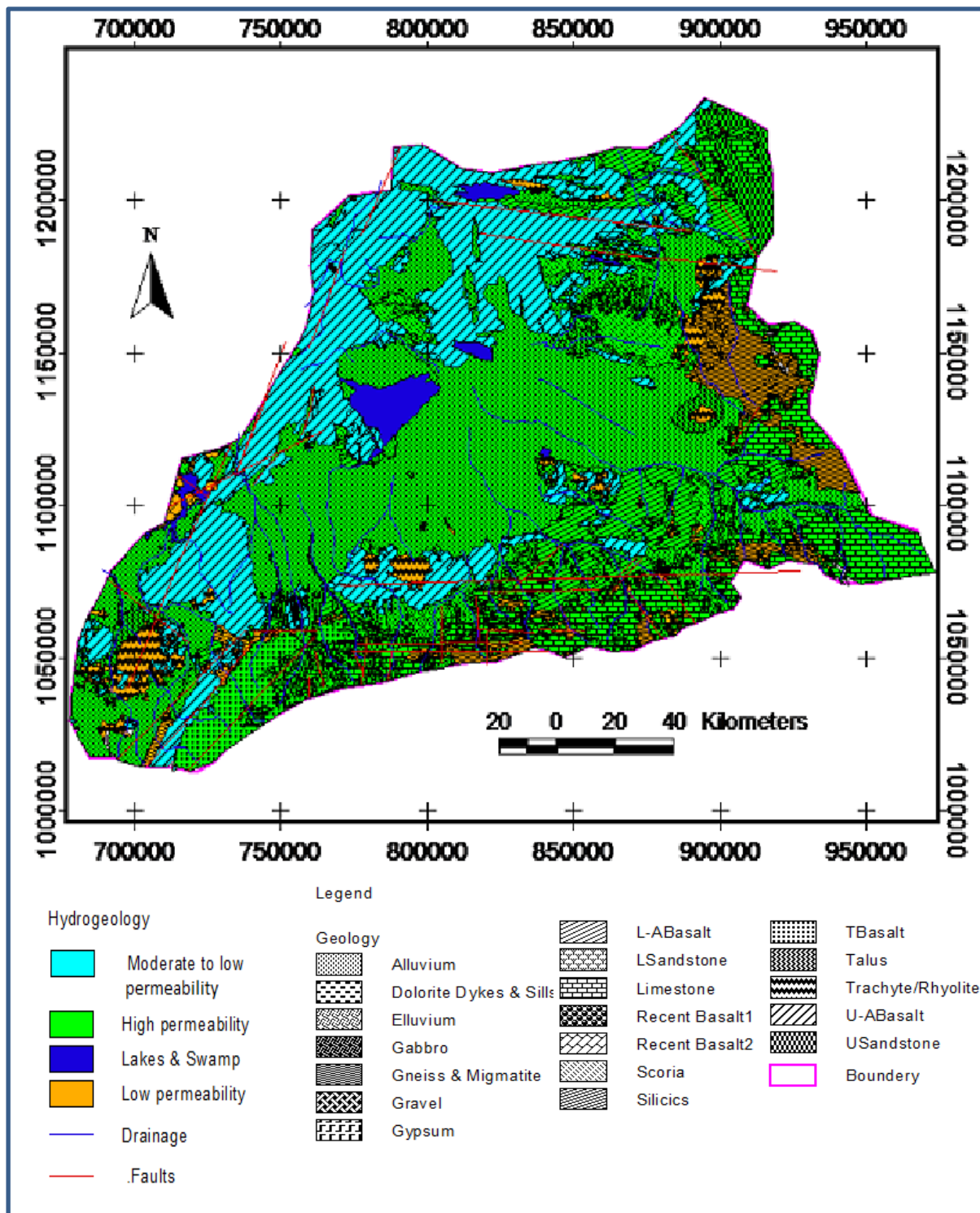


Figure 4.1 Simplified hydrogeological map of the study area (after OWWDSE, 2011)

The acidic volcanic rocks outcropping in Shinile plain are less fractured and less affected by secondary structures to support groundwater circulation and they have very low permeability and poor aquifers contrary to the basic rocks (dominantly basalts) of the study area.

#### **4.2.4 Recent/Quaternary Sediments**

These are the youngest and unconsolidated sediments with inter-granular permeability in the study area. They include alluvial deposits channel deposits and slop deposits. They are the results of erosion and deposition from the surrounding highlands and they cover most part of the low lying plains. Thickness of this formation varies from place to place and some well logs show that it can be greater than 300 meters. Grain size of these sediments decreases towards the north from the foot of the escarpment and this is expected as the coarse grains settle first during deposition. Based on some of the data obtained from wells drilled in these formations they are very good aquifers with high permeability. For instance, boreholes drilled to 150m depth in Afase and Alajer Villages in Afdem area have Transmissivity of  $3,012.48\text{m}^2/\text{day}$  and  $18.46\text{m}^2/\text{day}$  respectively (appendix 2). Simplified hydrogeological map of the study area is shown in figure 4.1.

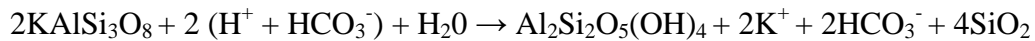
## 5. HYDROGEOCHEMISTRY

### 5.1 General

Hydrogeochemistry is the study of the chemical composition of natural waters. The chemical composition of natural waters results both from natural (geologic) and anthropogenic sources. The types and concentration of different chemical constituents in ground water depends on the processes that affected the water since it fell as rain. Among the factors that determine the level of major and trace elements in water are the content of solute in the original rain, the extent of reaction with rock and soil, loss of constituents by precipitation or absorption and loss of water because of evaporation, transpiration or reaction with minerals. Chemical composition of natural waters varies widely depending up on climate, hydrology and geology in a specific drainage area.

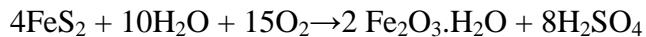
The most common chemical processes or reactions that affect chemistry of natural waters are:-

**Hydrolysis-** which involves reaction between mineral ions and ions of water ( $H^+$  and  $OH^-$ ),



K-feldspar                  carbonic acid;                  kaolinite (clay)                  silica

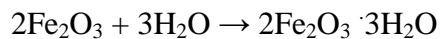
**Oxidation-** which is the reaction that occurs between oxygen and compounds, that is, oxygen is added to minerals and elements,



pyrite                                  limonite                                  sulfuric acid

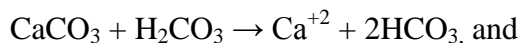
**Reduction-** the removal of oxygen from minerals and elements

**Hydration-** which involves the rigid attachment of  $H^+$  and  $OH^-$  to reacted compounds,

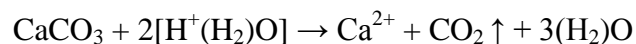


Hematite                          Limonite

**Carbonation-** which is the reaction of carbonate and bicarbonate ions with minerals



**Solution or dissolution-** which is the dissolving of soluble minerals in water or weak acids



Calcium carbonate + Aqueous acid  $\rightarrow$  Calcium ion (soluble) + Carbon dioxide + Water

As rain water infiltrates in to the ground and circulate in different geological media one or more of these reactions take place resulting in different composition of groundwater or hydrochemical facies which are the results of geochemical reactions along ground-water flow paths. This leads to regional variations in water composition that evolve in the direction of flow. In general isoconcentration contours of reacting dissolved constituents drawn on maps of water composition tend to align normal to the direction of ground-water flow (White et al. 1963, Back 1960, 1966). If the concentrations of reacting chemical constituents in water entering the ground vary spatially along the ground water recharge area hydrochemical facies will align parallel to the flow direction. In more complex cases, the concentration of reactive constituents may vary spatially and temporally along the recharge area, and may also evolve along the direction of flow. Thus the study and analysis of hydrochemistry data helps us to understand the sources of the water, recharge and discharge conditions, what kind of geological setting is there, sources and extent of pollution, sources of naturally occurring harmful constituents in the ground water and the chemical changes or evolution that the ground water undergoes from one place to another.

## 5.2 Data Quality

A total of 87 water chemistry data obtained from OWWDSE collected for Shinile zone groundwater potential assessment project are used for this study. Out of the 87 water sample data 46 samples are from boreholes, 30 samples are from hand dug wells, four samples are from springs and the remaining seven samples are from rivers. Location of these samples is more or less evenly distributed in the study area (Figure 5.2). The laboratory analysis results of the hydrochemical data used in this study are presented in annex 1. The hydrochemical analysis and field measured water quality variables (EC, pH) shows wide hydrochemical variations. EC and TDS vary from 313 to 14620 $\mu$ S/cm and 220 to 10700mg/l respectively. In general sodium and bicarbonate represent the dominant cation and anion, respectively. Before these data were used for analysis and interpretation they were checked for quality or accuracy of the laboratory analysis. In general two types of error are encountered in chemical analysis and they are precision or statistical errors which reflect random fluctuation in the analytical procedure and accuracy or systematic errors which indicate systematic deviations due to faulty procedures or interference during analysis. The accuracy of analysis for major ions is checked by using

electron neutrality or charge balance calculation. The charge balance can be calculated for both the cations (positively charged ions) and the anions (negatively charged ions) in units of milliequivalents per liter (meq/L). This unit of measurement takes into account both the differences in gram atomic weight (molar) units of each ion and the valence or charge units for each ion. The meq/L difference is compared using the following equation

$$\text{Error\%} = \left[ \frac{A - B}{\frac{A + B}{2}} \right] * 100$$

Where A is sum of cations in meq/L and B is sum of anions in meq/L.

The error should be within 5% for a high quality analysis. A 10% error is allowed if TDS is less than approximately 100 or more than 5000 mg/l. Accordingly the reaction error or charge balance of the samples is shown in figure 5.1.

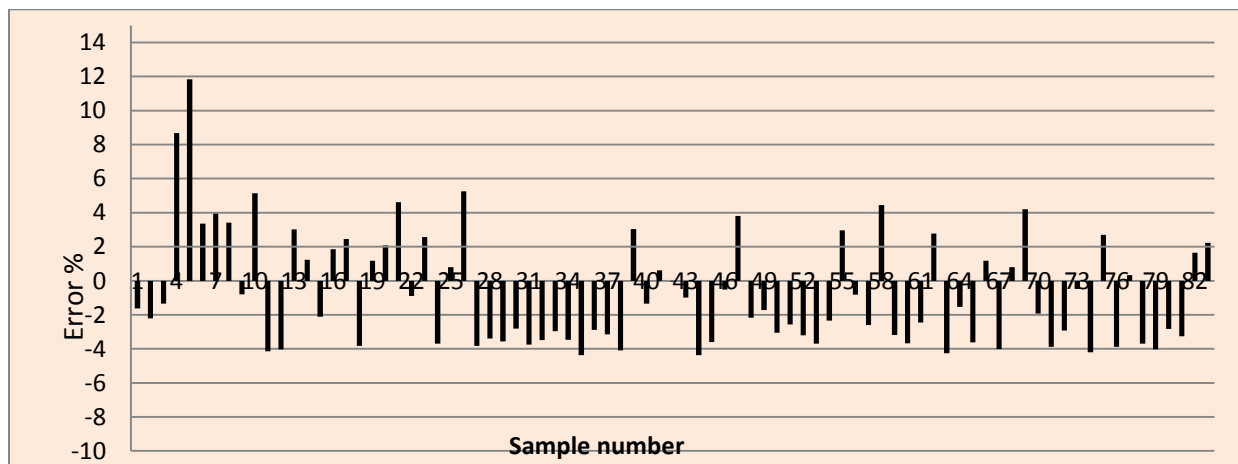


Figure 5.1 Charge balance graph of the water samples.

Even though some systematic error in the data set is observed as revealed by systematic negative reaction error (figure 5.1), this could be the result of overestimation of one or more of the anion compositions or under estimation of one or more of the cation species in the waters and the overall quality of the data is very good since the reaction error for most of the samples are less than 5% except for two samples from bore holes which show reaction error of 8.67 and 11.84 percent.

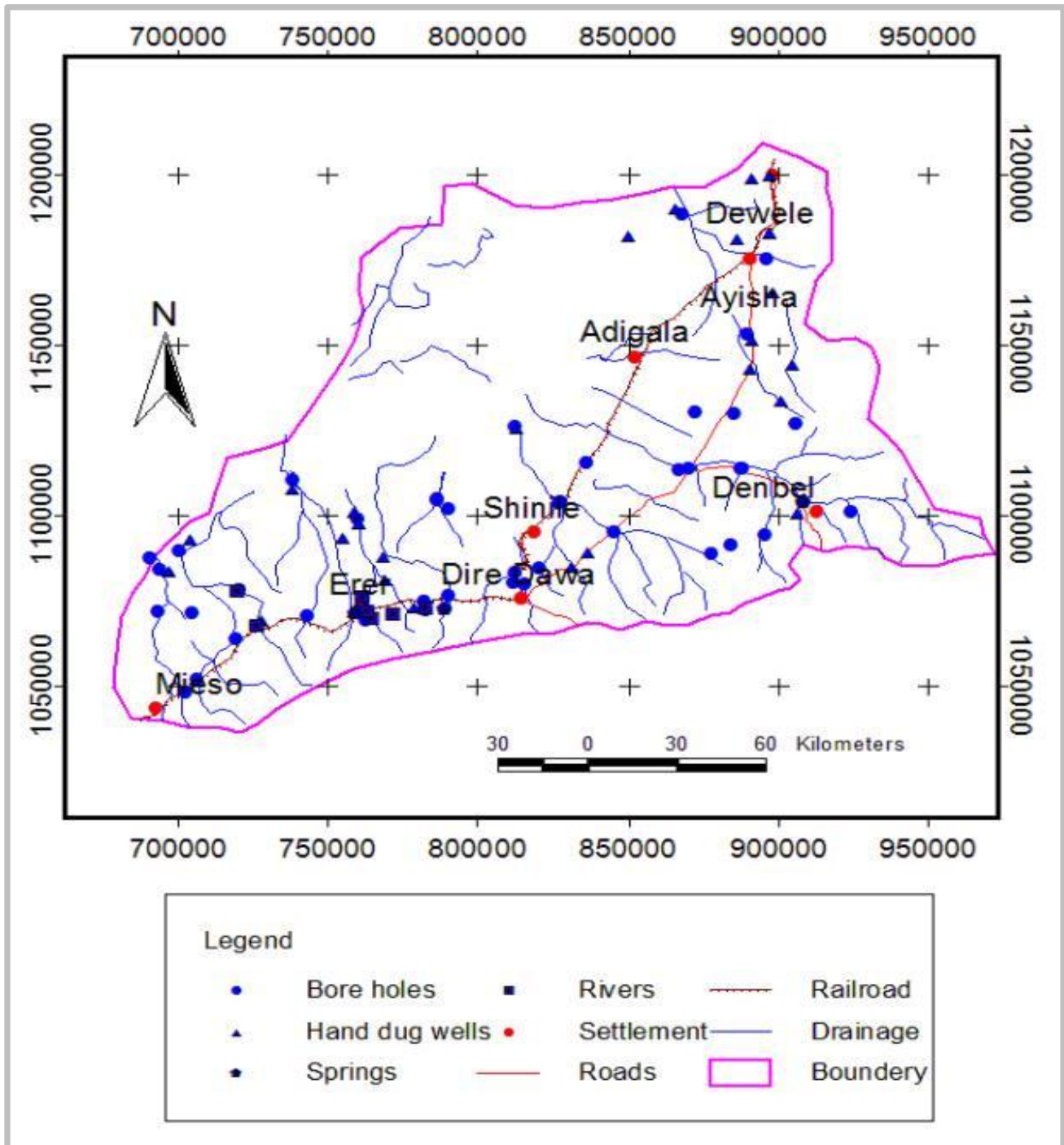


Figure 5.2 Location of the different water samples

### 5.3 Data Analysis

The chemical composition of surface and ground water is controlled by many factors that include composition of precipitation, mineralogy of the watershed and aquifers, climate and topography. These factors combine and create diverse water types that change spatially and temporally. To trace these changes and understand the hydro-chemical evolution of groundwater of the study area from physical and hydrochemical data of the water samples graphical and multivariate statistical methods were used.

The use of major ions as natural tracers (Back, 1966 ) has become a very common method to delineate flow paths in aquifers. Generally the approach is to divide the samples in to hydrochemical facies or water types, that is, groups of water samples with similar chemical characteristics that can then be correlated with location. The spatial variability observed in these natural tracers can provide insight in to aquifer heterogeneity and connectivity as well as the physical and chemical processes controlling water chemistry. Thus a robust classification scheme for partitioning water chemistry samples in to homogenous group can be an important tool for the successful characterization of hydrogeological systems (Guler et al 2002). A variety of graphical and multivariate statistical techniques have been devised since the early 1920s in order to facilitate the classification of waters with the ultimate goal of dividing a group of samples in to homogenous groups each representing a hydrochemical facies. Several graphical and multivariate statistical methods are available for this purpose and some examples are piper diagrams, stiff diagrams and pie diagrams from the graphical methods and hierarchical cluster analysis (HCA) and principal components analysis (PCA) from multivariate statistical methods.

Each of these methods have their advantages and disadvantages when used to present and analyze hydrochemical data. Most of the graphical methods are designed to simultaneously represent the total dissolved solid concentrations and the relative concentrations of certain major ionic species (Hem 1989). Though they can provide easily accessible information about the chemical composition of samples in a group they have serious limitations since they use only major ion concentrations to classify or group samples and they don't consider minor and trace elements which may sometimes behave conservatively in ground waters and be used more efficiently to group the water samples ( Guler *et al* 2002). In addition some of the graphical methods can only display one water sample as a mean value at a time ( Collins bar, pie and stiff

diagrams ) it is impractical to use them for large number of samples. Unlike the graphical methods multivariate statistical methods can use any combinations of chemical and physical parameters to classify water samples but their main limitation is that none of them can provide easily accessible information about the chemical composition of the samples in a group. In this study multivariate statistical method is used in conjunction with multi sample graphical techniques as suggested by Guler et al 2002 to classify and analyze the water samples to understand geochemical evolution of ground water in the study area.

### **5.3.1 Graphical Methods**

#### **5.3.1.1 Piper Diagram**

The Piper diagram is the most widely used graphical form of data presentation. The diagram displays the relative concentrations of the major cations and anions on two separate trilinear plots, together with a central diamond plot where the points from the two trilinear plots are projected. The central diamond-shaped field (quadrilateral field) is used to show overall chemical character of the water.

First all water samples from the four different sources are plotted on piper diagrams together and separately to see if they can be grouped in to distinct hydrochemical facies or water type groups based on their origin or sources. These diagrams can help us see that water type in the study area does not necessarily depend on source of the water, that is, water from bore holes springs, rivers and hand dug wells may have similar composition.

As it can be seen from the plots below the water samples from the different sources are clustered in to Ca-Na-HCO<sub>3</sub>, Ca-HCO<sub>3</sub>, Ca-Mg-HCO<sub>3</sub>, Na-Ca-HCO<sub>3</sub>, Na-HCO<sub>3</sub> with noticeable amounts of SO<sub>4</sub> and Cl and Na-Ca-SO<sub>4</sub>, Na-Ca-Cl, type waters. Ca-Mg-HCO<sub>3</sub> and Ca-HCO<sub>3</sub> type waters are dominant followed by Na-Ca-HCO<sub>3</sub> and Na-HCO<sub>3</sub> type waters. In addition the dominance of Ca, Na and HCO<sub>3</sub> concentration in waters of the study area is clearly observed from the piper plots. Ca-HCO<sub>3</sub> and Ca-Mg-HCO<sub>3</sub> types of waters are the dominant water type in the study area. Geochemical groundwater evolution analysis in different parts of the world reveal that these type of waters are often regarded as recharge area waters at their early stage of geochemical evolution draining basic volcanic rocks like basalts (Plummer et al., 1990; Adams et al., 2001; Ayenew et al., 2009).

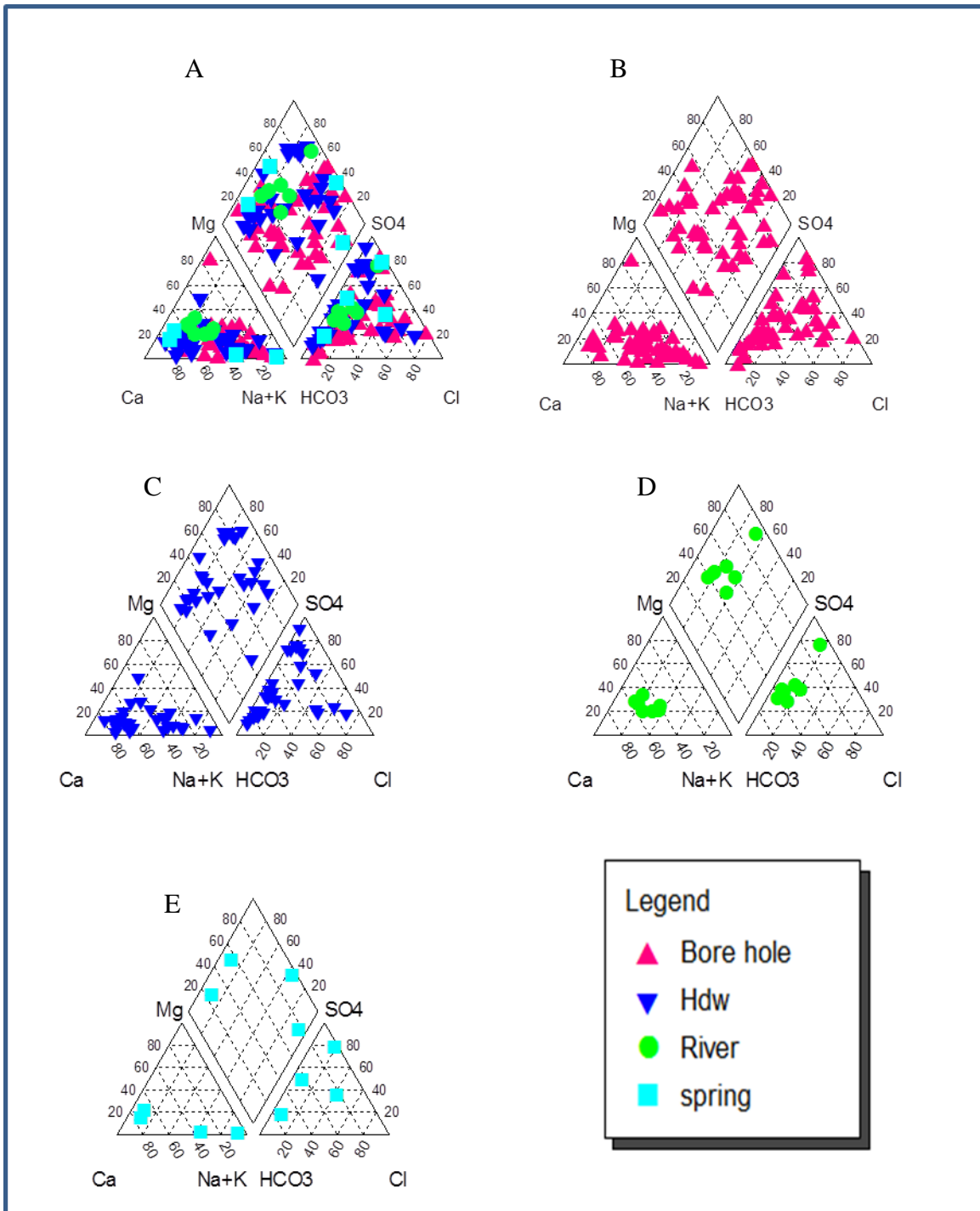


Figure 5.3 piper plots: A= all water samples, B= borehole waters, C= HDW waters, D= river waters and E= spring waters.

Na-Ca-HCO<sub>3</sub> and Na-Ca-Mg-HCO<sub>3</sub> type waters are the second dominant water type in the study area. This water types have relatively higher TDS and more concentrated when compared to the Ca-HCO<sub>3</sub> and Ca-Mg-HCO<sub>3</sub> type waters. According to (Demile et al. 2007) these types of waters are weakly mineralized waters that drain acidic volcanic rocks like rhyolites, trachytes, ignimbrite and tuff.

Piper plots of the water samples also show that Na-Ca-SO<sub>4</sub>, Na-Cl-SO<sub>4</sub>, Na-HCO<sub>3</sub>-SO<sub>4</sub> and Na-Ca-HCO<sub>3</sub>-SO<sub>4</sub> types of water are common in the study area. These types of waters are usually the results of water rock interaction with sedimentary deposits like evaporites and lacustrine deposits.

### **5.3.1.2 Pie Chart and Stiff Diagrams**

Pie charts and Stiff diagrams are very good to present individual water samples that can easily be recognized based on their major ion compositions. In this study they are used to present and interpret the mean group samples of the five water groups that are obtained using Q-mode statistical cluster analysis or HCA. Pie diagrams are easy to construct and present relative major ion composition in percent milliequivalents per liter (relative %meq/l).

#### **5.3.1.2.1 Results of the pie chart plots**

From pie charts of the mean samples of the five groups obtained by HCA presented in figure 5.4 we can identify some major ion concentration differences that might have played a role in classification of the water samples in to five groups by the hierarchical cluster analysis method. Group one samples have the highest percentage of Ca and bicarbonate when compared to the other four groups. This could be because water samples clustered in this group are recharge area waters draining basic volcanic aquifers like basalts or carbonate rocks like limestone and dolomite with short residence time in the ground. Water samples clustered in to group two are characterized by decrease in percentage of Ca and bicarbonate and increase in percentage of Na and Cl with no significant change in percentage concentrations of the other major ions. This is probably because water samples clustered in to group two are the result of change in concentration of group one waters along their flow path by replacement of Ca ions by Na or waters of this group may be recharge area waters draining volcanic rocks rich in feldspars like

rhyolite. Water samples of group three are identified by marked increase in their percentage of  $\text{SO}_4^{2-}$  concentration and decrease in that of their  $\text{HCO}_3^-$  and they are probably the result of dissolution of evaporite sediments like gypsum by group one and two waters. Group four waters are distinguished by very low percentage of  $\text{Mg}^{2+}$  and significant increase in their percentage concentration of  $\text{Na}^+$  and  $\text{SO}_4^{2-}$  and they may represent water coming from deeper source since most of the members of this group are thermal springs. The water sample clustered in group five has the highest percentage of Na and Cl and its bicarbonate concentration percentage is very small. This can be a highly evolved ground water dissolving local evaporite sediments on the rift floor like halite.

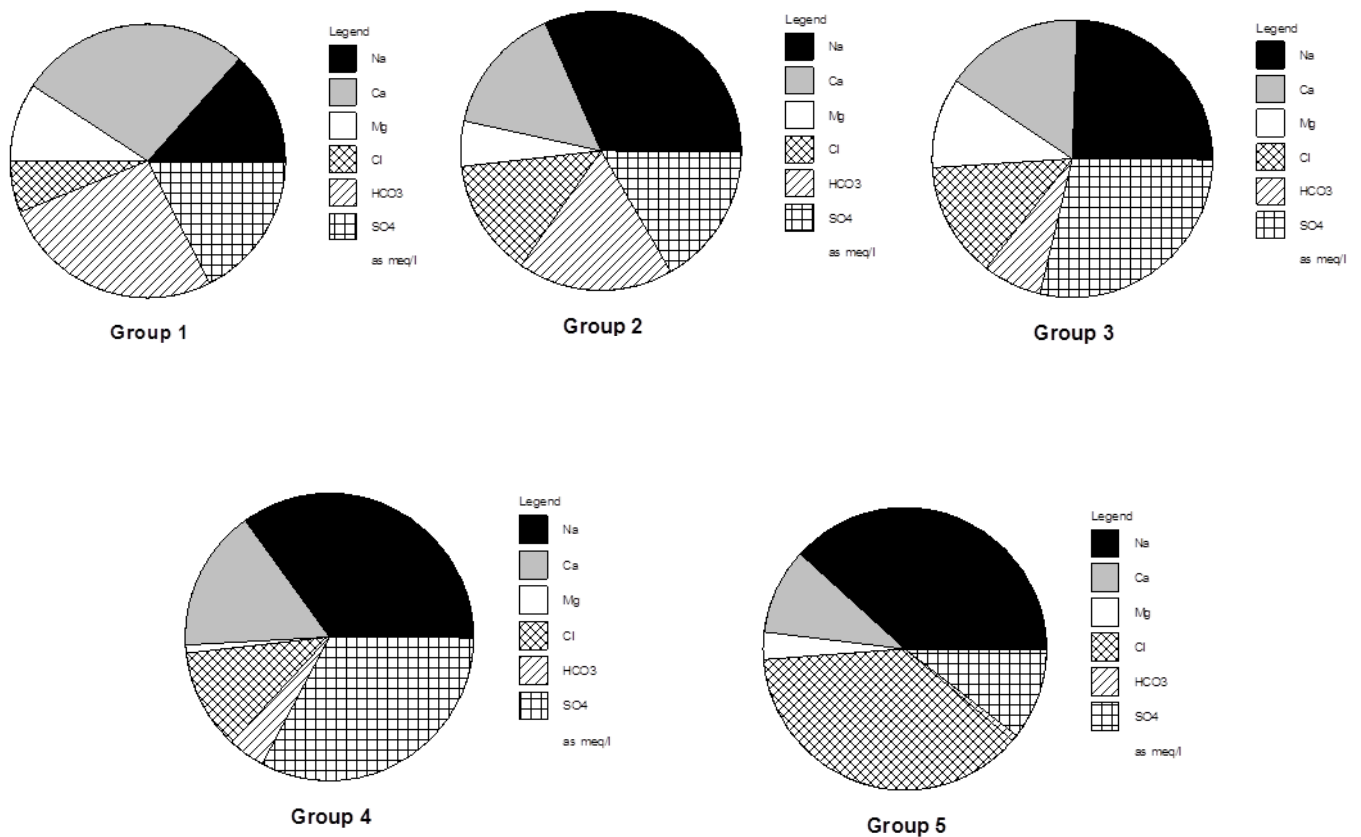


Figure 5.4 Pie diagrams of the group mean samples of the five water groups obtained from HCA.

### 5.3.1.2.1 Results of the Stiff diagram plots

The Stiff pattern diagram is a polygon that is created from three (or four) parallel horizontal axes extending on either side of a vertical zero axis (Stiff 1951). In this diagram, cations are plotted on the left of the axes and anions are plotted on the right, in units of milliequivalents per liter (meq/l). The Stiff diagrams are useful for making visual comparison of waters with different characteristics. As the actual concentration of water samples are used when plotting Stiff diagrams they are presented below in figure 5.5 to show variations in concentration between the five water groups obtained by HCA.

Water samples clustered in groups one and two have very low concentration of all the major ions when compared to the water samples in the other three groups which indicates they are dilute ground waters at their early stage of geochemical evolution that have not undergone significant water rock interaction. The difference between these two groups of water is that waters of group 2 have higher sodium and lower calcium concentration. This may indicate that waters of the two groups interact with different rock types after their recharge or that group two waters are the result of evolution of group one waters at its early stage. According to (Demile *et al.* 2007) Na-Ca-HCO<sub>3</sub> and Ca-Na-HCO<sub>3</sub> types of waters are weakly mineralized waters that drain volcanic rocks like rhyolites, trachytes, ignimbrite and tuff. But Ca-HCO<sub>3</sub> and Ca-Mg-HCO<sub>3</sub> types of waters are usually the result of water rock interaction at its early stage with Ca and Mg rich basic volcanic rocks like basalts and scoria. But they can also be ground water at an early stage of interaction with carbonate rocks like limestone which are commonly found outcropping along the escarpment in the study area.

It is clearly seen from the stiff diagrams below the remaining three water groups show a pronounced increase in salinity when compared to the above two groups of water. Group three waters show significant amount of increase in concentrations of all the major cations and anions. Group four waters also show a significant amount of increase in their concentrations of Na, Ca, Cl and SO<sub>4</sub> but their concentration of Mg and HCO<sub>3</sub> is almost the same as that of the members of group one and two. This may indicate that group three waters can be the result of geochemical evolution of waters of group one and two while group 4 waters may be ground waters with

different history of geochemical evolution and they can be ground waters related to deeper thermal source that passes through metamorphic rocks in the study area.

Group five water, that is put in a group of its own by the HCA shows interesting hydrochemical characteristics. It is ground water of very high salinity. Concentration of this water is approximately five to six times that of the water samples clustered in the other groups which can be observed from the scale of the stiff diagram used to plot its concentration. This water has extremely high concentration of Na and Cl when compared to the other cations and anions and its bicarbonate concentration is very small. This water can be water from deeper source dissolving a localized deposit of the evaporite like sodium chloride.

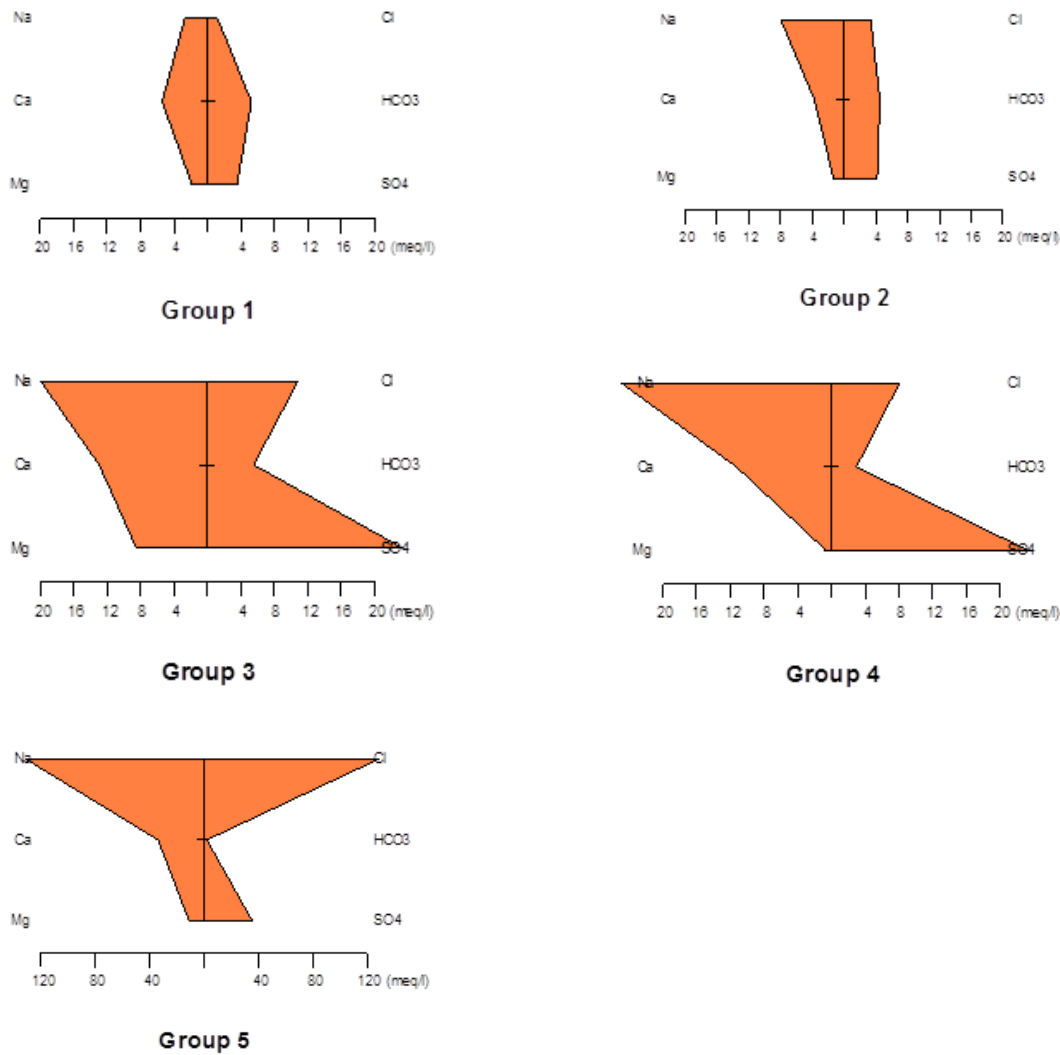


Figure 5.5 Stiff pattern diagrams of group mean samples of the five water groups obtained from HCA.

## 5.3.2 Multivariate Statistical Methods

### 5.3.2.1 Hierarchical Cluster Analysis

Multivariate statistics can be used to evaluate large amount of data in order to decipher patterns within the data set that otherwise might not be observed. Classifications of samples according to their parameters are known as Q-mode classifications. In this study Q-mode hierarchical cluster analysis (HCA) was used to classify the samples into distinct hydrochemical groups. HCA is a multivariate statistical technique used to classify hydrochemical observations so that the members of the resulting groups or subgroups are similar to each other and distinct from the other groups. The characteristics of the groups or sub-groups are not predetermined but can be obtained after the classification. The results obtained in HCA are justified according to their values in interpreting the data and in indicating realistic hydrochemical patterns representing field conditions. It is therefore not the number of members of a group that determines the robustness of HCA. It is possible that many single member groups that do not belong to any of the multi-member groups are placed in separate groups.

Eleven hydrochemical variables (consisting of EC, pH, Ca, Mg, Na, K, Cl, SO<sub>4</sub>, HCO<sub>3</sub>, F and NO<sub>3</sub>) were utilized in this analysis. TDS values are not used to avoid redundancy because they are directly correlated with EC. Prior to any multivariate statistical analyses, the data were arranged in an ( $n \times p$ ) matrix, representing the number of samples ( $n$ ), including bore holes, hand dug wells, rivers and springs, and the number of variables ( $p$ ), including major ions, F and EC. The elements of the data matrix ( $x_i, j$ ) consisted of the concentration of the  $j$ th hydrogeochemical constituent measured in the  $i$ th groundwater sample. The data is log transformed and a standardized data matrix was then generated by mean subtraction followed by division by the column standard deviation in order to reduce or restrict the influence caused by the variables that have the greatest or the smallest variances or magnitudes on the clustering result and assign equal weight to all variables. A detailed description of the advantages and uses of the HCA in hydrochemistry and the mathematical formulation behind HCA is thoroughly discussed in Güler et al. (2002).

Although there are a number of hierarchical clustering techniques, all of which are regularly applied to the earth sciences, the most widely used measure of ordering is Ward's criterion, which uses an analysis of variance approach that minimizes the sum of squares within the clusters and maximizes the variance between separate clusters based on Euclidean or straight line distance (Ward, 1963). After trying with the different HCA methods in this study the use of Ward's criterion produced the best result by clustering samples with similar hydrochemical composition together and identifying outlier samples with distinct composition in to separate groups. Accordingly the 87 water samples are clustered in to five groups which are shown in figure 5.6.

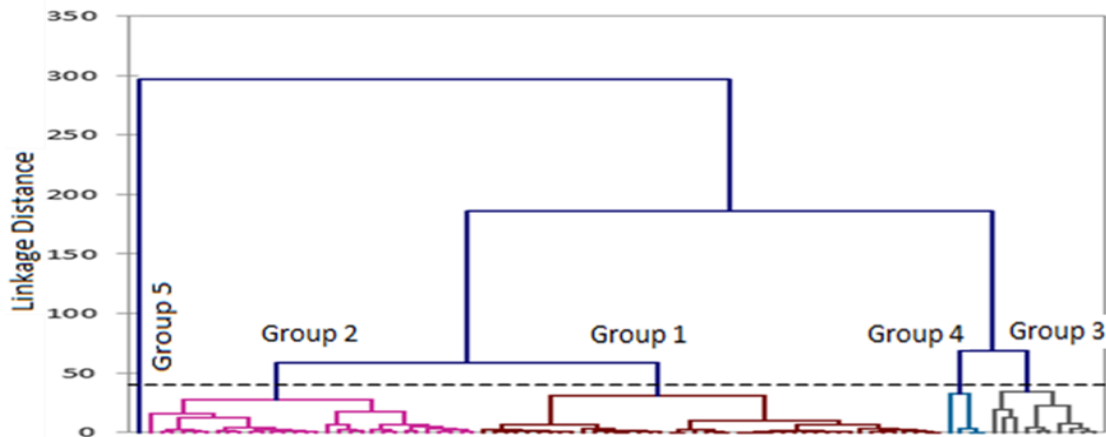


Figure 5.6 Dendrogram of the Q-mode hierarchical cluster analysis.

### 5.3.2.1.1 Results of the HCA

The dendrogram resulting from hierarchical cluster analysis (Fig. 5.6) displays the presence of five clusters. The water samples from bore holes, hand dug wells, springs and rivers are grouped according to the similarity of their hydrogeochemical compositions. The samples clustered under each group and the average values for each of the hydrochemical composition are presented in Table 1. The average values for each of the composition of the groups produced by the hierarchical cluster analysis reveal trends between them and they are the basis for the distinction of the subgroups.

Table 1 Mean concentrations (unit in mg/l except for EC in  $\mu\text{S}/\text{cm}$ ) for the groups derived from HCA

Water group	EC	TDS	PH	Na	K	Mg	Ca	Cl	SO4	HCO3	NO3	F
Group 1 (n=42)	930.8	622.62	7.5998	62.1	3.11	22	108.5	43.12	168.7	321.2	27.69	1.088
Group 2 (n=30)	1268	851.13	8.1197	182	6.71	16	74.54	120.4	201	274.8	67.29	1.626
Group 3 (n=10)	3830	2637.2	7.514	458	9.43	103	259.2	386.3	1123	339.6	19.84	1.263
Group 4 (n=4)	3508	2377.5	7.5425	571	15.9	7.8	225.7	284.5	1121	179.8	2.21	6.95
Group 5 (n=1)	14620	10700	7.7	3000	18	129	668.8	4560	1720	153	510	7.1

Numbers in parenthesis indicate the number of samples in each group

Water samples clustered in to group 1 generally have lower TDS and EC when compared to the other groups. They also show higher values of Ca, Mg, and HCO<sub>3</sub> compared to the members of group 2. Thus this group of water is seemed to be separated from the others based on the lower value of EC and higher concentrations of Ca, Mg, and HCO<sub>3</sub> of its members by the HCA. Group 2 samples also have lower TDS and EC like group 1 compared to the other three groups but they show higher value of PH, Na, NO<sub>3</sub> and Cl and low concentration of Ca unlike group one samples and this seems to be the basis for separation of the two groups from each other by the HCA. The main differences between members of group three and four are concentrations of Mg, NO<sub>3</sub> and HCO<sub>3</sub> which is much higher for group three and concentration of fluoride which is very high in group four samples. These are clearly the basis for separation between group three and four in addition to the higher value of EC in group three samples. Only one water sample is clustered in group five by the HCA and this is because the water sample is different from all the other water samples in its very high concentration of most of the major ions and this sample has the highest EC of all the water samples used for this study. A detailed description of the location, water type and geochemical evolution of the water samples clustered in to the five groups is given in table 2. Piper diagram of the water samples clustered in to the five groups by HCA showing the different water types in each group is given in figure 5.7 below.

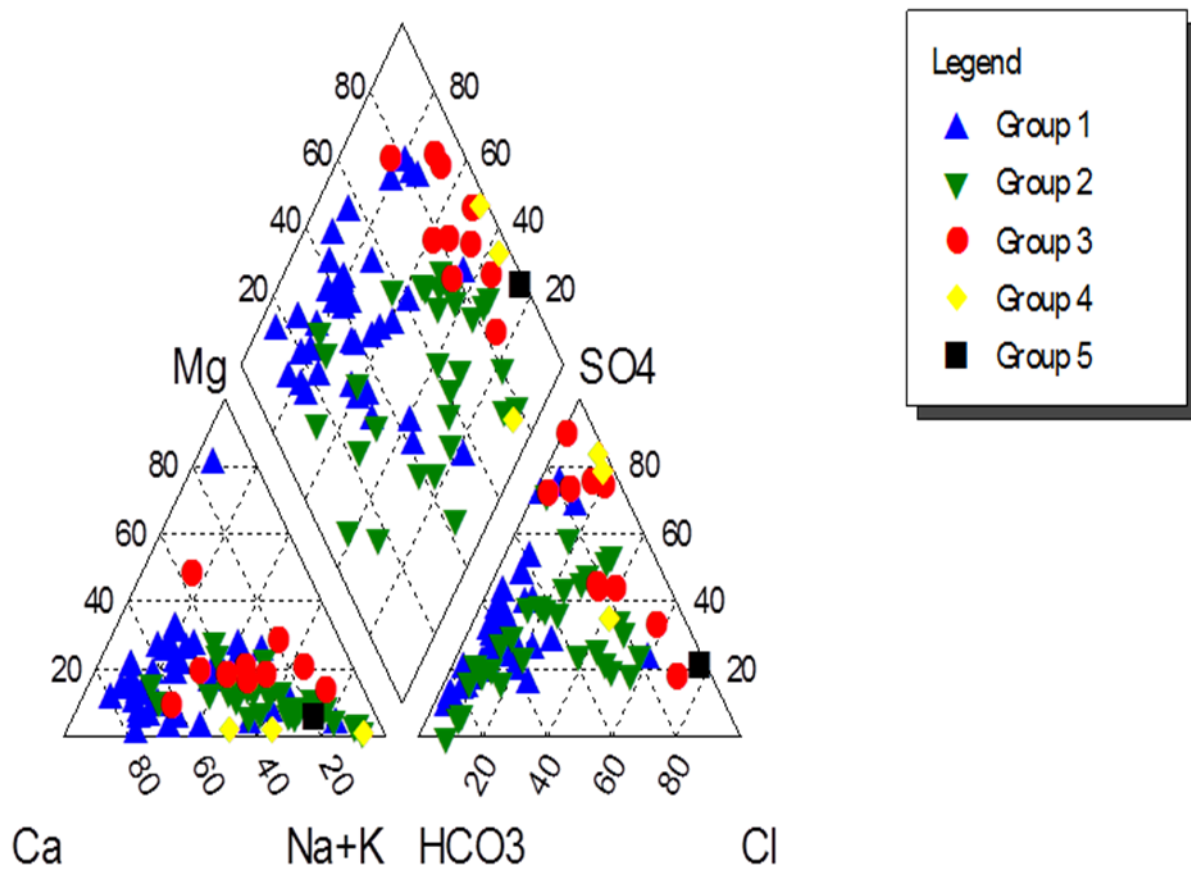


Figure 5.7 Piper diagram of water samples clustered into five groups by HCA.

Table 2 Description of water cluster groups (Numbers in the superscript indicate the number of samples of the group).

Cluster group	Description and interpretation
1 <sup>42</sup>	This group consists of samples from 18 bore holes, 17 hand dug wells, 5 rivers and 2 springs. They are characterized by low PH and very dilute chemistry ( $378\mu\text{S}/\text{cm} < \text{EC} < 1744\mu\text{S}/\text{cm}$ ). They are mostly Ca -HCO <sub>3</sub> , Ca-Mg-HCO <sub>3</sub> , Ca-Mg-Na-HCO <sub>3</sub> and Ca-Mg-HCO <sub>3</sub> -SO <sub>4</sub> types of water with subordinate amounts of SO <sub>4</sub> . They are generally found at higher elevations on the plateau and along the escarpment at the southern margin of the study area. Few members of this group are found on the rift floor and this could be the result of fault or fracture controlled shallow and fast ground water flow. The dominance of Ca and Mg in this group of water with their low value of EC suggest that they are recharge area waters that have not undergone pronounced rock water interactions in basic volcanic rocks or carbonate terrain and the existence of somewhat higher sulfate in these waters can be explained by concentration due to evaporation which is common in arid and semi-arid areas and/or by the existence of gypsum deposits found outcropping at some places along the escarpment.
2 <sup>30</sup>	This group consists of samples from 20 bore holes, 9 hand dug wells and 1 river. They are characterized by high PH and relatively higher concentration or salinity ( $313\mu\text{S}/\text{cm} < \text{EC} < 2520\mu\text{S}/\text{cm}$ ). Most of the samples in this group are Na-Ca-HCO <sub>3</sub> , Na-Ca-Mg-HCO <sub>3</sub> , Na-HCO <sub>3</sub> , Na-Ca-HCO <sub>3</sub> -SO <sub>4</sub> and Na-Ca-HCO <sub>3</sub> -SO <sub>4</sub> -Cl type waters. They are mostly located at southwestern and northeastern part of the study area but some members of this group are also found on the rift floor. The dominance of Na and general increase in salinity and EC of this group may indicate greater rock water interaction than group one. So this water group can be the result of evolution of group one waters along their flow path or they can be waters from different rock formation like trachyte and silicic volcanic rocks but with greater rock water interaction than the group one waters along their own flow path. The increase in concentration of Cl and SO <sub>4</sub> can be by enrichment from evaporation and dissolution of evaporite sediments.
3 <sup>10</sup>	This group consists of samples from 5 bore holes 4 hand dug wells and one river. They are characterized by moderately high PH very high salinity ( $3830\mu\text{S}/\text{cm} < \text{EC} < 6430\mu\text{S}/\text{cm}$ ) and they are Ca-Na-SO <sub>4</sub> , Mg-Ca-SO <sub>4</sub> -HCO <sub>3</sub> and Na-Mg-Cl-SO <sub>4</sub> types of water. Members of this group are all found on the rift floor. The very high EC of this group indicates that they are evolved ground waters with significant rock water interaction and they are the result of evolution of group one and two waters. The increase in concentration of SO <sub>4</sub> and Cl is from dissolution of evaporites common on the rift floor and the decrease in concentration of HCO <sub>3</sub> in this group can be explained by precipitation of calcite after saturation that takes out the bicarbonate ions.
4 <sup>4</sup>	This group consists of 2 hot springs and 2 bore holes samples. They are characterized by moderately high PH and high salinity ( $3240\mu\text{S}/\text{cm} < \text{EC} < 3870\mu\text{S}/\text{cm}$ ). The water type of the springs is Na-Ca-SO <sub>4</sub> and that of the bore holes is Na-Cl-SO <sub>4</sub> -HCO <sub>3</sub> . Samples of this group are localized in two places at the south western and south eastern part of the study area on the escarpment. Waters of this group are thermal waters from deeper aquifer where there is abundance of sulfur.
5 <sup>1</sup>	This group has only one sample and it is from a deep well at the center of the study area on the rift floor. This sample is characterized by moderately high PH and extremely high salinity ( $\text{EC} = 14620\mu\text{S}/\text{cm}$ ) The water type is Na-Cl-SO <sub>4</sub> and this could be the result of dissolution of a localized bed of evaporite deposit like halite. It is clear that the source of the evaporite deposit that caused high salinity of this sample is not found at a shallow depth because one sample from a hand dug well located very close to this bore hole is included in this study and it is grouped with water samples of group three which are relatively fresh and it has a different water type which is Ca-Na-SO <sub>4</sub> .

### 5.3.2.2 Principal Components Analysis

Factor analysis and principal components analysis are multivariate analytical techniques which are used to extract a subset of variables called factors that explain the variance observed in the original dataset. Factor analysis derives a subset of uncorrelated variables that explain the variance observed in the original dataset (Anazawa and Ohmori, 2005; Brown, 1998). In technical terms, common factor analysis represents the common variance of variables, excluding unique variance, and is thus a correlation-focused approach seeking to reproduce the inter-correlation among the variables. On the other hand, components (from PCA) reflect both common and unique variance of the variables and may be seen as a variance-focused approach that reproduces both the total variable variance with all components as well as the correlations. For this purpose PCA is far more commonly used than factor analysis (FA). However, it is common to use “factors” interchangeably with “components” in multivariate analysis. Factor analysis can be performed on any kind of scientific data to establish a pattern of variation among variables or reduce large data sets into factors for easy handling and interpretation. Because PCA is simply the generation of pairs of eigenvalues and eigenvectors, the data do not need to be normally distributed (Johnson and Wichern, 2002). Eigenvalues describe the amount of variation within the original data set explained by each principal component.

The total number of factors generated from a typical factor analysis indicates the total number of possible sources of variation in the data. Factors are ranked in order of merit. The first factor or component has the highest eigenvector sum and represents the most important source of variation in the data. The last factor is the least important process contributing to the chemical variation. Often the population variability for large data sets, such as those with large numbers of samples and variables, can be attributed to the first one, two, or three components (Johnson and Wichern, 2002). Factor loadings on the factor loadings tables are interpreted as correlation coefficients between the variables and the factors. In this study PCA was used to extract the principal factors corresponding to the different sources of variation in hydrochemistry of the study area.

Correlation coefficient is commonly used to measure and establish the relationship between two variables. It is a simplified statistical tool to show the degree of dependency of one variable to

the other. The correlation matrix of the eleven variables used for analysis that was generated by the PCA has been presented in Table 3.

Table 3 Correlation coefficient among hydrochemical parameters

Variable	EC	PH	Na	K	Ca	Mg	F	Cl	NO <sub>3</sub>	HCO <sub>3</sub>	SO <sub>4</sub>
<b>EC</b>	<b>1</b>										
<b>PH</b>	-0.140	<b>1</b>									
<b>Na</b>	0.960	-0.001	<b>1</b>								
<b>K</b>	0.429	-0.041	0.443	<b>1</b>							
<b>Ca</b>	0.781	-0.388	0.614	0.149	<b>1</b>						
<b>Mg</b>	0.624	-0.237	0.470	0.253	0.542	<b>1</b>					
<b>F</b>	0.495	-0.002	0.538	0.396	0.362	-0.045	<b>1</b>				
<b>Cl</b>	0.876	-0.036	0.916	0.366	0.604	0.438	0.418	<b>1</b>			
<b>NO<sub>3</sub></b>	0.558	0.075	0.631	0.109	0.347	0.137	0.201	0.690	<b>1</b>		
<b>HCO<sub>3</sub></b>	-0.039	-0.247	-0.054	0.074	-0.143	0.270	-0.271	-0.114	-0.087	<b>1</b>	
<b>SO<sub>4</sub></b>	0.787	-0.204	0.651	0.315	0.781	0.623	0.432	0.415	0.160	-0.096	<b>1</b>

### 5.3.2.2.1 Results of the Principal Components Analysis

The EC values exhibit high positive correlation with Ca, Mg, Na, Cl, SO<sub>4</sub> and NO<sub>3</sub>. Sulfate shows high positive correlation with Calcium and magnesium, 0.781 and 0.623 indicating common source of origin like dissolution of gypsum or anhydrite. Cl and Na possess a very good positive correlation (0.916) between each other. The high Na and Cl contents detected in certain samples may suggest the dissolution of chloride salts. Cl also shows strong correlation with NO<sub>3</sub> (0.69) this may indicate nitrate and some of the chloride could be from some common source like pollution of the ground water from anthropogenic effects like the use of fertilizers and pesticides. In addition Na show a strong positive correlation with Ca, F, K and Mg (0.614, 0.538, 0.443 and 0.470) respectively and this indicates that some of these constituents might have come from a common source like hydrolysis of silicate minerals.

The results obtained from the principal components analysis is presented in table 4 for the first three principal components which together account for 72.85% of the total variance in the hydrochemistry. Figure 5.8 shows factor loadings of the eleven variables for PC 1 and PC 2. PC1 represents about 46.99% of the variance and has high absolute loadings for EC, Ca, Mg, Na, K, F, SO<sub>4</sub> and Cl and probably represent dissolution reaction of carbonates and evaporite sediments

by ground water in the area. PC 2, which accounts for 15.29% of the total variance in hydrochemistry, contains high absolute loadings for pH, Mg, and HCO<sub>3</sub>; probably represent silicate hydrolysis reaction of volcanic rocks. PC3 which account for 10.58% of the variance in hydrochemistry contain high absolute loadings for NO<sub>3</sub> and HCO<sub>3</sub> and probably represent addition of contaminants to the ground water from anthropogenic sources like the use of fertilizers for agriculture.

Table 4 PCA factor loadings matrix

<b>variables</b>	<b>PC1</b>	<b>PC2</b>	<b>PC3</b>
<b>EC</b>	0.990	-0.013	0.055
<b>PH</b>	-0.180	0.663	0.249
<b>Na</b>	0.940	0.178	0.170
<b>K</b>	0.472	0.037	-0.045
<b>Ca</b>	0.810	-0.228	-0.265
<b>Mg</b>	0.616	-0.576	0.153
<b>F</b>	0.549	0.411	-0.455
<b>Cl</b>	0.870	0.218	0.292
<b>NO3</b>	0.574	0.368	0.530
<b>HCO3</b>	-0.080	-0.643	0.510
<b>SO4</b>	0.789	-0.243	-0.376
<b>Eigenvalue</b>	5.169	1.682	1.163
<b>Variability(%)</b>	46.994	15.289	10.576
<b>Cumulative%</b>	46.994	62.283	72.859

Figure 5.9 show the projection of the two PC scores (PC1 vs. PC2) for all the water samples of the study area in a 2D scatter-plot. According to Belkhiri L. *et al.* 2011 Compact PC distributions for majority of the water samples within groups suggest that all the water samples in their respective groups have similar chemistries hence similar flow paths or sources. This is true in the case of the five water groups of the study area identified by the HCA. Most of the water samples of the study area in each group are well separated in the PC space and compactly distributed within their respective groups indicating continuous variation of chemical properties of the samples. If distribution of the samples in the PC space is broad it may indicate changes in the water chemistry due to processes such as a source of contamination, dilution or abrupt changes in vertical-horizontal connectivity of the aquifer. As one can see from figure 5.9 this is not true for most of the water samples of the study area and distribution of the water groups in the PC space confirms the HCA classification.

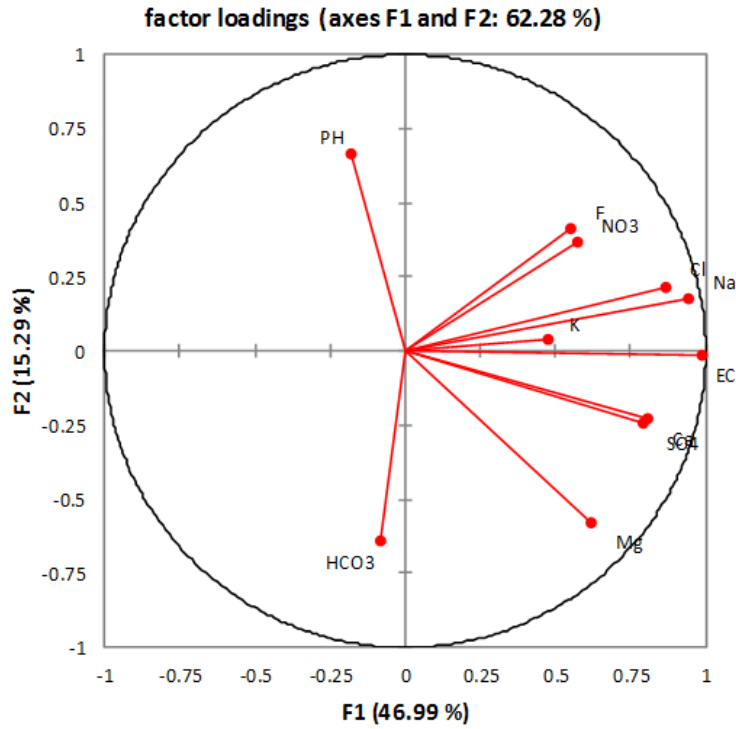


Figure 5.8 Factor loadings of the variables.

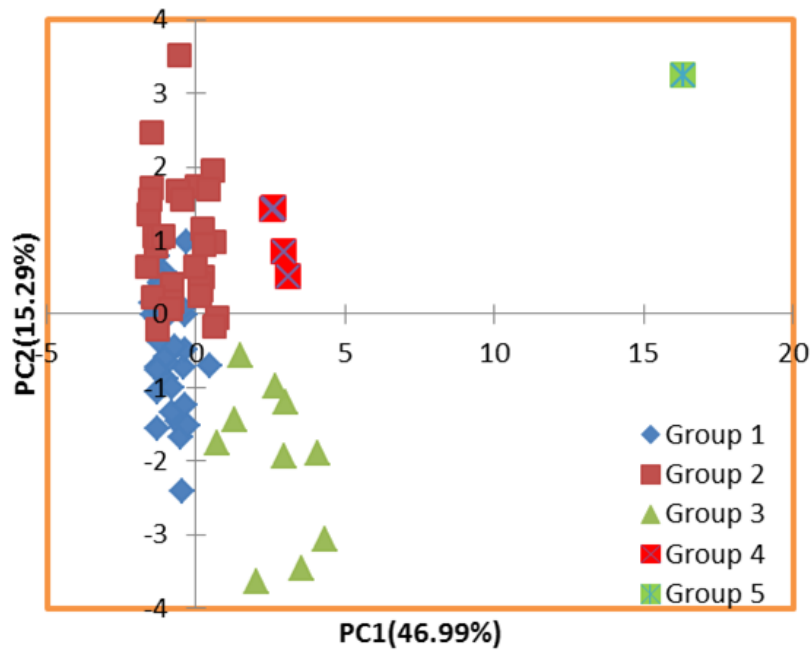


Figure 5.9 Plots of PC scores for PC1 versus PC2.

## 5.4 Evolution and Spatial Variation of hydrochemistry

Figure 5.10 shows the spatial distribution of the five cluster groups. The relationship between the statistically defined clusters of samples and geographic location was prepared by plotting group values for each sample. The five groups are separated geographically, as well as physiographically with good correspondence between spatial locations and the HCA results. Samples that belong to the same group are located in close proximity to one another suggesting more or less the same hydrogeochemical processes (evolution) and/or flow paths. The high degree of spatial and statistical coherence suggests that the changes between the principal hydrochemical facies define the hydrochemical evolution of ground water in the study area with distinct spatial patterns representing the rift floor, escarpment and highlands.

Most of the group one waters which have low TDS (average=622.62mg/l) and mainly composed of Ca-HCO<sub>3</sub>, Ca-Mg-HCO<sub>3</sub> and Ca-Na-Mg-HCO<sub>3</sub> water types with subordinate amount of SO<sub>4</sub> and Cl representing recharge area ground waters at their early stage of hydrochemical evolution draining basic volcanic rocks or carbonate sedimentary rocks are located on the highland and escarpment at the southern and south eastern part of the study area. Few members of this group are found in limited areas at the western and north eastern part of the study area on the rift floor and this could be the result of fault or fracture controlled shallow and fast ground water flow to those areas from the highland and escarpment.

Group two waters have relatively higher TDS compared to group one (average=851.13mg/l) and they are mainly composed of Na-HCO<sub>3</sub>, Na-Ca-HCO<sub>3</sub> and Na-Ca-HCO<sub>3</sub>-SO<sub>4</sub> type waters with higher amounts of SO<sub>4</sub> and Cl than group one. Members of this group probably represent ground water evolved from group one waters or recharge area waters draining silicic volcanic rocks, Mesozoic and quaternary sediments in the study area and most of them are located at the south western and north eastern part of the study area at lower elevations compared to the group one waters. Very few members of this group are also found at some places on the rift floor.

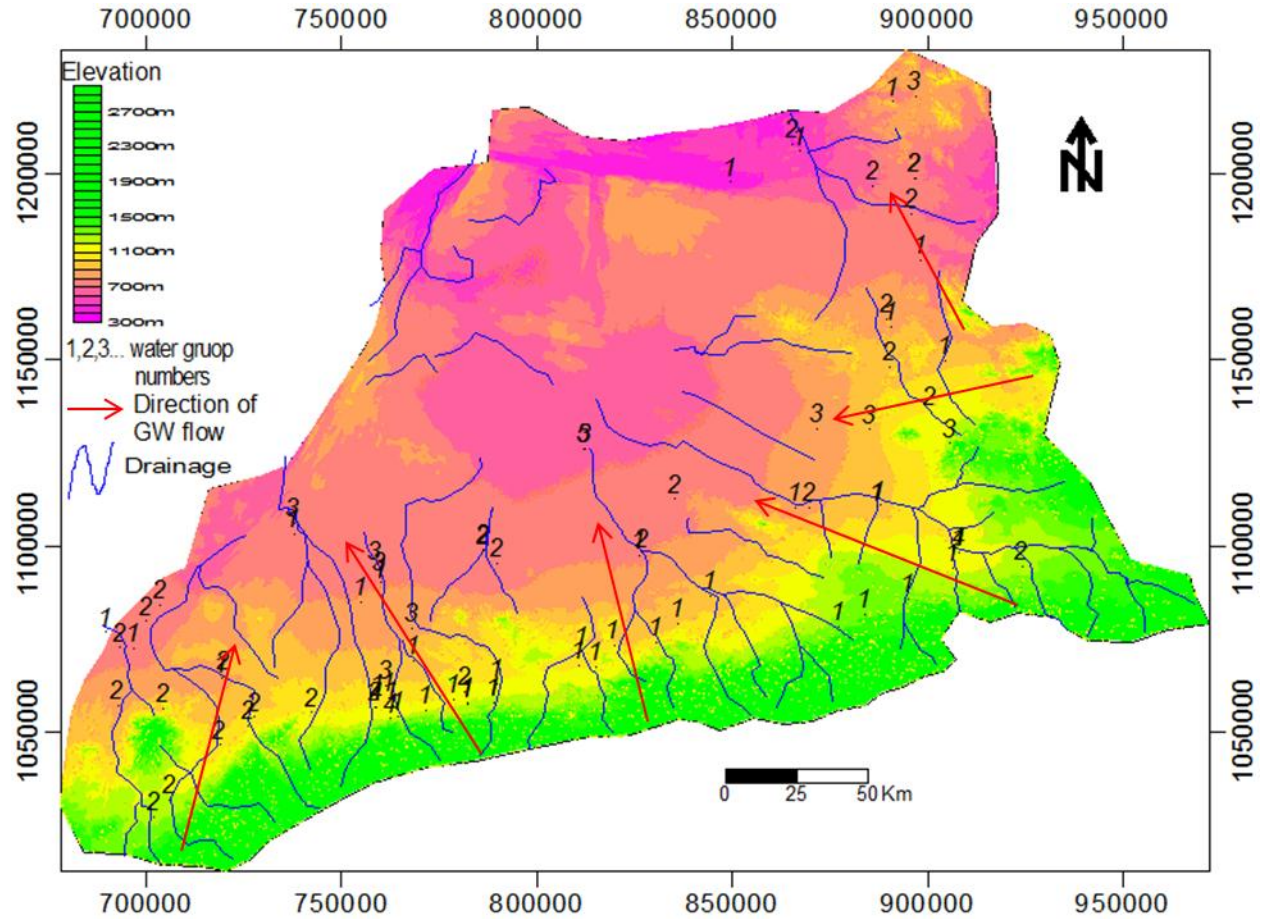


Figure 5.10 Distribution of the HCA water groups in the study area. The red lines indicate inferred direction of groundwater flow.

Group three waters have very high TDS (average=2637.2mg/l) which is typical of evolved ground waters and only exceeded by the member of group five and are mainly composed of Ca-Na-SO<sub>4</sub>, Mg-Ca-SO<sub>4</sub>-HCO<sub>3</sub>, Na-Ca-Cl and Na-Mg-SO<sub>4</sub>-Cl-HCO<sub>3</sub> types of water. They are mostly located on the rift floor at the central part of the study area. Group three waters are most likely the results of hydrochemical evolution of group one and two waters along their flow path due to rock water interaction with sedimentary rocks on the rift floor where evaporite deposits are common and this is reflected in the increased concentrations of SO<sub>4</sub> and Cl in waters of this group.

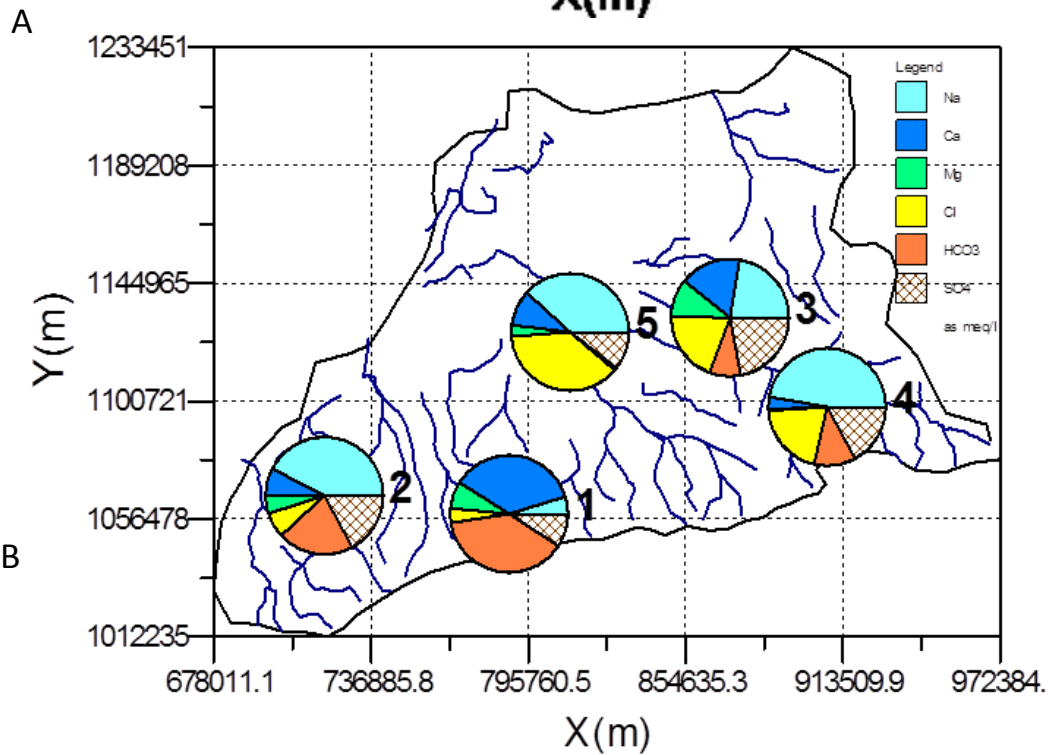
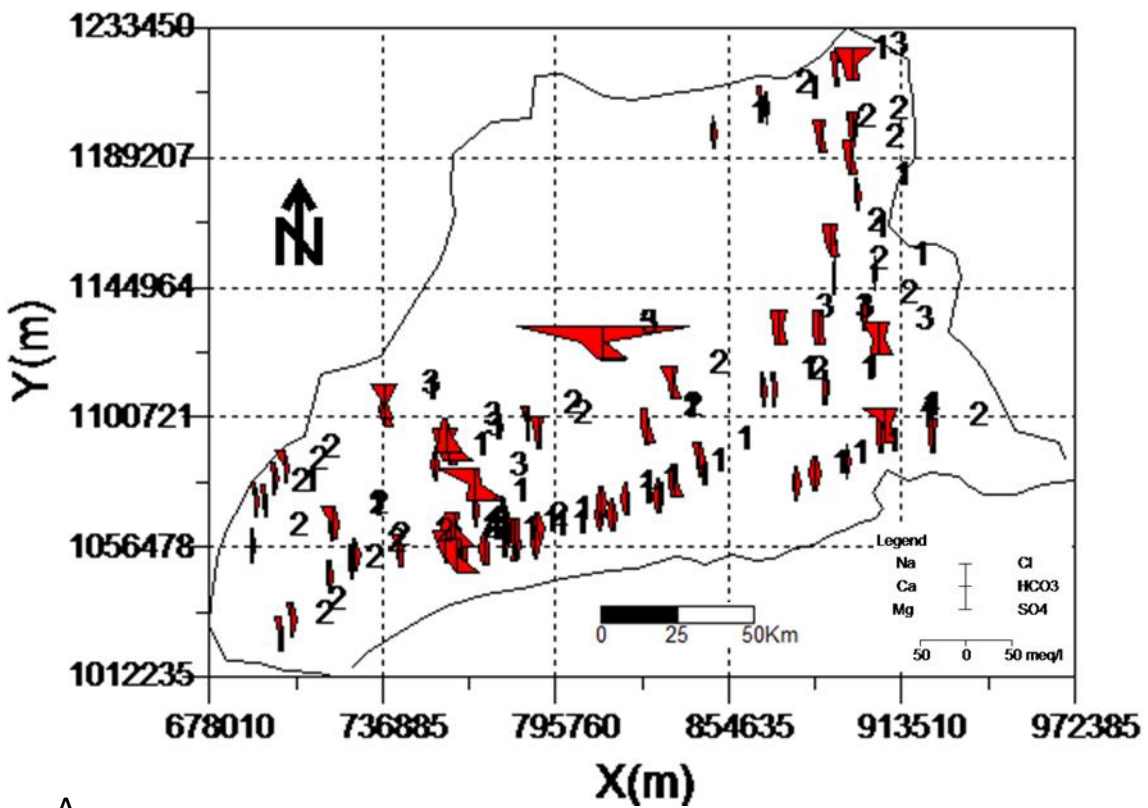


Figure 5.11 Stiff and pie diagram plots of the water samples on base map of the area.

A- Stiff diagram of samples in each group, B-pie diagrams of representative sample for each group

Group four waters have relatively lower TDS (average =2377.5mg/l) than the group three waters. Waters of this group are Na-Ca-SO<sub>4</sub> type and most of the members of this group are thermal springs. They are localized at two places in the southern part of the study area at the contact between the volcanic rocks and Mesozoic sediments and they are probably ground waters from deeper thermal sources dissolving the Mesozoic sediments. Group 5 water which has only one member has the highest total dissolved solids (TDS=10700mg/l) in the study area and It is Na-Cl-SO<sub>4</sub> type of water. This water sample is located at the central part of the study area on the rift floor and it is probably a ground water in contact with localized evaporite deposit of halite or a highly evolved ground water with very long residence time.

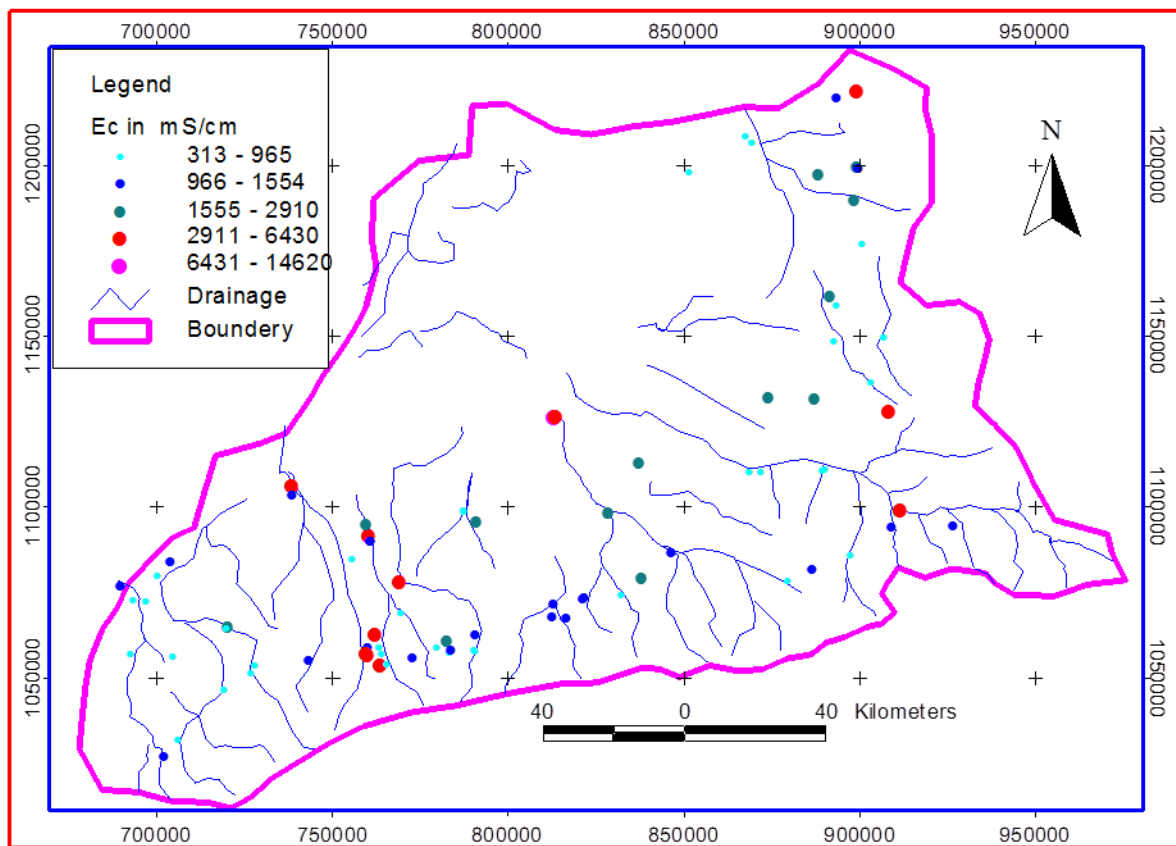


Figure 5.12 Electrical conductivity (EC) map of the study area.

The wide spatial variations of the hydrochemistry of natural waters can be observed from Stiff pattern maps and electrical conductivity (EC) maps. Stiff pattern diagrams visually allow us to

trace the flow paths (Stiff, 1951) and observe changes in concentrations that the ground waters undergo along their flow paths. For this purpose Stiff pattern diagrams of all the water samples clustered in to each of the five groups by the HCA are plotted on base map of the study area (figure 5.11A). From this figure it is observed that salinity of the water samples generally increases from group one to group five as one goes from the highland along the escarpment to the rift floor in the study area. Pie diagrams of the representative samples for each group is also plotted on base map of the study area (figure 5.11B) to show the general trend of variation of hydrochemical facies in the area.

Electrical conductivity map of the water samples also shows similar pattern increasing from the highland to the rift floor indicating the general increase in salinity of the water samples towards the rift floor since it is directly related to the total dissolved solids concentration of the water samples (figure 5.12).

## 5.5 Hydrogeochemical Processes

Reactions between groundwater and aquifer minerals have a significant role on water chemistry, which are also useful to understand the genesis of groundwater (Cederstorm 1946). Groundwater chemistry in general is regulated by diverse processes and mechanisms. Earlier in section 5.3.2.2.1 dissolution of carbonate and evaporite sediments followed by silicate hydrolysis of volcanic rocks are suggested to be the main geochemical processes that might be responsible for the observed variations in ground water geochemistry of the study area based on PCA results. Here some attempt is made to determine if these processes are really responsible for the observed variation by analyzing the relationship between major ion compositions of the water samples.

Calcium and magnesium are the dominant cations present in groundwater followed by sodium in the study area. Similarly, bicarbonate is the dominant anion followed by sulfate and chloride. In silicate terrain, if the calcium and bicarbonate in groundwater are solely originated from calcite, the equivalent ratio of dissolved  $\text{Ca}^{2+}$  and  $\text{HCO}_3^-$  in the groundwater is 1:2, whereas from dolomite weathering, it is 1:4 (Garrels and Mackenzie 1971; Holland 1978). Similarly, if the calcium and sulfate in groundwater is derived from dissolution of gypsum or anhydrite, then the  $\text{Ca}^{2+}/\text{SO}_4^{2-}$  ratio is almost 1:1 (Das and Kaur 2001). In  $\text{Ca}^{2+}$  vs  $\text{HCO}_3^-$  scatter diagram (Fig. 5.13 A), some groundwater samples follow the 1:2 line and some groundwater samples follow the 1:4

line indicating the contribution of both calcite and dolomite weathering on groundwater chemistry in the area but most of the groundwater samples show excess calcium which may indicate additional source of calcium. More over in  $\text{Ca}^{2+}$  vs  $\text{SO}_4^{2-}$  scatter diagram (Fig. 5.13 B), few samples fall along the 1:1 equiline ( $\text{Ca}^{2+} = \text{SO}_4^{2-}$ ) and most of them show excess calcium over sulfate. Groundwater samples following the 1:1 equiline seem to be derived from gypsum or anhydrite dissolution, whereas excess calcium indicates additional geochemical processes like silicate hydrolysis. Similarly, excess sulfate over calcium in some samples may express the removal of calcium from the system likely by calcite precipitation or additional sources of sulfur.

Mayo and Loucks (1995) explained that if  $\text{Ca}^{2+}/\text{Mg}^{2+}$  molar ratio is equal to one, dissolution of dolomite should occur, whereas a higher ratio is indicative of greater calcite contribution. Katz et al. (1998) also explained that the higher  $\text{Ca}^{2+}/\text{Mg}^{2+}$  molar ratio ( $>2$ ) is indicative of dissolution of silicate minerals. The  $\text{Ca}^{2+}$  versus  $\text{Mg}^{2+}$  scatter plot presented in fig. 5.13C shows that the  $\text{Ca}^{2+}/\text{Mg}^{2+}$  molar ratio for majority of the water samples from the study area is generally greater than 2 and some samples have this ratio equal to one which indicates the importance of silicate hydrolysis and dissolution of carbonates like calcite and dolomite in the study area. It can also be seen from fig.5.13C that some samples show  $\text{Ca}^{2+}/\text{Mg}^{2+}$  ratio less than 1 which may indicate the occurrence of calcite precipitation or replacement of  $\text{Ca}^{2+}$  by  $\text{Na}^+$  in some of the water samples.

Quantification of the products of silicate weathering are more difficult because the degradation of silicates is incongruent, generating a variety of solid phases (mostly clays) along with dissolved species (Das and Kaur 2001). However, silicate weathering can be understood by estimating the ratio between  $\text{Na} + \text{K}$  and total cations. The relationship between  $\text{Na} + \text{K}$  and total cations of the area (Fig. 5.13D) indicate that the majority of the samples are plotted near the  $\text{Na} + \text{K} = 0.5\text{Totalcation}$  line. This observation shows the involvement of silicate weathering in the geochemical processes, which contributes mainly sodium and potassium ions to the groundwater (Stallard and Edmond 1983; Sarin et al. 1989).

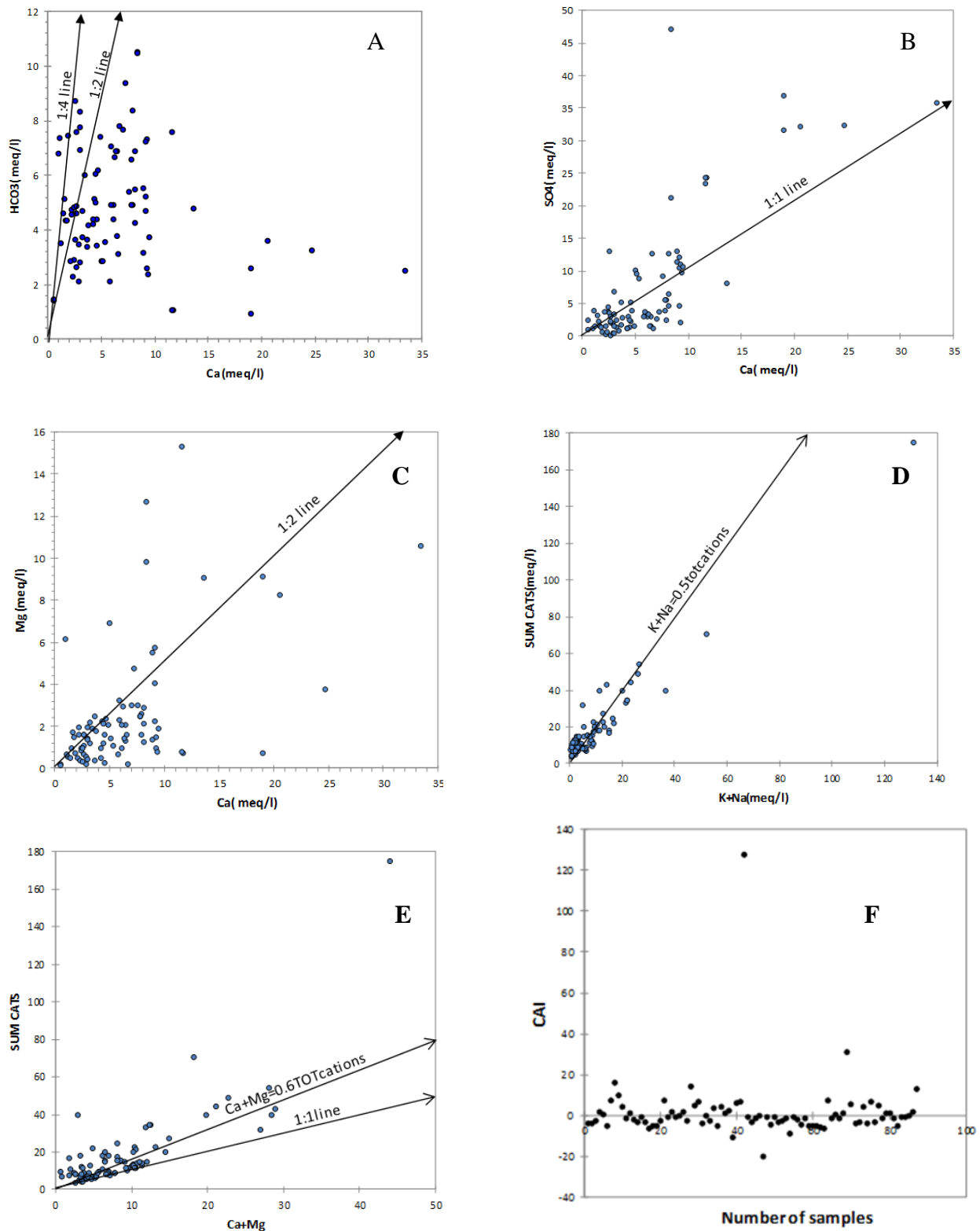


Figure 5.13 Relationship between the major ions: A= $\text{HCO}_3^-$  vs  $\text{Ca}^{2+}$ , B= $\text{SO}_4^{2-}$  vs  $\text{Ca}^{2+}$ , C= $\text{Mg}^{2+}$  vs  $\text{Ca}^{2+}$ , D=Total cations vs  $\text{K}^+ + \text{Na}^+$ , E= Total cations vs  $\text{Ca}^{2+} + \text{Mg}^{2+}$  and F = chloro-alkaline indices

In the plot of total cations versus  $\text{Ca}^{2+} + \text{Mg}^{2+}$ , figure 5.13E, some of the groundwater samples have a linear spread along 0.6:1 or  $\text{Ca}^{2+} + \text{Mg}^{2+} = 0.6\text{TOTcation}$  line and according to Subramani *et al.*, 2009 this indicates that some of these ions  $\text{Ca}^{2+} + \text{Mg}^{2+}$  are resulted from the weathering of silicate minerals. But a considerable number of the water samples also plot on and very near to the 1:1 line which indicates the significance of evaporite and carbonate dissolution in groundwater geochemistry of the study area.

The occurrence of ion exchange reactions in groundwater can be determined from calculations of chloro-alkaline indices of water samples. When there is an exchange between Ca or Mg in the groundwater with Na and K in the aquifer material, the chloro-alkaline index is negative, and if there is a reverse ion exchange, that is, if there is exchange between Na and K in the groundwater with Ca and Mg in the aquifer material the chloro-alkaline index of ground waters will be positive (Schoeller 1965, 1967 and Subramani *et al.*, 2009) where chloro-alkaline index of a given water sample is calculated as shown below.

$$CAI = CI - \left(\frac{Na+K}{Cl}\right), \text{ When concentrations of Na, K and Cl are in meq/l.}$$

Accordingly chloro-alkaline indices for the water samples of the study area are calculated and presented in figure 5.13F. Chloro-alkaline index of the water samples of the study area show both negative and positive values indicating the occurrence of both normal and reverse ion exchanges in the area but greater number of the water samples show negative chloro-alkaline index values which indicates the dominance of normal ion exchange in the study area.

## 5.6 Hydrochemistry and Water Quality

### 5.6.1 Hydrogen ion activity (pH)

According to Hem, 1992, Hydrogen ion activity or pH of natural waters mainly falls between 6 and 8.5 and it is controlled by interrelated chemical reactions that produce or consume hydrogen ions. Some of these reactions are dissociation of acidic solutes and dissolution of CO<sub>2</sub> that reduce the pH of water by producing H<sup>+</sup> or hydrogen ions and dissolution of carbonates and hydrolysis of silicate minerals that increase pH of natural waters by consuming hydrogen ions.

The pH of natural water is a useful index of the status of equilibrium reactions in which the water participates (Hem 1985).

The pH values of the water samples of the study area range between 6.99 and 8.64. The higher pH values of are generally associated with water samples of the group 2 which are mainly located at the south western, north eastern and at some places in the central part of the study area. This high PH is probably related to dissolution of carbonates and silicate hydrolysis reactions that the waters undergo along their flow path that consume hydrogen ions. The more evolved waters of group three and four in the area have generally lower pH and this might be due to the increase in concentrations of Cl<sup>-</sup> and sulfate in these waters that increase their acidity. From water quality point of view pH value of the water samples in the area is well in the range of the 2003 WHO standard of pH for drinking water which is from 6.5 to 9.5. PH distribution of the study area is shown in figure 5.14.

### 5.6.2 Total Dissolved Solids (TDS) and Electrical conductivity (EC)

Total dissolved Solids include all solid material in solution; therefore total dissolved solids concentration is approximately equal to the sum of the concentrations of all ions. On the other hand electrical conductivity of water is its ability to conduct an electric current at a specified temperature and it is usually measured in micro Siemens per centimeter or micromhos per centimeter (Weast, 1968). This ability of water to conduct electricity is due to the presence of charged ionic species in the water and as ionic concentrations increase, conductance of the water increases; therefore, electrical conductivity and TDS are directly related and conductance measurement provides an indication of ionic concentration or TDS of natural waters. Plot of

TDS vs. EC is presented in figure 5.16 and they are related for the study area with the equation  $TDS = 0.7018EC$  with  $r^2$  value of 0.9964.

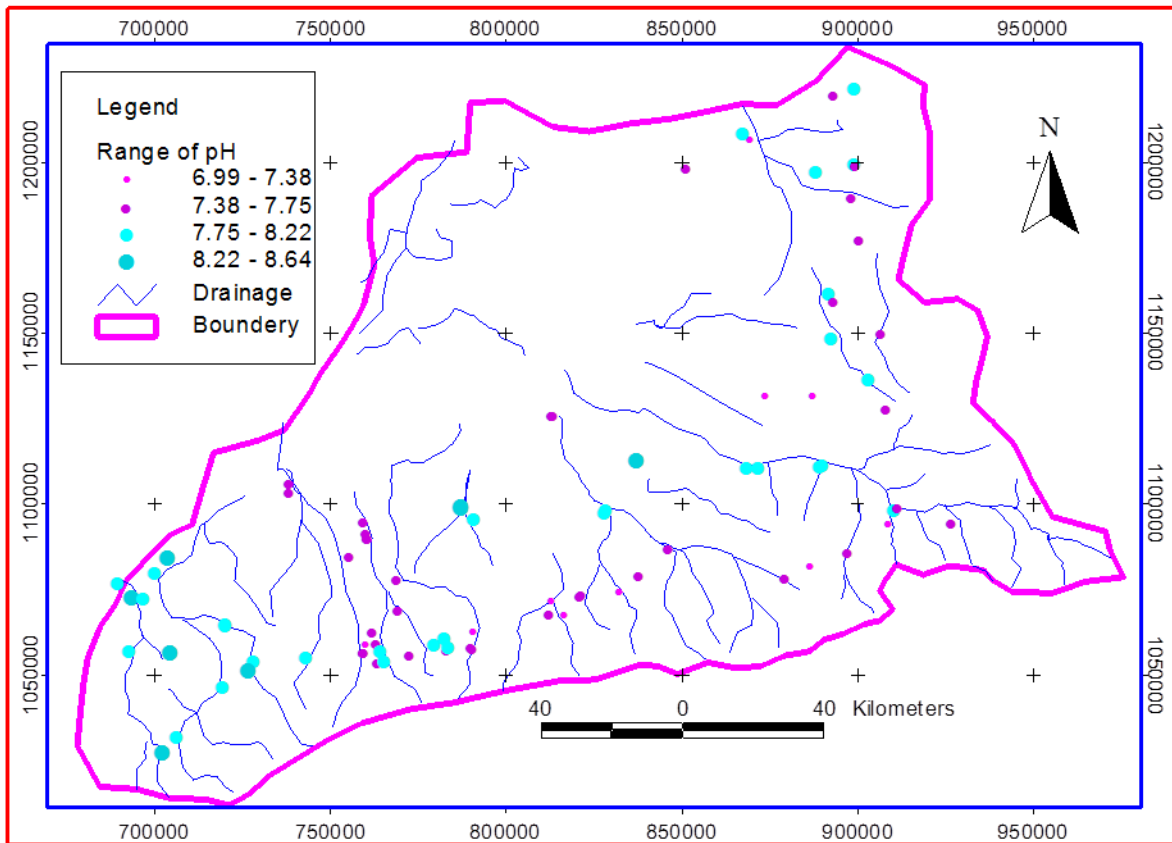


Figure 5.14 Distribution of pH in the study area.

On land surface, in the soil zone, and in groundwater zone to depths of many hundreds or thousands of meters, aluminosilicate minerals such as feldspar and mica are thermodynamically unstable and tend to dissolve when in contact with water. The dissolution processes cause the water to acquire dissolved constituents and the rock to become altered mineralogically (Freeze and Cherry 1979). TDS of natural water range from less than 10ppm of dissolved solids for rain and snow, to more than 300,000ppm for some brine. This variation in TDS can be indicative of the chemical property of the water and it can be used for simple classification of water.

The total dissolved solids concentrations of the water samples vary from 220mg/l to 10700mg/l. In general, TDS in the study area increases from the higher elevation areas of the plateau and escarpment towards the lower elevation areas of the rift floor. Most of the group one water samples at the southern part of the study area show very low values of TDS which indicates they are fresh and recharge area waters at their early stage of geochemical evolution. A very slight increase in TDS is observed in waters of group two at the south western and central part of the area following the direction of the ground water flow. Water samples of group three which are found on the rift floor and the thermal waters of group four have very high TDS values but the highest TDS value of 10700 belongs to Harey deep well which is located at the central part of the study area. Figure 5.15 shows variation of TDS in the area. As can be expected distribution of TDS is very similar to distribution of EC of the area presented in figure 5.12.

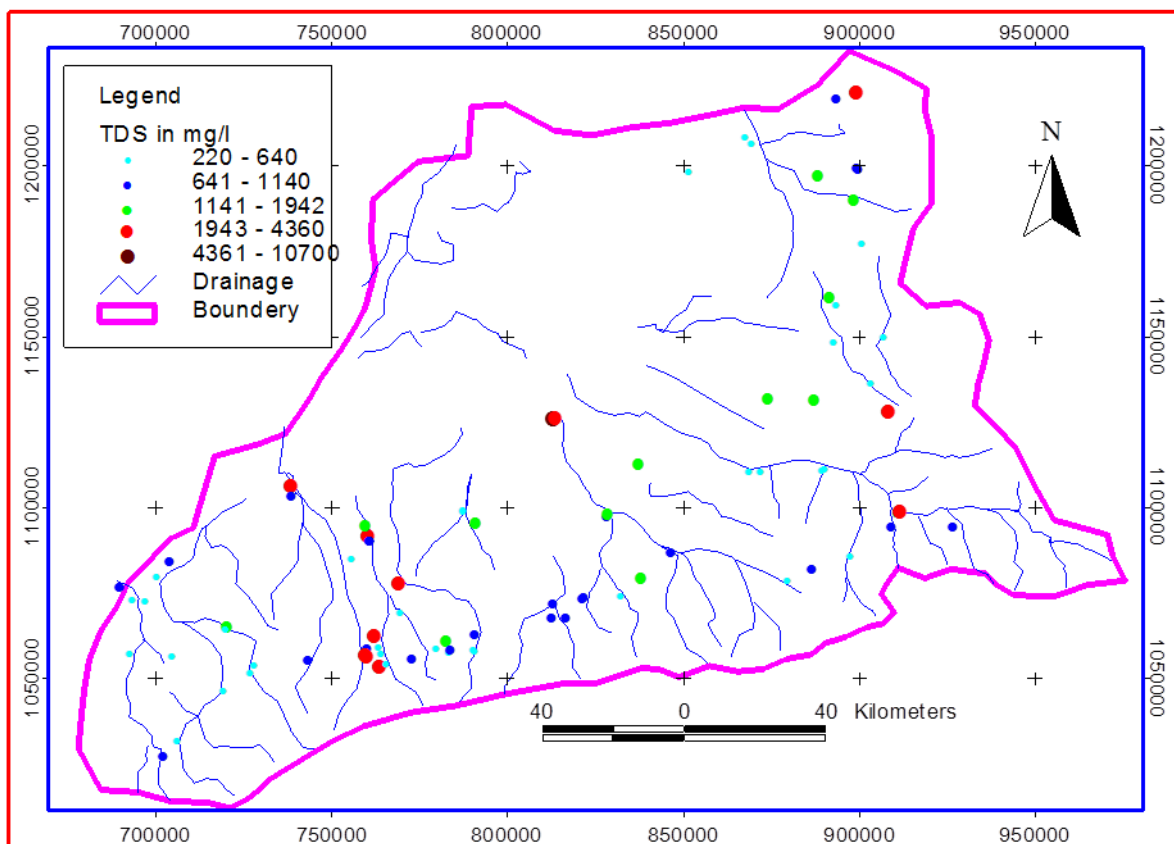


Figure 5.15 Spatial distributions of TDS in the area.

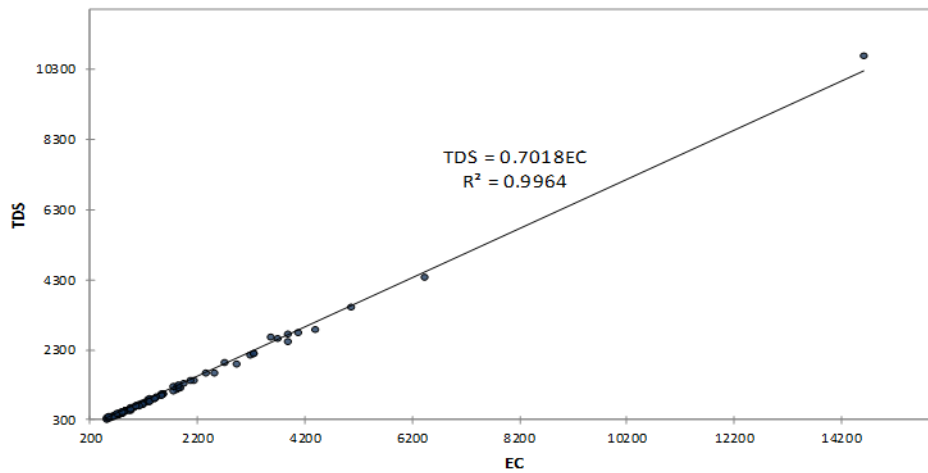


Figure 5.16 Relationship between EC and TDS.

### 5.6.3 Fluoride

High salinity and fluoride concentrations in groundwater are major problems in arid, semi-arid and rift valley regions in our country. Thus distribution of fluoride in the study area is examined to assess its impact on water quality. In nature F comes from chemical weathering product of igneous rocks, magmatic emissions, atmospheric dusts from continental sources and industrial pollution (Hem, 1970). According to Gerasimovskiy and Savinova (1969) the volcanic rocks of East Africa are richer in F than similar rocks in other parts of the world. Unlike many of its halogen group compounds of F have very low solubility and natural concentration of fluoride ranges from 0.01 to 10 mg/l (Fetter, 1994). But even very small amount of fluoride in drinking water cause health problems of dental and skeletal fluorosis and the maximum permissible concentration of fluoride in drinking water is 1.5 mg/l according to the 2003 WHO guidelines for drinking water quality.

Concentration of fluoride in ground water is governed by the solubility of its least soluble compound, which is usually calcium fluoride ( $\text{CaF}_2$ ). In solutions that contain sufficient amounts of calcium there may be equilibrium with respect to fluorite. Higher dissolved calcium in the groundwater brings about lower level of F (Hem 1970). In addition according to Tesfaye 1982 and Ayenew 2007, the most important sources of fluoride in the rift ground water are acidic volcanic rocks such as tuff, pumice and obsidian and emanations from geothermal systems. When we come to the study area both of these reasons seem to be the source of high

concentration of fluoride in the study area. Fluoride distribution of the study area is presented in figure 5.17.

Even though most of the water samples analyzed from the area have fluoride concentration below the 2003 WHO guideline standard of 1.5 mg/l (about 72.4%) the remaining 27.6% of the water samples have fluoride concentrations greater than 1.5 mg/l. These water samples with high fluoride concentrations are found at the south western, north eastern and central part of the study area. Generally samples with very low Ca concentrations have high concentration of F but the highest concentration of fluoride is associated with water samples of the group four which is mostly composed of thermal springs and the highly evolved water of group five. High concentration of fluoride in group four waters is an indication of contribution from geothermal source and high fluoride content of the group five water is probably due to the very low concentration of Ca which can be the result of precipitation as  $\text{CaCO}_3$  after saturation and/or replacement of Ca by Na ions in ion exchange reaction as the ground water evolved along its flow path.

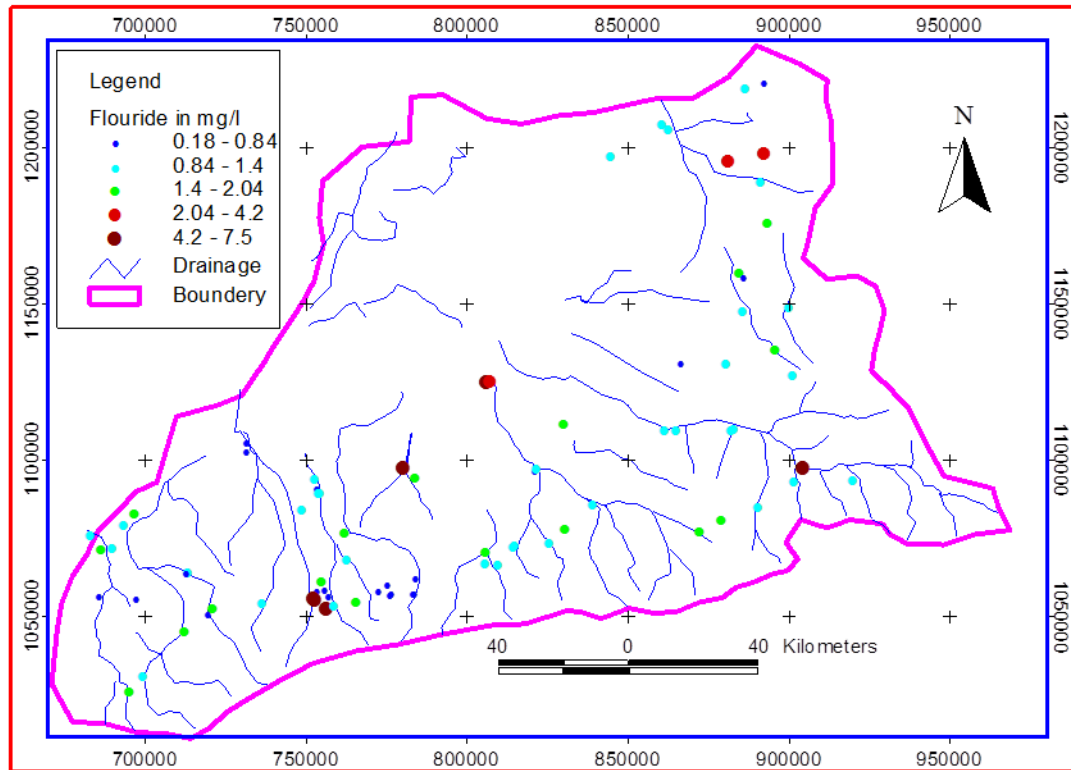


Figure 5.17 Spatial distribution of fluoride in the area.

#### 5.6.4 Other Water Quality Parameters

Other water quality parameters that are important according to the WHO guidelines for drinking water standards include Na, SO<sub>4</sub>, NO<sub>3</sub>, Cl and hardness. Sodium is the dominant cation in water samples of the study area and its concentration varies from 9.4 to 3000mg/l. About 29.9% of the water samples from the area have Na concentration greater than the 200mg/l of 2003 WHO standard for drinking water. Most of the high concentration is associated with waters of group three and five which are found on the rift floor and this could be the result of replacement of Ca by Na in ion exchange reactions and waters of group four which are from geothermal sources. Concentration of SO<sub>4</sub><sup>2-</sup> in the water samples vary from 0.13mg/l to more than two thousand mg/l and 21.8% of the samples have sulfate concentration greater than the 500mg/l WHO drinking standard. Higher sulfate concentration is also associated with waters of group 3, 4 and 5 but very few members of group 1 and 2 waters also show high concentration and this could be the result of dissolution of sulfate from evaporite sediments common in the area. Chloride concentration in

the water samples vary from 5.3mg/l to 4560mg/l and 14.8% of the samples have chloride concentration greater than the 250mg/l WHO drinking water standard. Higher chloride concentration is generally observed in waters of group 3, and 5 but group 4 waters and very few members of group 1 and 2 waters also show high concentration and this could be the result of dissolution of chloride from evaporite sediments common in the area and concentration of chloride from evaporation. Concentration of nitrate varies from 0.25mg/l to 510mg/l and about 29.9% of the samples show  $\text{NO}_3^-$  concentration greater than WHO 2003 standard of 50mg/l. High value of nitrate is generally found in group two which is probably the result of contamination of ground water from anthropogenic sources like the use of fertilizers and wastes of domestic animals like cattle. Hardness of the water samples vary from 36 to 2204 mg/l and 74.8% the water samples have hardness greater than the maximum WHO limit of 200mg/l and this could be the result of dissolution of carbonate rocks that mainly contribute calcium and magnesium.

### 5.6.5 Agricultural Water Quality

At present construction of large irrigation project is being undertaken in Shinile zone for utilization of the good ground water potential of the study area for agriculture. Thus determination of suitability of the groundwater in the area for agriculture is very important. The relative concentration of Na with respect to Ca and Mg is very important for the suitability of ground water for agricultural purposes. Sodium when present in the soil in exchangeable form replaces calcium and magnesium adsorbed on the soil clays and cause dispersion of soil particles decreasing permeability and aeration of the soil. This harms plant growth by limiting the uptake of air and water. Sodium Adsorption Ratio (SAR) is an index that expresses the relative activity of sodium ions in exchange reactions with the soil. This ratio measures the relative concentration of sodium to calcium and Magnesium using the following equation;

$$\text{SAR} = \frac{\text{Na}}{\sqrt{\frac{\text{Ca} + \text{Mg}}{2}}} \quad \text{where concentrations of Ca, Na and Mg are in meq/l}$$

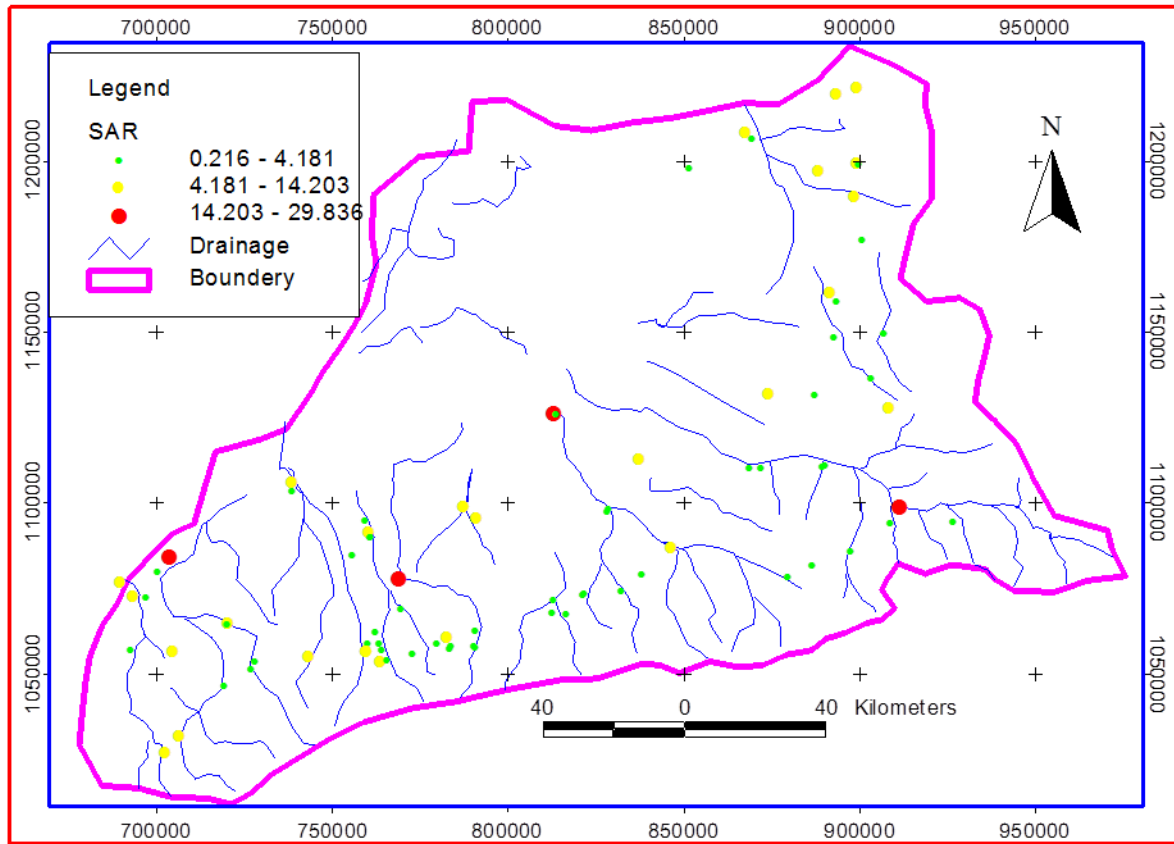


Figure 5.18 Spatial distribution of SAR in the area.

The SAR value of water samples of the study area varies from 0.22 to 29.84. As it can be seen from figure 5.18 above, high values of sodium adsorption ratio are generally found at lower elevations on the rift floor except at one place at the southeastern part of the study area where a very high value of SAR is observed on the highland and this is probably due to high sodium content of the thermal springs in the area.

## 6. CONCLUSION AND RECOMMENDATION

### 6.1 Summary and Conclusion

The main objective of this study was to assess the geochemical evolution of groundwater from plateau to the rift floor by analyzing hydrochemical data using conventional graphical methods and multivariate statistical methods. The study area which is chosen to include the three physiographic regions covers a total area of 34793 square kilometers and it is found in Somali national regional state in the eastern part of Ethiopia. To fulfill this objective water chemistry data of eighty seven water samples from the area obtained from OWWDSE are analyzed and interpreted. The eighty seven water samples are collected from forty six bore holes; thirty hand dug wells, seven rivers and four springs (appendix 1). Location of all the water samples is given in figure 5.2

Prior to using the data for interpretation and the intended purpose, the water chemistry data is checked for quality or accuracy of the laboratory analysis. This involves calculation of reaction error for ionic compositions. Reaction error calculations reveal that the error is less than 5% for most of the water samples (figure 5.1) which indicates the quality of the data is very good for the purpose of this study. After the data is checked for quality all water samples from the four different sources are plotted on piper diagrams together and separately to see if they can be grouped in to distinct hydrochemical facies or water types based on their origin or sources (figure 5.3). These plots showed that water type in the study area does not necessarily depend on source of the water, that is, water from bore holes springs, rivers and hand dug wells may have similar composition. In addition the piper plots showed the diversity of the water types in the area.

Hierarchical clustering analysis (HCA) was used to classify the samples into distinct hydrochemical groups. Eleven variables (EC, PH, Ca, Mg, Na, K, HCO<sub>3</sub>, NO<sub>3</sub>, Cl, SO<sub>4</sub> and F) were used for the clustering analysis and this resulted in classification of the eighty seven water samples in to five different groups.

Pie charts which are used to present relative major ion compositions of water samples in percent milliequivalent per liter and Stiff pattern diagrams which are used to present the actual major ion concentrations of water samples in milliequivalent per liter were used to present mean group

values for each of the five water groups to show the variations in relative and actual concentrations of the major ions among the five water groups (figure 5.4 and 5.5).

The relationship between the statistically defined clusters of samples and geographic location was prepared by plotting group values for each sample. Samples that belong to the same group are located in close proximity to one another suggesting more or less the same hydrogeochemical processes (evolution) and/or flow paths. Figure 5.10 shows the spatial distribution of the five cluster groups.

The wide spatial variations of the hydrochemistry of natural waters can be observed from Stiff pattern maps and electrical conductivity (EC) maps. Stiff pattern diagrams visually allow us to trace the flow paths (Stiff, 1951) and observe changes in concentrations that the ground waters undergo along their flow paths. For this purpose Stiff pattern diagrams of all the water samples clustered in to each of the five groups by the HCA are plotted on base map of the study area (figure 5.11 A). Pie diagrams for representative sample for each of the groups are plotted on base map of the area to show trend of variation of hydrochemical facies in the area (figure 5.11B). EC map of the water samples is also presented in figure 5.12. From these figures it is observed that salinity of the water samples generally increases from group one to group five as one goes from the highland to the rift floor in the study area.

Based on analysis of the eighty seven water samples using the different methods discussed above the following conclusions are made about the ground water evolution in the study area.

- The Q-mode hierarchical cluster analysis classified the water samples in to five distinct groups with different hydrochemical compositions that are separated geographically, as well as physiographically with good correspondence between spatial locations and the HCA results.
- In general salinity and concentration of the water samples increases from highland areas to the rift floor.
- Water type in the study area changes from Ca-HCO<sub>3</sub> and Ca-Mg-HCO<sub>3</sub> dominated type on the highlands to Na-HCO<sub>3</sub> and Na-HCO<sub>3</sub>-SO<sub>4</sub> dominated type on the escarpment to Mg-Ca-SO<sub>4</sub>-HCO<sub>3</sub>, Ca-Na-SO<sub>4</sub> and Na-Cl-SO<sub>4</sub> types on the rift floor following the direction of the ground water flow.

Principal component analysis, another multivariate statistical method, is employed to analyze the water samples to identify geochemical processes that are responsible for the observed variation in hydrochemistry of the area. The first three principal components accounted for 72.85% of the total variance in the hydrochemistry. The first principal component which showed high absolute loadings for EC, Ca, Mg, Na, K, F, SO<sub>4</sub> and Cl explained 46.99% of the observed variance and most probably represents dissolution reactions of carbonates and evaporite sediments which are responsible for putting these elements in to ground water. The second principal component which showed high absolute loadings for pH, Mg, and HCO<sub>3</sub> explained 15.29% of the observed variance in hydrochemistry and most probably represents silicate hydrolysis reaction. The third principal component which account for 10.58% of the variance in hydrochemistry contain high absolute loadings for NO<sub>3</sub> and HCO<sub>3</sub> and probably represent addition of contaminants to the ground water from anthropogenic sources.

PC scores for the first two principal components of the water samples clustered in to the five water group by HCA is plotted in a 2D scatter-plot(PC1 vs. PC2,figure 5.9) and majority of the water samples of the study area in each group are well separated in the PC space and compactly distributed within their respective groups. According to Belkhiri L. *et al.* 2011 this shows that all the water samples in their respective groups have similar chemistries hence similar flow paths or sources.

The relationship among the major ion compositions of the water samples are analyzed to determine if the geochemical processes suggested based on the PCA results are really responsible for the observed variations in hydrochemistry of groundwater in the study area. The results of this analysis clearly indicated the occurrence of dissolution reaction of evaporite deposits and carbonate sediments as well as silicate hydrolysis reactions in the study area confirming the PCA results. Chloro-alkaline indices of the water samples are also calculated and this indicated the occurrence of both normal and reverse ion exchange reactions in the study area.

Finally water quality of the study area is assessed from domestic use and agricultural point of view. This showed that pH of the water samples in the area is well in the range of the 2003 WHO standard of pH for drinking water which is from 6.5 to 9.5 but fluoride concentration in 27.6% of the water samples exceed the 2003 WHO standard of 1.5 mg/l. In addition Na concentration in 29.9% of the water samples, sulfate concentration in 21.8% of the water

samples, chloride concentration in 14.8% of the water samples and nitrate concentration in 29.9% of the water samples are greater than the WHO 2003 standard limit for drinking water of 200, 500, 250 and 50 mg/l respectively. In the case of hardness 74.8% of water samples analyzed from the area have hardness greater than the 2003 WHO maximum limit of 200mg/l.

Water quality of the area is assessed from agricultural point of view and distribution of sodium adsorption ratio of the water samples is mapped. This showed that high SAR values are found at two places in the area. One is at the south eastern part of the area on the highland which is due to high Na content of the thermal springs in the area and the second place is at the northern and central part on the rift floor which is related to the increased Na concentration of the highly evolved waters of the area.

## 6.2 Recommendations

The following recommendations are made based on previous discussions and conclusions stated above.

- Isotope hydrologic studies using environmental isotopes of  $\delta^{18}\text{O}$ ,  $\delta^2\text{H}$  and  $\delta^{13}\text{C}$  should be conducted in the area to confirm the output of this study and especially to determine if the highly evolved waters on the rift floor are the result of water recharged from the adjacent southern highland dissolving evaporites and lacustrine sediments along their relatively short flow paths or if they are from water recharged at some other far places following deeper flow paths with very long residence time discharging in the area. These isotope studies are also recommended to identify if the sources of major ions in the relatively less evolved highland waters are Mesozoic sediments or volcanic rocks both of which are common in the area.
- Defluoridation of drinking water is recommended in parts of the study area which have high concentration of fluoride in ground water to mitigate the adverse health effects of fluoride.
- Measures should be taken to reduce the negative effects of sodium on agriculture at the north, central and south eastern parts of the study area where the ground waters showed high values of SAR if they are to be used for irrigation purposes.

## References

- Ashley, R P. and Burley, M.J., 1994. Controls on the occurrence of fluoride in groundwater in the rift valley of Ethiopia. In: Groundwater Quality, pp. 45–54, (Nash, H. and McCall, G.J.H., eds). Chapman and Hall, London.
- Belkhiri, L. 1\*, Boudoukha, A.2 and Mouni, L. 3, 2011. A multivariate Statistical Analysis of Groundwater Chemistry Data. *Int. J. Environ. Res.*, 5(2):537-544, Spring 2011
- Fetter, C.W., 1994. Applied Hydrogeology. 3rd edition, Prentice – Hall, New Jersey. 695pp
- Freeze R. Allan and Cherry John A., 1979. Groundwater. Prentice – Hall, New Jersey. 616pp.
- Freeze R. Allan and Cherry John A., 1979. Groundwater. Prentice – Hall, New Jersey. 616pp.
- Giday Woldegebriel, Aronson, J.L. and Walter, R.C., 1990. Geology, geochronology, and rift basin development in central sector of the Main Ethiopian Rift. *Geological Society of America Bulletin* 102:439–458. [B34.022].
- Gizaw B, 1996. The origin of high bicarbonate and fluoride concentrations in waters of the Main Ethiopian Rift Valley, East African Rift system. *J Afr Earth Sci* 2:391–402.
- Guler, C., Geoffrey, D., John, T., McCray, E., 2002. Evaluation of graphical and multivariate statistical methods for classification of water chemistry data. *Hydrogeology Journal*, 10, 455 – 474.
- Habteab Zerai and Jiri Sima, 1986. Hydrogeology and Hydrochemistry of the Dire Dawa area. Ethiopian Institute of Geological Survey, Addis Ababa.
- Hem, J.D., 1989. Study and interpretation of the chemical characteristics of natural waters, US. Geol. Surv. Water Supply Paper 2254, 272 pp.
- J.E. Koonce, Z. Yu\*, I.M. Farnham, K.J. Stetzenbach, 2006. Geochemical interpretation of groundwater flow in the southern Great Basin, *Geosphere*; April 2006; v. 2; no. 2; p. 88–101; doi: 10.1130/GES00031.1

- Johnson, R.A., and Wichern, D.W., 2002. Applied multivariate statistical analysis (fifth edition): Upper Saddle River, New Jersey, Prentice Hall, 767 pp.
- L. R. Bentley<sup>1</sup>, O. Mrklas<sup>2,\*</sup>, S. R. D. Lunn<sup>2</sup> and A. Chu<sup>3</sup>, 2006. Principal component analyses of groundwater Chemistry data during enhanced bioremediation. *Water, Air, and Soil Pollution* (2006) 169: 395–411.
- Meng, S.X., Maynard, J.B., 2001. Use of statistical analysis to formulate conceptual models of geochemical behaviour: water chemical data from the Botucatu aquifer in Saõ Paulo state, Brazil. *J. Hydrol.* 250, 78–97.
- Mengesha Tefera, Tesfaye Chernet, Werkinah Haro, 1996-2008. Explantion of the Geological Map of Ethiopia 1:2,000,000 scale. Ethiopian Institute of Geological Survey, 79pp.
- Minalah Bushura, (2007) Numerical Groundwater Flow Modeling Of the Dire Dawa Area, Unpublished MSc thesis, Addis Ababa University.
- Molla Demlie, Stefan Wohnlich, Tenalem Ayenew, 2008. Major ion hydrochemistry and environmental isotope signatures as a tool in assessing groundwater occurrence and its dynamics in a fractured volcanic aquifer system located within a heavily urbanized catchment, central Ethiopia. *Journal of Hydrology* (2008) 353, 175– 188.
- Molla Demlie, Stefan Wohnlich, Frank Wisotzky & Birhanu Gizaw, 2007. Groundwater recharge, flow and hydrogeochemical evolution in a complex volcanic aquifer system, central Ethiopia. *Hydrogeology Journal* DOI 10.1007/s10040-007-0163-3.
- Molla Demlie, Stefan Wohnlich, 2006. Soil and groundwater pollution of an urban catchment by trace metals: case study of the Addis Ababa region, central Ethiopia. *Environ Geol* (2006) 51: 421–431 DOI 10.1007/s00254-006-0337-7.
- Morbedelli, L., Nicoletti, M., Petrucciani, C., Piccirillo E.M., 1975. Ethioian South – Eastern Plateau and Related Escarpment. K – Ar ages the Main Volcanic Events (Main Ethiopian Rift from 8<sup>0</sup>10' to 9<sup>0</sup>00' lat. North). In “Afar Depression of Ethiopia” eds. A. Pilger

- and A. Rosler. Schweizerbart, Stuttgart, 362 – 369.
- OWWDSE, 2011. Shinlle Zone climate and hydrology report. Unpublished report, Addis Ababa, 2011, 103pp.
- OWWDSE, 2011. Shinlle Zone Groundwater Assesment Project. Unpublished report, Addis Ababa, 2011,165pp.
- Schoeller, H.1967. Geochemistry of groundwater—an international guide for research and practice (Chap. 15, pp. 1–18).
- Seifu Kebede, Yves Travi, Tamiru Alemayehu, Tenalem Ayenew, 2005. Groundwater recharge, circulation and geochemical evolution in the source region of the Blue Nile River, Ethiopia. *Applied Geochemistry* 20 (2005) 1658–1676
- Seifu Kebede, Yves Travi, Asfawossen Asrat, Tamiru Alemayehu, Tenalem Ayenew & Zenaw Tessema, 2007. Groundwater origin and flow along selected transects in Ethiopian rift volcanic aquifers. *Hydrogeology Journal*, 2007. DOI 10.1007/s10040-007-0210-0.
- Stiff H. A. 1951. The Interpretation of Chemical Water Analysis by Means of Patterns. *Journal of petroleum technology*, v. 3no. 10 pp15-17
- Subramani T. Rajmohan N. ·Elango L. , 2009. Groundwater geochemistry and identification of hydrogeochemical processes in a hard rock region, Southern India. *Environ Monit Assess* (2010) 162:123–137 DOI 10.1007/s10661-009-0781-4.
- Tenalem Ayenew and Tamiru Alemayhu, 2001. Principles of hydrogeology. Department of geology and geophysics, Addis Ababa University, 125pp.
- Tenalem Ayenew\*, Shimeles Fikre, Frank Wisotzky, Molla Demlie and Stefan Wohnlich , 2009 Hierarchical cluster analysis of hydrochemical data as a tool for assessing the evolution and dynamics of groundwater across the Ethiopian rift. *International Journal of Physical Sciences* Vol. 4 (2), pp. 076-090, February, 2009 Available online at <http://www.academicjournals.org/IJPS> ISSN 1992 - 1950 © 2009 Academic Journals

- Tenalem Ayenew, Molla Demile, Wohnlich S., 2008. Hydrogeological framework and occurrence of groundwater in the Ethiopian aquifers. *Journal of Africa and Earth Science* 52, 97 – 113.
- Tenalem Ayenew, 2005. Major ions composition of the groundwater and surface water systems and their geological and geochemical controls in the Ethiopian volcanic terrain. *Journal of Radioanalytical and Nuclear Chemistry*, Vol. 257, No. 1., 11–16 pp. *SINET: Ethiop. J. Sci.* 28(2): 0379–2897.
- Tenalem Ayenew, 2007. The distribution and hydrogeological controls of fluoride in the groundwater of central Ethiopian rift and adjacent highlands. *Environ Geol*, 54, 1313 – 1324.
- Todd, T.D., 1980. *Groundwater Hydrology*. John Wiley and Sons, New York.
- WHO, 2003. *Guidelines for drinking water quality*. Report WHO, Geneva, 139 pp.
- WHO, 2004. *Guidelines for Drinking-water Quality*. 3<sup>rd</sup> edition, 1, Recommendations.

## Appendices

### Appendix 1 Water chemistry data used for the study

Location	source	X	Y	TDS	EC	PH	Na	K	Mg	Ca	Cl	SO4	HCO3	NO3	F	Fe	PO4	NH3	Turbidity (NTU)
Biyobahay #7	Bore hole	887740	1110869	388	564	7.82	71	5.1	21.1	32.8	23.66	72	264	19.29	1.3	0.01	0.03	0.33	2.19
Biyobahay#5	Bore hole	886994	1110571	414	597	7.79	63	6	24	44.8	21.84	77.6	290	27.43	1.2	0.01	0.03	0.38	0.37
Biyobahay#6	Bore hole	866349	1110283	406	594	7.78	57	4.7	14.4	64	28.21	66.1	287	17.59	0.9	0	0.15	0.41	0.37
Mete #3	Bore hole	786149	1099151	452	719	8.61	140	3.8	2.4	11.2	117.8	51.2	87.8	0.4	1.8	0	0.19	0.23	4.7
Mete #2	Bore hole	786138	1098605	580	938	8.64	196	3.8	1.92	11.2	118.77	121	90.3	0.51	6.8	0.02	0.9	0.17	3.7
Harawa TW	Bore hole	826331	1097377	672	965	7.78	101	4.6	30.2	72.8	27	250	222	20.9	0.7	0.02	0.3	0.3	0.37
Aydora TW	Bore hole	759581	1091435	3530	5070	7.47	600	9.7	111	380	358.2	1771	159	43.4	0.8	0.01	0.3	3.1	0.37
Asbuli TW	Bore hole	737767	1106062	2174	3190	7.5	485	7.7	84	100	614.1	485	176	44.5	0.7	0.01	0.2	0.9	0.37
Jama Dere TW	Bore hole	871717	1131593	1902	2910	7.33	284	11	69.6	184	381.41	584	288	20.72	0.8	0.96	0.41	0.52	1.1
Magal Adi	Bore hole	781594	1060728	1218	1874	7.82	250	3.3	29	92.7	218.2	185	378	198.2	0.6	0.02	0.09	0.69	1
Alcho	Bore hole	782134	1057523	448	681	7.56	9.4	1	74.9	19	10.5	52.6	415	0.39	0.6	0.06	0.04	0.68	0
Hurso	Bore hole	789629	1062713	910	1390	7.25	66	0.7	57.5	144	79.8	180	573	41.48	0.7	0.03	0.06	1.46	1
Bike	Bore hole	742434	1055100	766	1177	7.93	196	10	11.5	48.6	76.95	212	294	1.48	1.3	0.01	0.11	0.12	1
Sisilu	Bore hole	719876	1064805	1360	1937	8.14	385	4.1	23.9	59.3	96.9	326	508	210.3	1.1	0.03	0.47	0.16	3
Afdem	Bore hole	718770	1046429	556	854	7.88	78	10	14.3	88.9	57.95	69.9	371	30.54	1.8	0.12	0.16	0.14	4
Sala'a	Bore hole	704353	1056263	470	682	8.56	129	6.4	6.44	24.3	47.4	71.1	214	56.8	0.2	0.02	0.25	0.02	5
Alijir	Bore hole	699990	1079698	520	793	7.94	115	7.3	12.9	53.2	26.6	0.13	464	7.5	1.2	0.01	0.13	0.05	6
Komiye	Bore hole	705842	1031637	520	800	8.18	129	5.6	9.2	38	34.2	26.8	454	6.4	1.2	0.05	0.44	0.44	7

Continued ...

Afase	Bore hole	693369	1072568	558	857	8.4	142	3.7	11.5	30.4	37.05	112	314	0.35	1.5	0	0.36	0.11	0
Butuji	Bore hole	692621	1057125	332	509	8.22	40	4.7	19.3	44.1	19	13.9	280	0.25	0.7	0	0.26	0.14	1
Gedamayitu	Bore hole	660081	1077855	1170	1798	8.17	340	11	10.6	48.6	314.41	178	178	78.5	1.6	0	0.15	0.06	4
Mulu	Bore hole	702038	1027095	750	1097	8.26	178	5.9	11.5	51.7	87.4	168	224	123	1.5	0.05	0.13	0.11	4
Qantras(palace)	Bore hole	762457	1053520	2610	3680	7.65	460	7.3	9.2	380	188.1	1521	56.1	0.84	5.6	0	0.06	0.77	0
Keleme	Bore hole	789029	1057941	528	789	7.7	20	1.5	16.1	129	24.7	78.3	420	8.6	0.8	0	0.19	1.01	1
Barak	Bore hole	819664	1073154	688	1033	7.73	26	2.4	31.3	160	32.3	264	299	14.6	1	0.01	0.04	1.22	2
Biyaman	Bore hole	758909	1056571	2190	3240	7.52	500	10	9.2	236	199.5	1168	64.9	2.8	7.5	0.06	0.1	3.26	18
Durdur	Bore hole	867541	1206305	360	514	7.07	44	7	2.3	57	21.85	88.6	130	58.3	1.2	0.01	0.28	0.16	1
Sanajif	Bore hole	905579	1127633	2780	4060	7.55	515	33	154	167	551	1022	642	1.34	1.1	0.08	0.42	3.3	1
Degago	Bore hole	889513	1161153	1642	2520	7.81	284	10	16.6	179	247	548	338	42.3	1.5	0	0.13	1.35	3
Biyedidley	Bore hole	885169	1131358	1420	2120	6.99	208	8.4	49.6	182	285.95	502	318	1.6	1.4	0.02	0.15	1.8	2
Arabi	Bore hole	908076	1098123	460	686	7.78	73	4.3	19.8	53.2	24.7	96.3	297	36.4	1.3	0	0.07	0.4	0
Keranle	Bore hole	884002	1081638	688	1056	7.25	45	2.8	19.3	160	43.7	114	510	27.9	2	0	0.05	1.36	1
Semekab	Bore hole	877409	1078318	542	828	7.52	53	2.2	25.3	98.8	24.7	73	452	19.7	1.9	0	0.06	0.54	2
Hagarwein	Bore hole	924150	1094497	1050	1541	7.6	154	8.2	25.3	129	182.4	148	229	282.6	0.9	0.02	0.09	0.57	1
Dembel	Bore hole	894991	1085654	440	677	7.43	38	3	23	68.4	11.4	41.3	366	30.5	1.1	0	0.1	0.45	0
Ayisha	Bore hole	896011	1189512	1450	2050	7.64	242	5.2	36.8	152	205.2	444	329	131.2	1.3	0.01	0.12	0.56	4
Shinile Town	Bore hole	811477	1071736	780	1191	7.19	69	1.3	36.8	141	91.2	129	468	62.3	1.5	0.01	0.05	1.02	1
Mermarsa	Bore hole	810949	1067896	822	1261	7.45	68	1.7	11.5	185	116.85	103	447	94.4	1.3	0.02	0.05	0.76	1
Harewa	Bore hole	826859	1098079	1270	1803	8.12	218	7	26.2	162	29.45	610	260	57	1	0.01	0.02	1.05	2
Milo	Bore hole	835448	1112659	1660	2340	8.59	380	3.3	19.3	131	285.95	610	190	96.1	1.9	0.01	0.06	0.52	1
Meto	Bore hole	789759	1095378	1200	1845	8.09	258	16	19.3	91.2	290.7	246	209	50.5	1.6	0.01	0.03	0.2	1
Harey	Bore hole	811834	1126149	10700	14620	7.7	3000	18	129	669	4560	1720	153	510	7.1	0.32	0.02	12.8	2

Continued ...

Tome	Bore hole	815089	1067392	778	1182	7.16	36	1.6	27.6	182	33.25	220	440	30.94	1.2	0.06	0.04	1.26	3
Dure	Bore hole	869872	1110383	410	609	8.18	75	5.3	18.4	34.2	30.4	63.8	267	41.2	1.1	0	0.1	0.35	1
Harmukale	Bore hole	844495	1086563	846	1291	7.69	188	3	17.5	60.8	81.7	164	473	12.3	1.3	0	0.08	0.44	3
ka'a	Bore hole	689741	1076778	670	1013	7.83	204	4.3	5.98	28.1	100.7	149	281	27.8	1.4	0.12	0.27	0.1	0
Harey	HDW	812228	1126012	2656	3560	7.4	260	5.7	46	494	19.95	1549	199	53.6	2.9	0.07	0.03	0.31	1
Durdur	HDW	865378	1208169	566	869	8.04	130	4.4	5.98	41.8	73.15	182	174	1.13	1.2	0	0.15	0.1	4
Gerbale	HDW	898235	1176996	420	642	7.52	48	3.2	3.22	90.4	15.2	111	269	2.42	1.5	0.05	0.29	0.21	1
Biyman	HDW	758548	1056732	1030	1554	7.6	192	16	12.9	108	95.95	429	218	58.6	1.1	0.01	0.22	1.01	45
Aydora	HDW	759959	1090176	900	1381	7.61	78	0.6	17.9	185	31.4	529	159	21	1.2	0.05	0.06	0.69	1
Aydora2	HDW	759968	1090121	890	1275	7.5	60	0.8	9.7	188	29.5	467	146	42.6	1.1	0	0.08	0.37	4
Girmame- Maras	HDW	778533	1058777	510	786	7.78	35	5.3	27.6	87.4	24.7	146	312	3.76	0.4	0.13	0.19	0.41	76
Asbuli	HDW	737763	1103347	930	1295	7.63	58	4.8	23	190	10.45	509	227	4.99	0.6	0.09	0.1	0.43	366
Dimitu	HDW	759331	1058654	760	1168	7.38	52	0.8	29.9	156	38	185	403	16.4	0.8	0.01	0.09	0.94	4
khelwine	HDW	758665	1094670	1942	2690	7.67	110	8.2	186	232	49.4	1124	464	0.5	1	0.13	0.05	3.9	3
Oerdela	HDW	754872	1084824	598	906	7.62	52	0.4	11.5	122	16.15	162	300	63.6	1.3	0.06	0.13	0.38	2
Tabi	HDW	768100	1077704	4360	6430	7.75	1200	2.4	120	167	233.7	2261	639	16.3	1.7	0.07	0.12	3.86	26
Sedit	HDW	768587	1069065	380	575	7.56	26	0.4	5.98	85.1	7.6	58.6	268	26.8	1.1	0.02	0.13	0.34	3

Continued ...

Gode	HDW	762251	1059159	530	806	7.51	41	3.7	2.3	133	12.4	56.8	476	2.1	0.7	0.01	0.21	0.4	1
Der Ela	HDW	727546	1053854	510	780	8.03	90	17	16.6	60.8	26.6	70.6	422	2.03	1.6	0.07	0.33	0.21	7
Asili	HDW	703512	1084032	1066	1522	8.5	345	2.4	7.82	21.3	67.45	187	448	168.3	1.9	0.02	0.28	0.12	6
Afase	HDW	696625	1072311	550	821	7.81	117	1.4	8.28	53.2	24.7	145	283	53.6	1.1	0.02	0.22	0.07	6
Adele (Motorized)	HDW	896807	1199109	1140	1750	7.97	208	3.5	28.1	117	290.7	152	301	94.8	1.7	0	1.29	0.26	2
Helele	HDW	900533	1136277	396	604	8.1	27	4.1	12	83.6	22.8	53.4	257	58.6	2	0	0.15	0.16	7
Kalebed	HDW	836068	1079158	1270	1740	7.57	120	4.4	66.7	179	95.95	628	192	20.3	1.6	0.01	0.06	1.98	2
Degajebis	HDW	830565	1074025	640	947	7.29	19	3	15.2	162	18.05	226	336	22.8	0.9	0	0.12	0.95	1
Derega	HDW	906387	1094041	852	1307	7.18	122	6.6	39.1	118	110.2	177	431	29.3	1.4	0	0.19	0.75	1
Dewele	HDW	896839	1221097	2860	4400	7.86	600	3.8	110	274	1130.5	389	292	14.85	0.8	0	0.14	1.19	1
Adele	HDW	896864	1199059	986	1517	7.74	160	4	25.3	122	241.3	148	269	93.5	4.2	0.01	0.27	0.34	4
Meramedobes	HDW	890871	1158904	246	378	7.54	12.5	5	6.9	57	5.7	18.6	213	22.8	0.7	0.01	0.28	0.11	1
Biyekobobe	HDW	890392	1148331	220	313	8.08	17.5	4.6	4.6	45.6	8.55	32	139	34.6	1.1	0	0.12	0.09	2
Anajog	HDW	885900	1196777	1296	1839	8.17	300	7	17.5	102	216.6	457	174	90.6	2.9	0.01	0.22	0.28	1
Umerguluf	HDW	849541	1197910	380	546	7.56	41	3.5	4.6	72.2	15.2	83.5	206	50.6	1.1	0	0.17	0.18	3
Kebrehauso	HDW	891132	1219589	942	1436	7.75	180	6.4	8.28	116	271.7	148	130	50.59	1.3	0.01	0.29	0.39	3
Biyegurgur	HDW	904417	1149757	274	400	7.68	13.5	4.9	5.52	60.8	7.6	25.9	172	60.4	1.3	0	0.27	0.12	1

Continued ...

Bona	River	761206	1062468	2748	3870	7.62	320	4.7	100	412	238.5	1546	220	1.6	1.5	0	0.3	2.8	34
Upper Erer	River	764416	1054223	480	736	7.99	28	1.9	26.2	89.7	22.8	120	305	22	1	0	0.13	0.82	0
Girmame	River	771686	1055856	920	1383	7.48	84	2.9	34.9	163	86.45	311	420	9.7	1.5	0	0.08	1.4	1
Halcho	River	782321	1057930	722	1098	7.96	48	1.7	35.9	125	69.35	162	406	2.1	0.8	0	0.19	1.4	1
Erer town	River	763074	1057045	400	627	8.12	27	2.8	26.7	64.6	22.8	119	227	17.1	0.6	0	0.07	0.53	3
Sisilu	River	719468	1064329	500	708	7.94	69	5.1	21.6	74.5	19.95	139	255	43.8	0.5	0.02	0.24	0.34	139
Afdem	River	726111	1051504	390	550	8.58	52	4.9	19.3	53.2	46.55	114	161	1.39	0.6	0.04	0.13	0.33	6
Keleme(hot)	Spring	789346	1057715	531	794	7.69	19.7	1.8	17.1	127	25.2	76.2	421	8.6	0.8	0	0.29	1.34	2.5
Biyman(hot)	Spring	758410	1056782	2201	3250	7.5	497	9.9	9.32	232	197.9	1170	65.2	2.8	7.5	0.08	0.14	4.57	24
Barak	Spring	819997	1073344	691	1038	7.71	25	2.2	30.4	157	31.1	265	300	15	1.2	0.01	0.14	1.62	18
Arab (hot)	Spring	908876	1098723	2520	3870	7.48	825	36	3.68	51.7	551	628	533	2.4	7.2	0.01	0.09	0.08	1

## Appendix 2 Well data of some of the wells in in the study area.

Location	X	Y	Z	Well depth (m)	Well size (inch)	Casing size (inch)	Q (l/s)	SWL (m)	DWL (m)	TDD (m)	Pump position (m)	Transmissivilty (m <sup>2</sup> /day)	Sp.Capacity (l/min/m)	storativity
Biyo Bahay Irrigation #4	227840	1111091	959	180	12	8	19	46.4	53.5	7.03			24.56	
Biyo Bahay SW #7	228536	1110869	965	174	12	8	22	41.9	62.3	20.4	119.75	334	31.5	2.44x10 <sup>-15</sup>
Biyo Bahay SW#5	229915	1110283	979	185	12	8	24	37.4	57.4	20	89.75	114.8	37.67	3.93x10 <sup>-9</sup>
Biyo Bahay SW #6	229175	1110571	971	180	12	8	24	35.9	67.7	31.8	95.75	260.6	39.25	1.59x10 <sup>-13</sup>
Mete (artesian) Irrigation #3	786149	1099151	741	210	12	8	28	2(above surface)	3.9	5.9	83.75	1162		1.36x10 <sup>-4</sup>
Mete Irrigation #2	786138	1098605	738	158	12	8	19	0.58	48.8	48.2	113.75	1148	1965.51	1.56x10 <sup>-4</sup>
Jama Dere TW	214296	1131593	831	250	12	8	3	84.7	125	40	155	56	4.51	9.55x10 <sup>-2</sup>
AydoraTW	759581	1091435	792	250	10	6	6	7.8	12.7	4.96	95	117.8	72.58	7.56x10 <sup>-3</sup>

Continued.....

Harawa TW	826331	1097377	790	250	12	8	24	32.7	63.7	31	71.75	113	42.5	1.54x10 <sup>-1</sup>
Asbuli TW	737767	1106062	711	227	12	8	8	119	121	2.3	191.5	1374	3001	4.11x10 <sup>15</sup>
Aseliso TW (TW-1)	801859	1057371	1251	220	10	6		80.12	81	0.87				
Aseliso SW1(NPW- 1)	802293	1057401	1244	220	16	12	50	73.57	74.5	0.94	100	2420		
Aseliso SW 2(NPW-2)	801838	1057385	1250	214	16	12	50	80.93	82.3	1.41	100	1400		
Aseliso SW3(NPW- 3)	801309	1057318	1259	252	16	12	50	89.54	90.8	1.3	100	2620		
Aseliso SW 4(NPW-4)	801632	1057297	1261	218	16	12	50	90.13	94.9	4.77	110	1630		
Alaydege plain (LA1)	633633	995257	962	252	14	10	20	101.2	139	37.6	210	102.4	32	
Alaydege plain (LA3)	627464	1015684	823	192	14	10	50	75.66	76.8	1.12	110	39528	2679	
Alaydege plain (AP1)	652507	996029	1118	350	14	10	6	62.27	118	56.1	110	10	9.2	
Alaydege plain (AP2)	641424	1007510	892	257	14	10		72.95						

Continued ...

Alaydege plain (LA2)	635543	1021775	817	236	14	10	34	68.42	94.8	26.4	110	325	77.24	
Alaydege plain (AP5)	645334	996709	996	310	14	10	4	149.9	173	23.5	270	10	10.21	
Alaydege plain (AP8)	662292	1043646	822	300	14	10	12	71.74	161	89.6	240	8	8	
Alaydege plain (LA5)	636415	1039961	733	263	14	10	50	3.6	30.2	26.6	70	161	1.88	
Alaydege plain (AP3)	643798	1019148	835	288	14	10	16	86.4	215.5	129	150	34.3	0.38	
Ka'a	689741	1076778	750	320	10	6	8	26.02	29.63	3.61				
Biyo bahay #2	227352	1111272	960	156	12	8	24	51.8	64.8	13	124		<u>112.6</u>	
Dhagago	227938	1164988	824	113	10	6	1.5	6.78	91.9	85.1	101		1.26	
Hulabora	748960	1050023	1226	67.6	12	6	4	67.6	134	66.4	140.5		3.62	
Biyo bahay #1	225930	1110971	952	129	10	6	5.6	54.7	60.41	5.69	76.73		60	
kurfa sawa	697094	1027068	1246	172	12	6	4.6	33.8	105.8	72	122.5		3.87	

## DECLARATION

I, the undersigned, declare that this thesis is my original work and has not been presented for a degree to any other university and that all sources of materials used for the thesis have been duly acknowledged.

Diriba Mengesha

Signature: \_\_\_\_\_

Date of submission: \_\_\_\_\_

Advisor: Seifu Kebede (PhD)

Signature: \_\_\_\_\_